

AFRL-VS-HA-TR-98-0038

**STUDY OF LOW AND HIGH FREQUENCY Lg
FROM EXPLOSIONS AND ITS APPLICATION TO
SEISMIC MONITORING OF THE CTBT**

**Indra N. Gupta
Robert A. Wagner**

**Multimax, Inc.
1441 McCormick Drive
Largo, MD 20774**

25 January 1998

**Final Report
17 July 1995 - 31 December 1997**

Approved for public release; distribution unlimited.



**DEPARTMENT OF ENERGY
Office of Non-Proliferation
and National Security
WASHINGTON, DC 20585**



**AIR FORCE RESEARCH LABORATORY
Space Vehicles Directorate
29 Randolph Road
AIR FORCE MATERIEL COMMAND
HANSCOM AFB, MA 01731-3010**

DTIC QUALITY INSPECTED 3

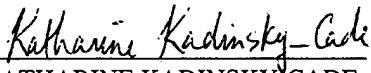
20000426 054


SPONSORED BY
Department of Energy
Office of Non-Proliferation and National Security

MONITORED BY
Air Force Research Laboratory

The views and conclusions contained in this document are those of the authors and should not be interpreted as representing the official policies, either express or implied, of the Air Force or U.S. Government.

This technical report has been reviewed and is approved for publication.


KATHARINE KADINSKY-CADE
Contract Manager


CHARLES P. PIKE, Deputy Director
Integration and Operations Division

This report has been reviewed by the ESD Public Affairs Office (PA) and is releasable to the National Technical Information Service (NTIS).

Qualified requestors may obtain copies from the Defense Technical Information Center. All others should apply to the National Technical Information Service.

If your address has changed, or you wish to be removed from the mailing list, or if the addressee is no longer employed by your organization, please notify AFRL/VSOS-IM, 29 Randolph Road, Hanscom AFB, MA 01731-3010. This will assist us in maintaining a current mailing list.

Do not return copies of the report unless contractual obligations or notices on a specific document requires that it be returned.

REPORT DOCUMENTATION PAGE

Form Approved
OMB No. 0704-0188

Public reporting burden for this collection of information is estimated to average 1 hour per response, including the time for reviewing instructions, searching existing data sources, gathering and maintaining the data needed, and completing and reviewing the collection of information. Send comments regarding this burden estimate or any other aspect of this collection of information, including suggestions for reducing this burden, to Washington Headquarters Services, Directorate for Information Operations and Reports, 1215 Jefferson Avenue Highway, Suite 1204, Arlington, VA 22202-4302, and to the Office of Management and Budget, Paperwork Reduction project(0704-0188), Washington, DC 20503.

1. AGENCY USE ONLY (Leave blank)		2. REPORT DATE 1/25/98		3. REPORT TYPE AND DATES COVERED Final Report, 17 Jul 95 to 31 Dec 97	
4. TITLE AND SUBTITLE Study of Low and High Frequency Lg from Explosions and Its Application to Seismic Monitoring of the CTBT				5. FUNDING NUMBERS F19628-95-C-0176	
6. AUTHOR(S) Indra N. Gupta and Robert A. Wagner				PE 69120H PR DENN TA GM WU AP	
7. PERFORMING ORGANIZATION NAME(S) AND ADDRESS(ES) Multimax, Inc. 1441 McCormick Drive Largo, MD 20774				8. PERFORMING ORGANIZATION REPORT NUMBER MM-02-98-002	
9. SPONSORING / MONITORING AGENCY NAMES(S) AND ADDRESS(ES) Air Force Research Laboratory Hanscom AFB, MA 01731-3010 29 Randolph Road Contract Manager: Katharine Kadinsky-Cade/VSBS				10. SPONSORING / MONITORING AGENCY REPORT NUMBER AFRL-VS-HA-TR-98-0038	
11. SUPPLEMENTARY NOTES This research was sponsored by the Department of Energy, Office of Non-Proliferation & National Security, Washington, DC 20585					
12a. DISTRIBUTION / AVAILABILITY STATEMENT Approved for public release; distribution unlimited				12b. DISTRIBUTION CODE	
13. ABSTRACT (Maximum 200 words) Most source discriminants make use of the prominent regional phase Lg, so that a complete understanding of the generation and spectral characteristics of Lg from explosions is essential for improved and reliable monitoring of the Comprehensive Test Ban Treaty (CTBT). Our research provides valuable new information regarding the origin of both low and high frequency Lg. The low-frequency (up to about 2 Hz) part of the Lg spectra (including the most prominent peaks and nulls) appears to be due to the near-source scattering of explosion-generated Rg into S. Excellent agreement between observations and theory leaves no doubt regarding the contribution of Rg-to-S scattering to the low-frequency Lg from explosions. The high-frequency Lg appears to originate from explosion-generated cracks around the source region. Evidence for these results comes mostly from analysis of broadband regional data from over 40 Nevada Test Site (NTS) and several Kazakh Test Site (KTS) explosions. The results obtained in this study not only improve our understanding of broadband Lg from explosions, but also provide potentially useful source discriminants. Knowledge of the physical basis of discriminants is important to CTBT monitoring because a physical understanding of how and why they work allows for the prediction of discrimination performance in different geologic settings where adequate seismic data may not be available.					
14. SUBJECT TERMS Lg, regional phases, Rg scattering, source discrimination, seismic monitoring, NTS, Kazakh, Lop Nor, CTBT				15. NUMBER OF PAGES 88	
				16. PRICE CODE	
17. SECURITY CLASSIFICATION UNCLASSIFIED	18. SECURITY CLASSIFICATION OF THIS PAGE UNCLASSIFIED	19. SECURITY CLASSIFICATION OF THIS ABSTRACT UNCLASSIFIED	20. LIMITATION OF ABSTRACT SAR		

TABLE OF CONTENTS

EXECUTIVE SUMMARY	1
1. INTRODUCTION	2
1.1 RESEARCH OBJECTIVES	2
1.2 OUTLINE OF ISSUES AND RELATED EARLIER WORK	2
1.2.1 <i>Mechanism of Generation of Low-Frequency Lg from Explosions</i>	2
1.2.2 <i>High Frequency S or Lg from Explosions</i>	3
2. ANALYSIS OF LOCAL AND REGIONAL DATA FROM NTS SHOTS	5
2.1 NARROW BANDPASS FILTERING AND SPECTRAL NULLS	5
2.2 DEPENDENCE OF SPECTRAL NULLS ON SHOT DEPTH	8
2.3 RESONANCE IN RG AND SPECTRAL PEAK IN LG FROM YUCCA FLAT EXPLOSIONS	16
3. ANALYSIS OF REGIONAL DATA FROM EXPLOSIONS IN OTHER REGIONS	25
3.1 SPECTRAL NULLS IN LG FROM KAZAKH EXPLOSIONS	25
3.2 CHINESE NUCLEAR TESTS AT LOP NOR	34
3.3 AZGIR PNE AT ILPA ARRAY	34
4. HIGH FREQUENCY S AND LG FROM NUCLEAR EXPLOSIONS	37
4.1 IMPORTANCE OF HIGH-FREQUENCY S OR LG	37
4.2 COMPARISON OF SEISMIC DATA FROM TAMPED AND DECOUPLED EXPLOSIONS	37
4.2.1 <i>Analysis of Local Data from Azgir Tamped and Decoupled Explosions</i>	37
4.2.2 <i>Re-examination of Salmon/Sterling Data at Local Distances</i>	37
4.3 HIGH FREQUENCY LG FROM NUCLEAR EXPLOSIONS RECORDED AT REGIONAL DISTANCES	43
4.3.1 <i>Analysis of Regional Data from NTS Explosions</i>	43
4.3.2 <i>Results from Analysis of High Frequency Data from Station NLS</i>	50
4.3.3 <i>Analysis of Regional Data from Kazakh Explosions</i>	50
5. APPLICATION TO REGIONAL DISCRIMINATION	54
5.1 SCATTERING OF RG INTO S AND REGIONAL DISCRIMINATION	54
5.2 EVALUATION OF DISCRIMINANTS USING GALILEE GROUND-TRUTH DATASET	54
5.3 DISCUSSION OF RESULTS	65
6. CONCLUSIONS AND RECOMMENDATIONS	71
7. ACKNOWLEDGMENTS	72
8. REFERENCES	73

EXECUTIVE SUMMARY

Most source discriminants make use of the prominent regional phase Lg, so that a complete understanding of the generation and spectral characteristics of Lg from explosions is essential for improved and reliable monitoring of the Comprehensive Test Ban Treaty (CTBT). Our research provides valuable new information regarding the origin of both low and high frequency Lg. The low-frequency (up to about 2 Hz) part of the Lg spectra (including the most prominent peaks and nulls) appears to be due to the near-source scattering of explosion-generated Rg into S. Significant correlation between period of the observed peak in the network-averaged Lg spectra and known depths of the Paleozoic layer suggests that the spectral peaks are associated with resonance caused by sharp impedance contrast in the source region. The observed null frequencies in the Lg spectra are in agreement with those expected from Rg due to a CLVD source at about one-third the shot depth. Evidence for these results comes mostly from analysis of broadband regional data from over 40 Nevada Test Site (NTS) and several Kazakh Test Site (KTS) explosions. Limited data from Lop Nor and Azgir shots provide additional support. Methods of analysis include narrow bandpass filtering, network-averaging, spectral ratios, and comparison of results with those from synthetics. Excellent agreement between observations and theory leaves no doubt regarding the contribution of Rg-to-S scattering to the low-frequency Lg from explosions.

The high-frequency Lg appears to originate from explosion-generated cracks around the source region. A comparison of the phase ratios, Pg/Lg and Pn/Lg from an explosion nearly surrounded by earlier shots whose estimated damage zones intersect its shot point, with the phase ratios from the earliest of these shots suggests that the high frequency (about 8 to 16 Hz) S or Lg from explosions is due to the generation of new cracks created by a tamped explosion. Evidence supporting a cracking mechanism also comes from a comparison of deeper and shallower shots for their frequency dependence of Pg/Lg and Pn/Lg for shots at NTS and KTS, respectively, and from re-examination of local data for Salmon and the decoupled shot in its cavity, Sterling.

These new concepts regarding the generation of Lg from explosions suggest useful methods for discriminating between earthquakes and explosions (including whether cavity decoupled or tamped). Detailed analysis of local and regional phases from known mine blasts and earthquakes in the Galilee region recorded at two stations of the Israel Seismic Network led to several interesting ideas for improvements in source discrimination at regional distances. The results obtained in this study significantly improve our understanding of the observed low and high frequency Lg from explosions. Knowledge of the physical basis of discriminants is important to CTBT monitoring because a physical understanding of how and why they work allows for the prediction of discrimination performance in different geologic settings where adequate seismic data may not be available.

1. INTRODUCTION

1.1 Research Objectives

Seismic monitoring of the Comprehensive Test Ban Treaty (CTBT) requires robust regional discrimination capabilities, especially at low magnitudes. A clear understanding of the generation, propagation, and spectral characteristics of regional phases and their dependence on various near-source parameters is essential for improving the reliability and transportability of regional discriminants from one region to another. Lg is often the largest seismic phase from both explosion and earthquake sources recorded at regional distances so that, in some cases, Lg may be the only reliably observed phase on seismic records. Furthermore, numerous studies have demonstrated the usefulness of Lg for detection, source discrimination, and yield estimation of underground nuclear explosions. Ratio of S- to P-wave energy (or Lg/Pn and Lg/Pg for regional data) has so far been found to be the most promising regional discriminant for earthquakes and explosions. However, a full understanding of the generation of broadband Lg, essential for providing confidence in our ability to monitor the CTBT, is largely lacking. In this study, available data from a large number of explosions with known ground truth, recorded at both local and regional distances, have been analyzed to provide not only a better understanding of Lg and its dependence on various near-source parameters but also improved source discrimination and depth estimates. Use of broadband data provides information on the relative advantages of using low- or high-frequency data. One of the most difficult problems in treaty monitoring is the identification of decoupled shots. Differences in the mechanisms of seismic wave generation from decoupled and normal explosions have been investigated by analyzing broadband regional and closer-distance data from decoupled shots and others (such as overburied shots). The research results enhance understanding of the broadband characteristics of Lg and other regional phases and improve the transportability of regional discriminants from one region to another.

1.2 Outline of Issues and Related Earlier Work

1.2.1 Mechanism of Generation of Low-Frequency Lg from Explosions

There is still no general agreement regarding the generation of low-frequency Lg from underground explosions. Spallation of near-surface layers over ground zero has been suggested as a significant source of Lg (*e.g.* Day and McLaughlin, 1991) but “no observational evidence convincingly demonstrates that spall has an important effect on regional seismic signals” (Patton and Taylor, 1995). Gupta *et al.* (1991a, 1992) provided observations and a theoretical model suggesting that the near-source scattering of explosion-generated Rg into S makes a significant contribution to the low-frequency Lg. This mechanism explains why the low-frequency Lg from explosions is so large that it destroys the discrimination capability of Pn/Lg amplitude ratios at frequency of about 1 Hz. Most evidence for this hypothesis came from analysis of regional data from nuclear explosions at both Nevada and East Kazakh test sites. Independent support for this mechanism also came from an examination of the source spectra

of Lg from East Kazakh and Novaya Zemlya explosions by Israelsson (1992), and from analysis of Lg spectral ratios from Yucca Flat (NTS) explosions by Patton and Taylor (1995). Analyses of seismic data from the recent Non-Proliferation Experiment (NPE) and several NTS nuclear explosions by Walter *et al.* (1994) and Mayeda and Walter (1994) also found Rg-to-S scattering to have a dominant role in generation of the low-frequency Lg. Note that significant near-source Rg-to-S scattering can be caused by several factors such as: laterally varying structure of the Yucca Flat basin (Stead and Helmberger, 1988; Gaffet, 1995), near-surface velocity heterogeneity (Xie and Lay, 1994), and incomplete dissipation by anelastic attenuation (Jih, 1995). It is also interesting to note that Rg is known to be important in both near-source and near-receiver scattering of seismic phases (*e.g.*, Gupta *et al.*, 1990, 1993).

An explanation for the pronounced spectral nulls in the observed Lg spectra of several Yucca Flat (NTS) explosions was provided by Patton and Taylor (1995) by suggesting that the Rg waves must originate mainly from a CLVD source and the low-frequency null is due to an excitation null in Rg for a buried CLVD source. For a homogeneous semi-infinite medium, one can determine (*e.g.*, Aki and Richards, 1980; pp. 315-335) that the CLVD spectral null frequency occurs approximately at $V/(16h)$ where V is the P-wave velocity and h is depth of the CLVD source (Poisson's ratio of 0.25 is assumed). This means that the null frequency is inversely proportional to source depth and directly proportional to medium velocity. For layered media, the CLVD null frequency in Rg for a given source depth can be computed and its comparison with the observed spectral nulls can be used for estimating source depth if one can establish a relationship between the centroid depth of the CLVD source and the explosion depth. Modeling of the observed Lg with the help of synthetics may also provide other source and near-source information. Rg is stronger for shallow sources such as mining explosions and rockbursts than for deeper sources such as earthquakes. An investigation of the spectral nulls and other characteristics of the low-frequency Lg from a large number of explosions with known ground truth is essential for understanding the scattering mechanism and its influence on source discrimination.

1.2.2 High Frequency S or Lg from Explosions

There appears to be lack of agreement regarding the generation of S (at short distances) or Lg (at regional distances) at higher (above 3 Hz) frequencies from explosions. Analysis of Salmon and Sterling data by Blandford and Woolson (1979) and Gupta *et al.* (1986) found relatively greater decoupling of Sterling for S or Lg than for P at higher frequencies. But Denny and Goodman's (1990) analysis of near-field data from Salmon and Sterling indicated no difference in frequency dependence of the phase ratio P/S at higher frequencies for tamped versus decoupled explosions. More recently, a comparison of data from several decoupled, overburied, and normally buried (tamped) explosions by Blandford (1995a) indicated significantly lower S than P for the decoupled and overburied shots, suggesting that the difference may be useful as a discriminant in this case. This analysis included Adushkin's (1992) data on P and S waves from Soviet tamped and decoupled shots in salt and showed the amplitude ratio P/S to be much greater for the decoupled shot (up to 50 times greater at 20 Hz). In order to explain these observations, Blandford (1995a, b) suggested the hypothesis that the S radiation comes from cracks created by the tamped explosion. In theory, a decoupled shot will not cause cracks (a

non-linear effect) because decoupling implies that the cavity boundary remains linear. Blandford's (1995a) analysis also indicated that the higher frequency S/P should decrease with shot depth because of greater overburden pressure which should inhibit cracking. However, an examination of Blandford's (1995a) and some other data by Murphy and Barker (1995) led them to conclude that the seismic characteristics of decoupled and coupled explosions are generally quite similar. According to Blandford (1995b), "the problem of high-frequency S generation from cracks is unsolved and there is no assurance that the high frequency S actually comes from such cracks". In the 1992 Report on the DARPA Seismic Identification Workshop, Blandford *et al.* (1992) recommended that the current research on the Lg/P discriminants be followed up with further empirical, experimental, and theoretical development of discriminants based on high-frequency S/P ratios. Earlier, by using the relatively high-frequency (3 Hz peak) Long Range Seismic Measurements (LRS) instrument, Blandford *et al.* (1981) concluded that the S/P ratio would work well as a regional discriminant throughout the United States if averaged over several stations. More recently, higher frequencies have provided more reliable and robust discriminants than the more conventional discriminants based on the use of frequencies lower than about 5 Hz. In their study of discrimination between NTS explosions and earthquakes, Walter *et al.* (1995) noted improved performance at higher frequencies. Kennett (1989) provided theoretical arguments, supported by observations, that the Pn/Sn ratio would perform better as a source discriminant at higher frequencies. Another example is the regional discrimination study of explosions and earthquakes in the eastern United States by Kim *et al.* (1993) who observed significantly improved discrimination capability of the amplitude ratio P/Lg in the 5-25 Hz band than in the lower frequency bands. The use of high frequencies led to source discrimination without regard to whether the explosions were single-hole shots or quarry blasts.

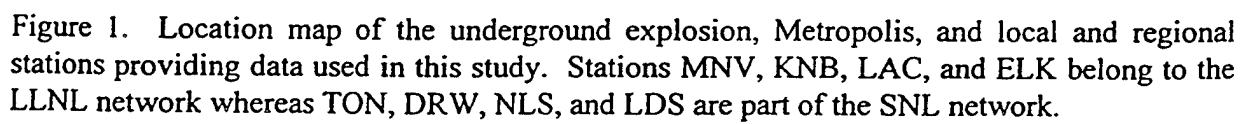
In their comparison of regional phases from NTS and KTS, Gupta *et al.* (1992) observed a large difference in the frequency dependence of Pn/Lg. They offered a possible explanation in terms of the large difference in the crustal structure and shot medium velocities of the two test sites. This explanation is based on the theoretical results of Frankel (1989) according to which the higher-frequency Lg originates from the pS phase and the shot-point velocity strongly influences the degree to which pS is trapped and contributes to Lg (see Gupta *et al.*, 1992, Figure 19). Such a mechanism would, however, indicate no difference in frequency dependence of the phase ratio P/S at higher frequencies for tamped versus decoupled explosions. Walter *et al.* (1995) observed strong dependence of the higher-frequency Pn/Lg on gas porosity of the shot medium. Since gas porosity, medium velocity, and shot depth are strongly correlated (Walter *et al.*, 1995), their results are in agreement with both Blandford's (1995a) hypothesis and Frankel's (1989) theoretical results. It is important to distinguish between the two possible but distinct origins of high frequency S from explosions so that the scope and limitations of the regional discriminant S/P are clearly understood.

2. ANALYSIS OF LOCAL AND REGIONAL DATA FROM NTS SHOTS

2.1 Narrow Bandpass Filtering and Spectral Nulls

A comprehensive study of the generation of Lg from underground nuclear explosions and its dependence on source and near-source parameters requires analysis of large amounts of data for which detailed ground truth information is available. This is mostly the situation for only the NTS explosions, although limited source information is now available for several Kazakh Test Site (KTS) explosions. Therefore, we first investigated regional and other data from NTS shots (Gupta and Zhang, 1996). The time-varying spectral characteristics of the observed seismic arrivals are examined by using a narrow bandpass filtering (NBF) technique which provides amplitudes for various values of group velocity and period. The NBF technique, described in detail by Seneff (1978), has been employed by several investigators (*e.g.*, Kafka, 1990) to study Rg from shallow sources. The group velocity curves are computed by using a moving zero-phase Gaussian filter. The period axis represents the central period of the filter and the velocity axis is simply epicentral distance/travel-time. The filter is applied at each period, the energy envelope computed, and the energy envelope curves are represented in the form of a two-dimensional matrix that is contoured.

Digital, broadband data from several NTS explosions recorded at both local and regional distances are available from Los Alamos National Laboratory (Edwards and Baker, 1993; Taylor, 1993). NBF analysis was first carried out on local data from the nuclear explosion Metropolis (10 March 1990, $m_b = 5.0$, depth 469 m) at several recording stations, covering the distance range of 114 to 274 km (Edwards and Baker, 1993). Figure 1 shows the locations of Metropolis, field deployment stations DM, MV, LM, and HD at local and near-regional distances (Edwards and Baker, 1993), Sandia National Lab (SNL) stations TON, DRW, NLS, and LDS, and Lawrence Livermore National Lab (LLNL) stations ELK, MNV, LAC, and KNB. Using the vertical component data from the intermediate-period system (which records velocity at frequencies above the seismometer period of 5 sec), NBF results from four stations are shown in Figure 2 in which the vertical axis is group velocity. At the three short distances (Figures 2a, b, c), the direct fundamental-mode Rayleigh (which includes the short period Rg with group velocity less than 2 km/sec) is well recorded, but the NBF show a sharp drop in amplitude for the shorter periods. A possible explanation is that, within a few km of the source, the shorter-period Rg is scattered into S waves which travel with a velocity of about 3 km/sec, considerably higher than the velocity of the shorter-period Rg. A spectral null at a period of about 1.7 sec is observed in energy traveling with a velocity of about 1 to 4 km/sec, which includes not only Rg but also S-wave group arrivals such as Sg and Lg. At larger distances (Figure 2d), the spectral null is clearly observed in Lg, which has become the dominant phase because of greater attenuation with distance of Rg. The spectral null in the Rg-S wave group at shorter distances also appears in Lg at regional distances, indicating that the Rg spectrum is imprinted onto the scattered S waves. These results strongly support the importance of the CLVD source and the near-source scattering of explosion-generated Rg into S waves and subsequently into Lg, in agreement with the earlier study of Patton and Taylor (1995).



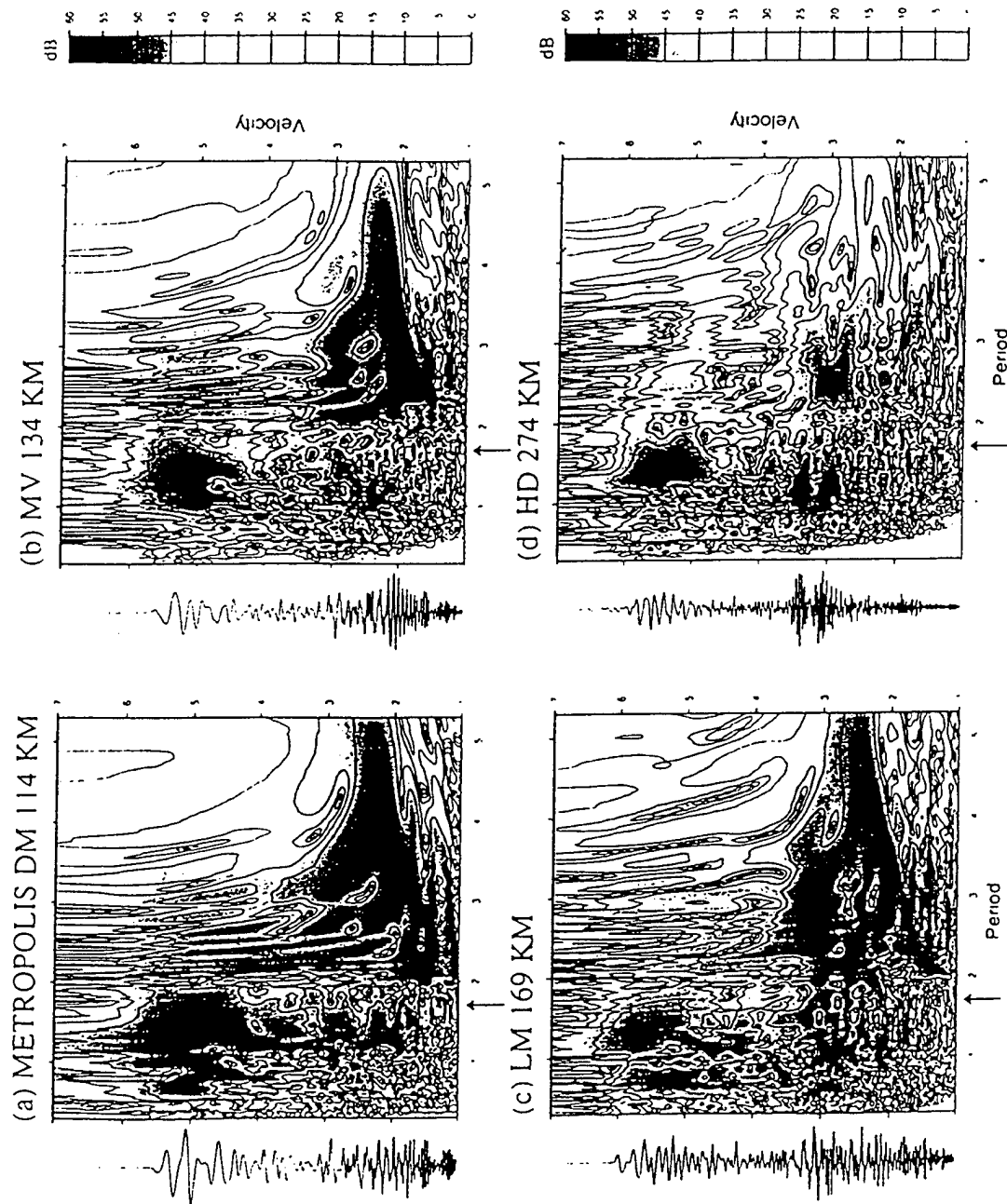


Figure 2. Narrow bandpass filtered records of Metropolis at four different distances indicating progressive (with distance) scattering of Rg (group velocity less than 2 km/sec) into Lg (group velocity about 3 km/sec) and spectral null at period of 1.7 sec in both Rg and Lg.

We also analyzed regional data from stations that recorded, in addition to Metropolis, two more Yucca Flat explosions, Texarkana (10 February 1989, $m_b = 5.2$, depth 503 m) and Tulia (26 May 1989, $m_b = 3.7$, depth 396 m), separated by about 5 km (Figure 3). NBF analyses of the vertical component, long-period data, with peak response at slightly less than 0.1 Hz (Taylor, 1993), from station TON are shown in Figure 4. Prominent spectral nulls in the S-wave group or Lg, with velocity of about 3 km/sec, are observed at periods of 1.5 and 1.3 sec for Texarkana and Tulia, respectively. NBF of Tulia recorded at DM also suggests a null at period of about 1.3 sec. The observed difference in null period for Texarkana and Tulia are likely to be due to several factors such as differences in their shot depths, medium velocities, and yield.

2.2 Dependence of Spectral Nulls on Shot Depth

The dependence of spectral null frequency on shot depth is investigated by analyzing Lg from 22 Yucca Flat explosions (Table 1 and Figure 3) well recorded at all four broadband stations (MNV, KNB, LAC, and ELK) of the LLNL network. The sources of data in Table 1 were Carter (1992) and personal communications from Nancy Howard, Howard Patton, and Bill Walter (all at the Lawrence Livermore National Lab). Table 1 includes the work-point velocity (velocity of compressional waves over a small interval around the shot point) and the overburden velocity (average compressional-wave velocity between the shot point and the surface) both of which suggest considerable lateral variation. Using 51.2 sec long Lg windows, multitapered spectra were obtained for each of the four stations and corrected for attenuation by using the path-dependent $Lg(Q)$ values in Patton (1988). Instrument response correction was not applied since the velocity response of the LLNL broadband stations is nearly flat from about 0.05 to 4.0 Hz and we are interested mainly in frequencies less than 3 Hz. Following Blandford (1981), who used network averaging for improved discrimination, we also obtained the network-averaged spectra by averaging (on log scale) the four single-station spectra. As an example, results for Metropolis are shown in Figure 5 which indicates distinct nulls at each of the four stations. The average null frequency at about 0.68 Hz appears stable, since the null frequencies show only a small variation from one station to another. Similar results based on use of the four SNL stations are shown in Figure 6 which again shows distinct nulls at each station, and the average null frequency is again 0.68 Hz. The consistency of spectral nulls in Figures 5 and 6 rules out the possibility of these nulls owing their origin to factors such as site effects or multipathing.

Results from eight shots, arranged in order of decreasing shot depth and recorded at MNV, are shown in Figure 7a whereas the LLNL network-averaged spectra are shown in Figure 7b. As expected, spectral nulls in the network-averaged spectra are considerably more distinct and reliable than those from a single station. The network-averaged spectra were used to determine the spectral-null frequencies (included in Table 1). Both Figures 7a and 7b indicate an increase in the null frequency with decreasing shot depth, but the increase in null frequency is at first very small and becomes much larger for shallower depths. It should be noted that the null frequencies in Table 1 also indicate some regional variation for shots with nearly the same shot depth. For example, the individual station and average spectra for Paliza (Figure 8) show a spectral null at about 0.78 Hz, whereas those for Metropolis, with shot depth differing by only 3

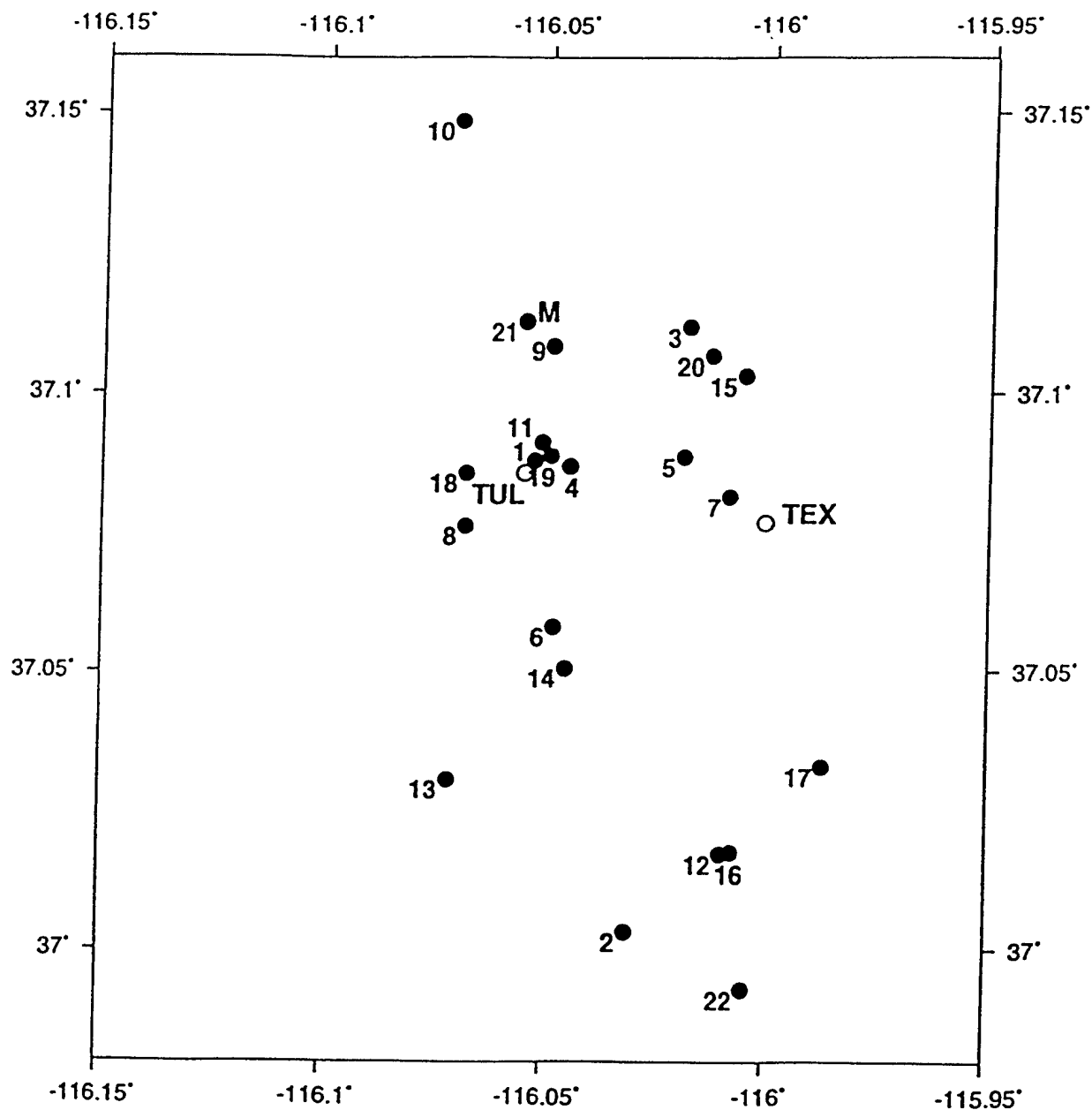


Figure 3. Location map of 22 underground explosions used in this part of the study, including Metropolis (denoted by M), with numbers corresponding to those in Table 1. Locations of two additional shots Texarkana and Tulia (denoted by TEX and TUL, respectively), are also shown.

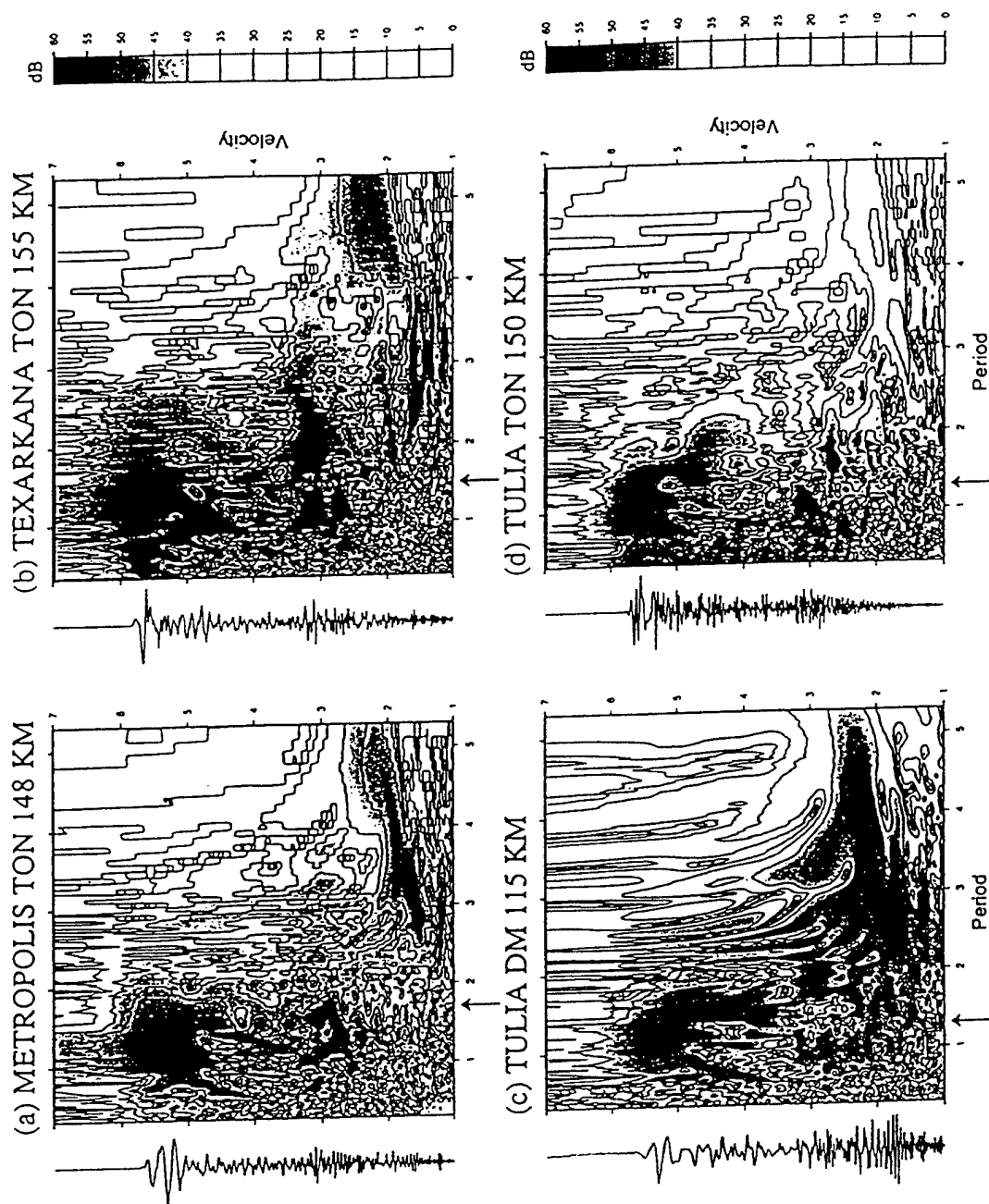


Figure 4. Similar to Figure 2 for the nuclear explosions Metropolis, Texarkana, and Tulia, with shot depths 469, 503, and 396, respectively. The spectral nulls appear to vary with both shot depth and subsurface structure.

Table 1: Yucca Flats Explosions and Associated Lg Null Frequencies

No	Date	Name	m_b USGS	Shot Depth H (m)	Work- Point Velocity (km/sec)	Over- burden Velocity V (km/sec)	Null Fre- quency f (Hz)	CLVD Depth (m) h= V/(16 f)	h/H
1	06 Sep 79	HEARTS	5.8	640	2.688	1.763	0.55	200	0.31
2	22 May 80	FLORA	3.8*	335	1.704	1.257	0.85	92	0.28
3	14 Nov 80	DAUPHIN	4.1	320	2.010	1.420	0.82	108	0.34
4	15 Jan 81	BASEBALL	5.6	564	2.830	1.970	0.55	224	0.40
5	16 Jul 81	PINEAU	3.3*	204	1.530	1.125	1.00	70	0.34
6	04 Sep 81	TREBBIANO	3.8*	305	1.850	1.465	0.80	115	0.38
7	01 Oct 81	PALIZA	4.9	472	2.294	1.497	0.78	120	0.25
8	11 Nov 81	TILCI	4.8	445	2.140	1.600	0.80	125	0.28
9	12 Nov 81	ROUSANNE	5.3	518	2.410	1.580	0.60	165	0.32
10	03 Dec 81	AKAVI	4.6	494	2.100	1.730	0.82	132	0.27
11	28 Jan 82	JORNADA	5.9	640	2.405	1.695	0.53	200	0.31
12	17 Apr 82	TENAJA	4.5	357	2.344	1.310	0.86	95	0.27
13	10 Dec 82	MANTECA	4.6	413	2.250	1.610	0.90	112	0.27
14	11 Feb 83	COALORA	4.1*	274	1.870	1.340	0.82	102	0.37
15	26 May 83	FAHADA	4.4	384	2.070	1.500	0.82	114	0.30
16	02 Aug 84	CORREO	4.7	335	2.085	1.305	0.84	97	0.29
17	21 May 88	LAREDO	4.3	350	2.110	1.600	0.91	110	0.31
18	30 Aug 88	BULLFROG	5.0	489	2.474	1.622	0.80	127	0.26
19	13 Oct 88	DALHART	5.9	640	2.180	1.770	0.56	198	0.31
20	15 Nov 89	MULESHOE	3.4*	244	1.790	1.330	0.87	96	0.39
21	10 Mar 90	METROPOLIS	5.0	469	2.073	1.515	0.68	139	0.30
22	21 Jun 90	AUSTIN	4.0	351	1.920	1.370	0.85	101	0.29

Mean h/H = 0.31

* Local magnitude

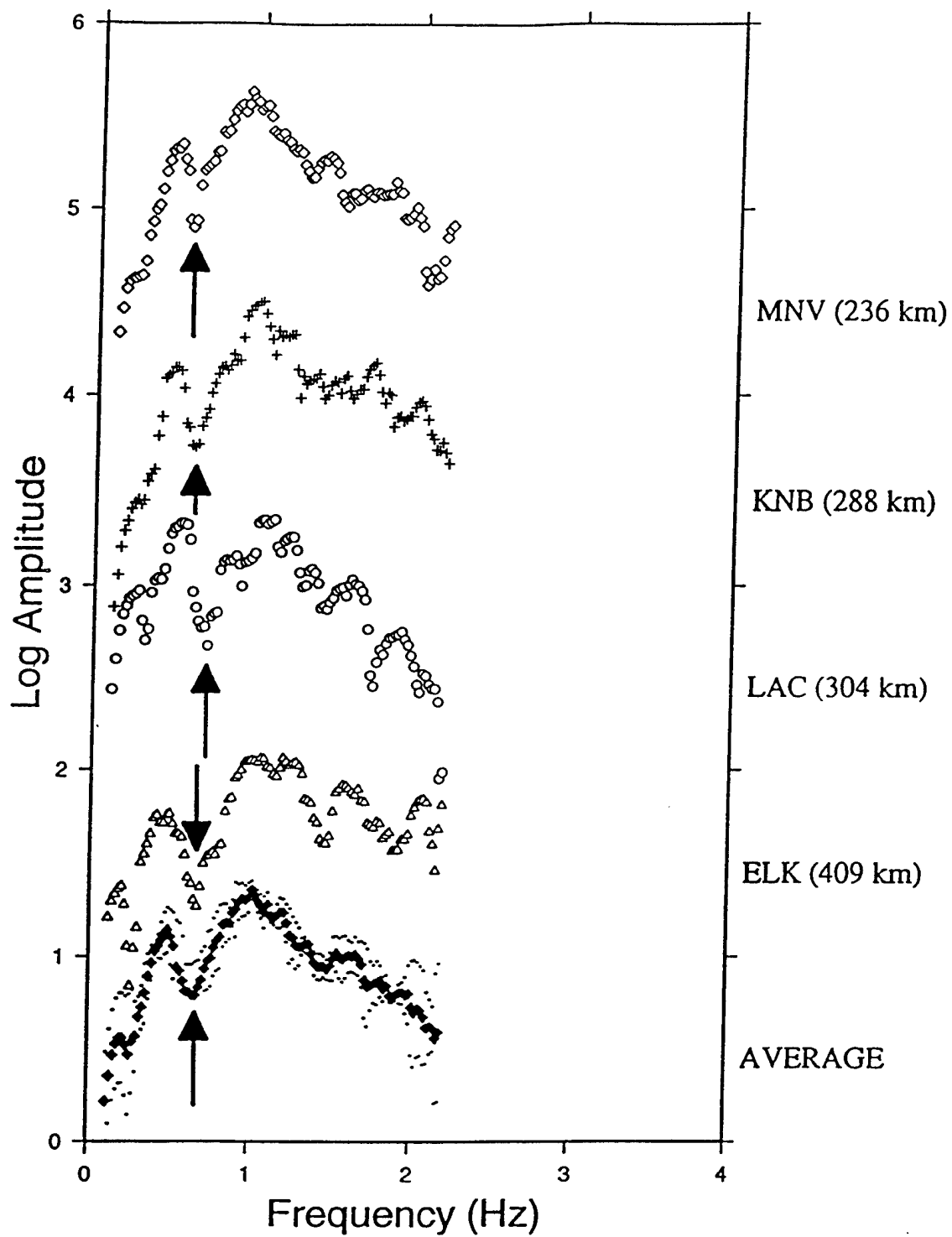


Figure 5. Single-station and network-averaged Lg spectra, based on LLNL stations, for Metropolis, indicating a spectral null at frequency of about 0.7 Hz.

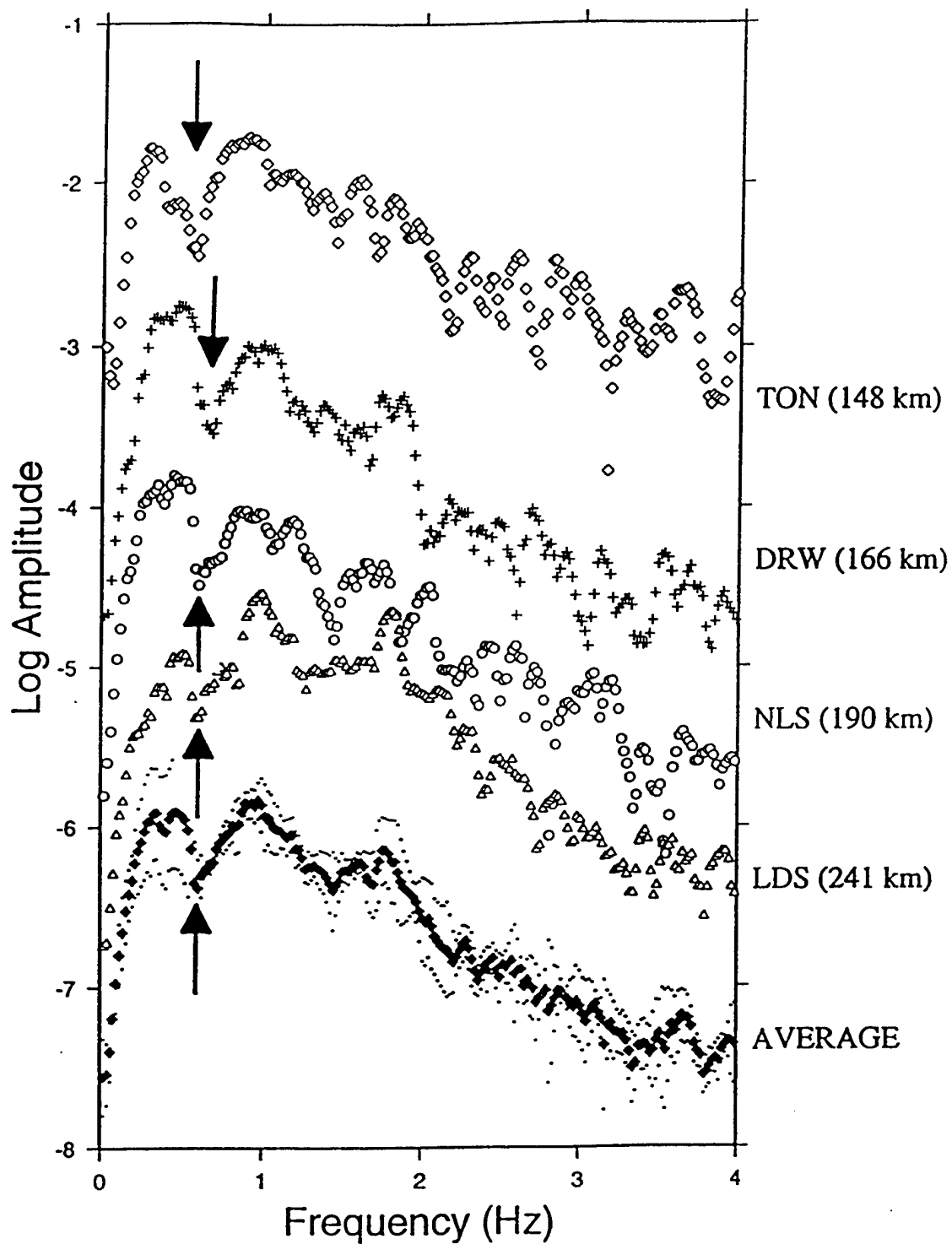


Figure 6. Single-station and network-averaged Lg spectra, based on SNL stations, for Metropolis, again indicating a spectral null at frequency of about 0.7 Hz.

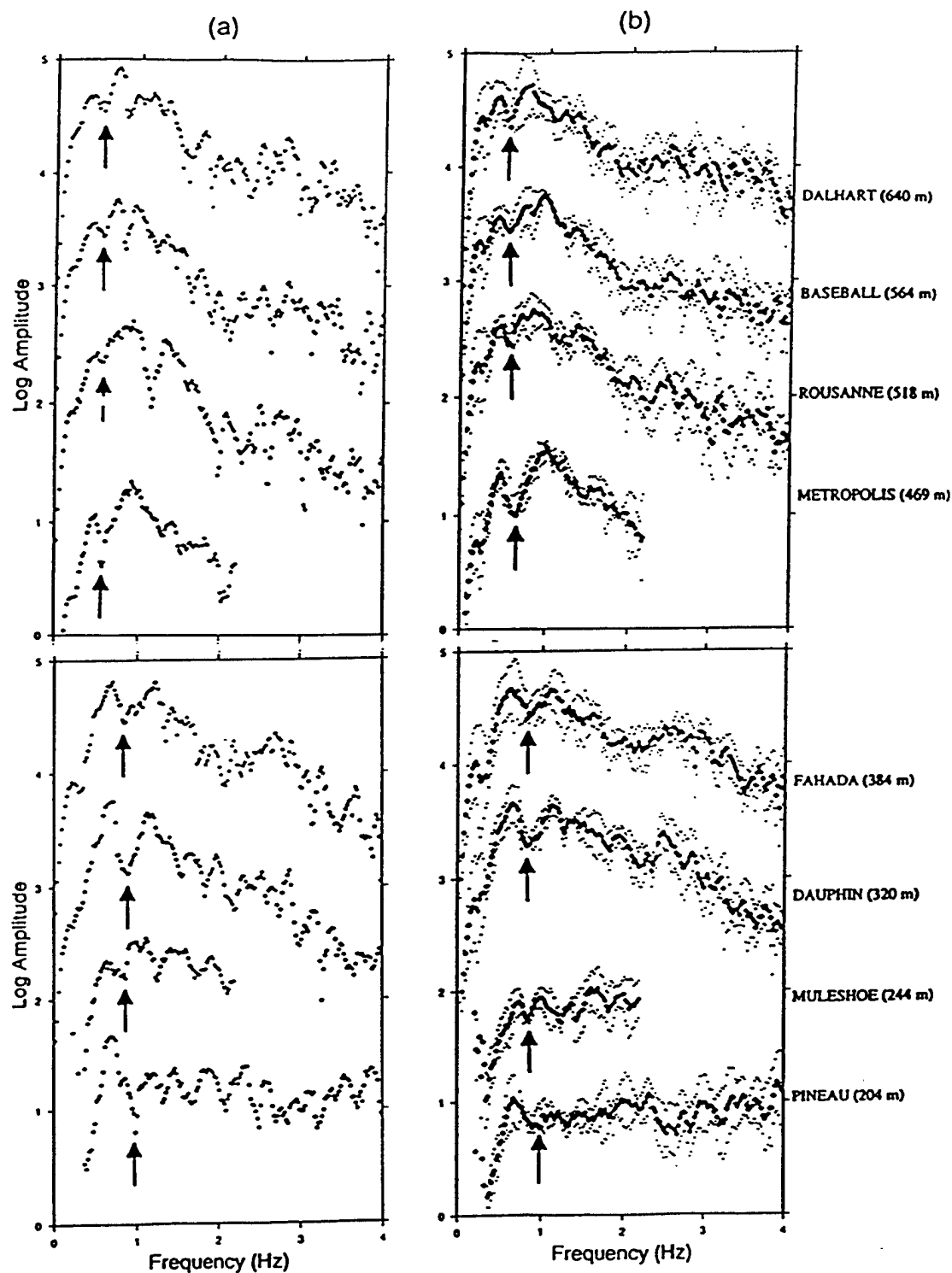


Figure 7. Spectra of Lg for eight explosions at Yucca Flat with shot depths as indicated, based on (a) data from a single station, MNV, and (b) network-averaged over all four LLNL stations, showing systematic increase in spectral null frequency (indicated by arrows) with decreasing shot depth; the increase in null frequency is very small at first but becomes larger for shallower depths.

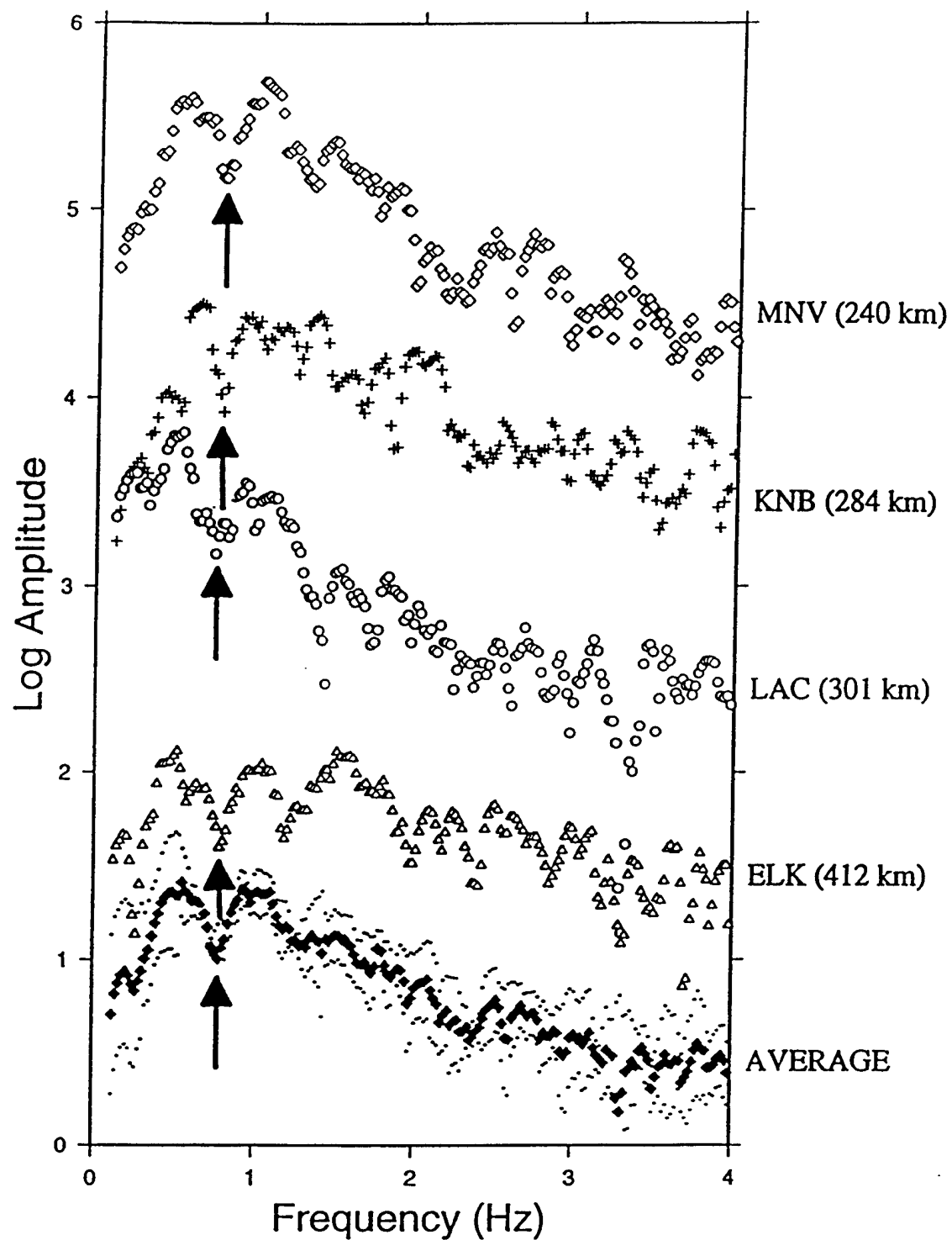


Figure 8. Single-station and network-averaged Lg spectra, based on LLNL stations, for Paliza, indicating a spectral null at frequency of about 0.8 Hz.

m, have a spectral null at 0.68 Hz (Figures 5 and 6). The main reason for this variation is probably the presence of significant lateral variation in the subsurface as also shown by the large variation in both work-point and overburden velocities (Table 1). Note that the work-point velocity for Paliza is considerably greater than that for Metropolis although the overburden velocity for Paliza is slightly less than that for Metropolis.

In order to understand the observed variation in spectral null frequency with depth of the Yucca Flat explosions, the wavenumber integration technique described by Herrmann and Wang (1985) was used for generating the Rg synthetics for vertically-oriented CLVD sources at various depths. The crustal velocity model of Patton and Taylor (1995, Table 1, SMU Velocity Model), was used and the source was assumed to be an impulse. The epicentral distance was taken to be only 20 km, since the Rg-to-S scattering should occur near the explosion source. The spectra of Rg for various depths of the CLVD source are shown in Figure 9 in which the spectra for source depth of 250 m appears to be identical with that in Patton and Taylor (1995, Figure 14). It is interesting to note that the increase in the null frequency is very slow at first but becomes much larger for shallower depths, remarkably similar to the observed variation in Figure 7. Figure 10 shows the dispersion curves for group and phase velocity of the fundamental-mode Rayleigh wave for the same Yucca Flat crustal model as used for the synthetics in Figure 9. The group velocity has a prominent minimum at about 0.5 Hz, which may be responsible for the peaks in the spectra of synthetics in Figure 9.

The crustal model used in deriving the synthetics in Figure 9 comprises a top-most layer 600 m thick with P-wave velocity of 1.8 km/sec. The overburden velocities in Table 1 show a large variation (from about 1.1-2.0 km/sec) with mean value of about 1.5 km/sec. This means that there are large lateral variations in medium velocity, and the crustal model used in the synthetics is only approximately valid. This may also explain the difference between the shapes of the observed (Figure 7) and the theoretical (Figure 9) spectral nulls (the observed nulls for source depths of 250-150 m are much broader than the theoretical). It seems, however, that for frequencies below 2 Hz, the homogeneous half-space model is a fairly good approximation to the layered NTS model (Gupta *et al.*, 1991b), so that a rough estimate of depth of the CLVD source for an explosion will be $V/(16f)$ where V is its overburden velocity and f is its observed spectral null frequency. These estimates, included in Table 1, suggest that depth of the CLVD source for each explosion is on the average about 0.31, or one-third of its shot depth. Linear regression of V/f versus shot depth with zero intercept (Figure 11) indicates a correlation coefficient of 0.91 and a mean slope of 4.9, which again suggests the depth of the CLVD source to be, on the average, $4.9/16$ or about one-third of the shot depth.

2.3 Resonance in Rg and Spectral Peak in Lg from Yucca Flat Explosions

Near-field displacement time histories from several nuclear tests in the Yucca Flat region have suggested vertical compressional-wave resonance with the resonance period independent of explosion yield and depth (Rodean, 1981). There is a considerable impedance mismatch between the Paleozoic rocks and the overlying alluvium and tuff. The wave period was found to be equal to four P-wave transit times between the free surface and the Paleozoic rock surface (Rodean, 1981). This resonance phenomenon may be related to Rayleigh wave generation by

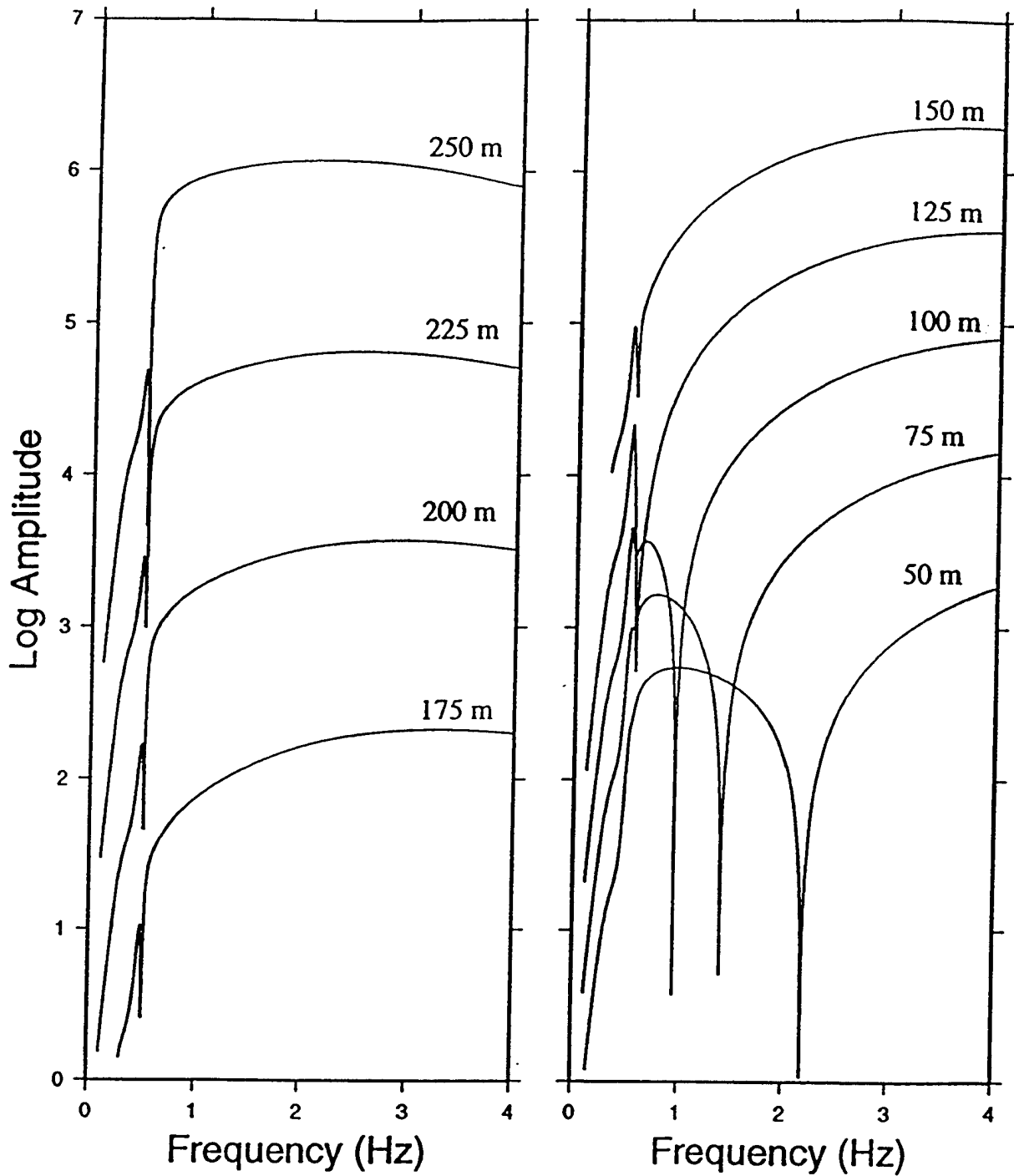


Figure 9. Spectra of Rg synthetics for CLVD source at various depths for crustal velocity model of Yucca Flat used by Patton and Taylor (1995). The increase in the null frequency with decrease in source depth is extremely small at first but becomes much larger for shallower depths, similar to the observed variation in Figure 7.

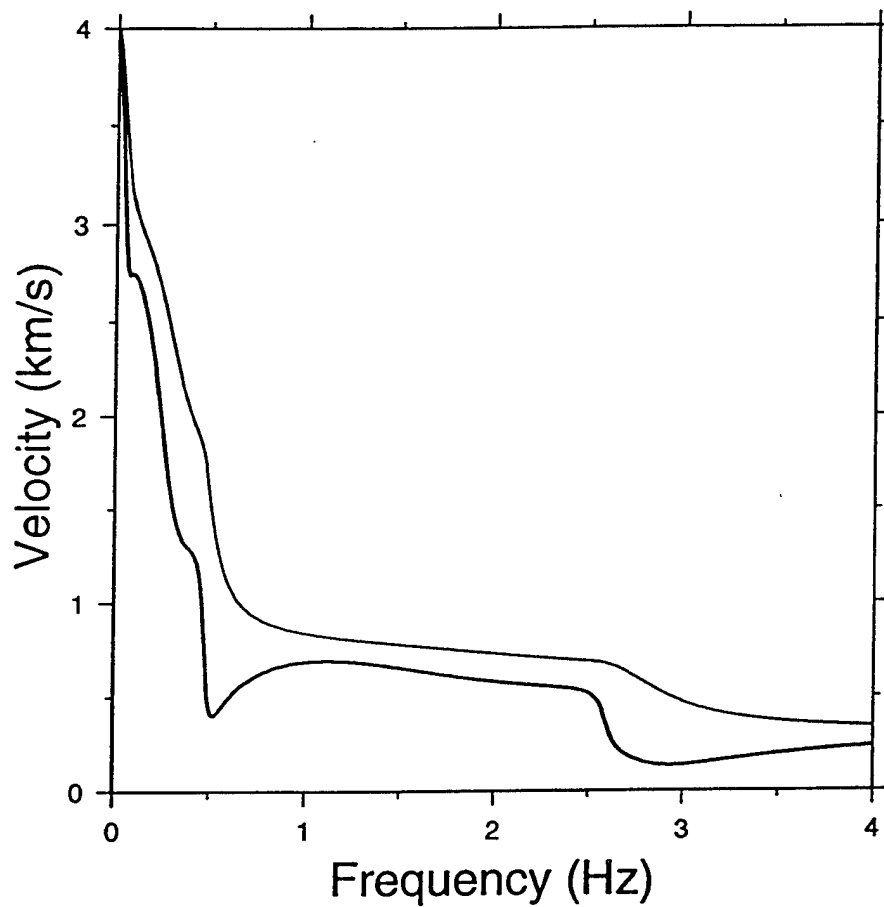


Figure 10. Dispersion curves for group (lower curve) and phase velocity for the fundamental Rayleigh mode for the Yucca Flat crustal structure used in Figure 9. Note the prominent minimum in group velocity at about 0.5 Hz.

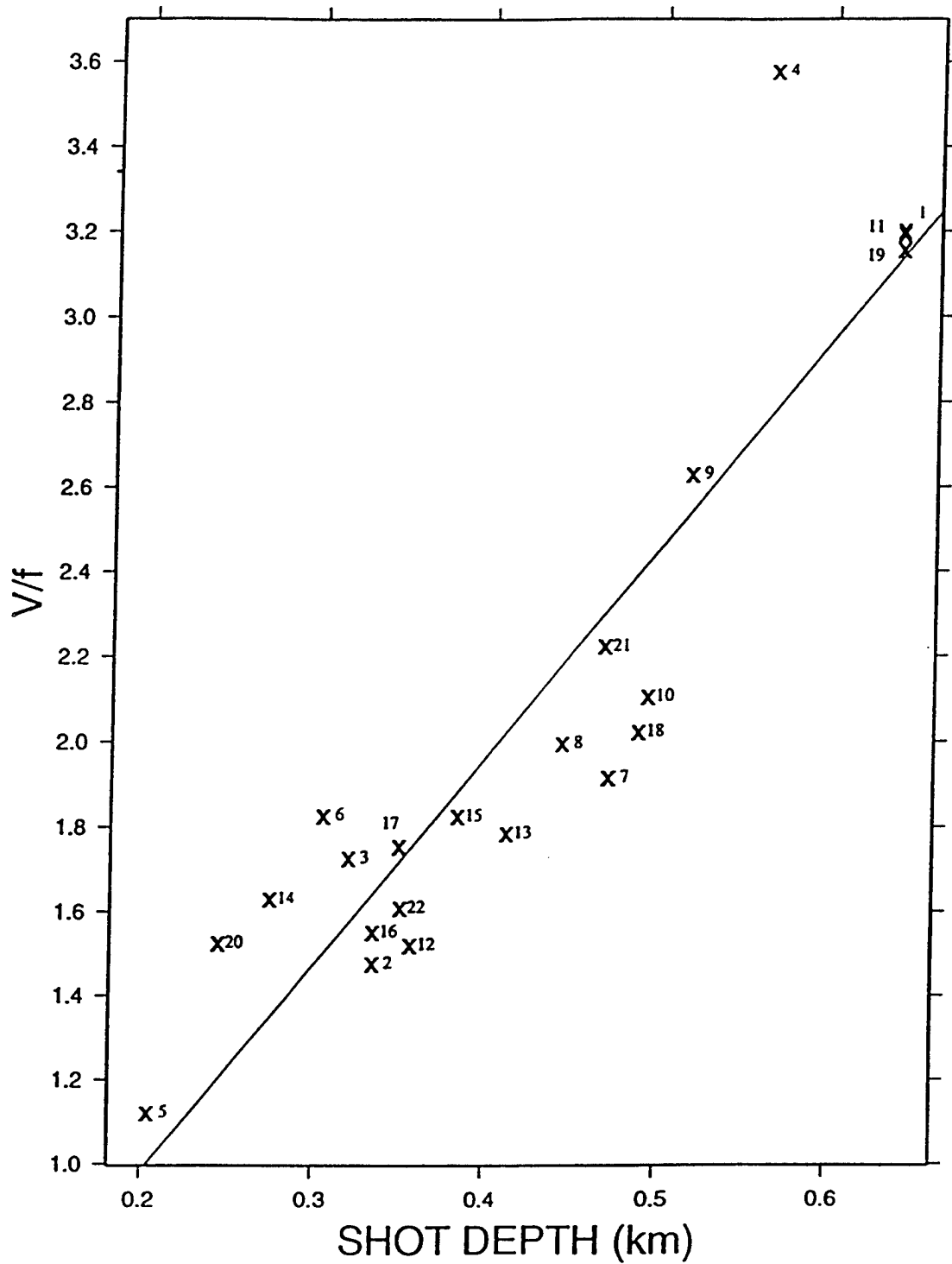


Figure 11. Plot of V/f (where V is the overburden velocity and f is the $Lg(NULL)$ frequency) versus shot depth for 22 explosions listed in Table 1. Linear regression, with zero intercept, shows a mean slope of 4.90 and correlation coefficient of 0.91.

explosions because, as noted by Hudson and Douglas (1975), when a sharp impedance contrast exists in a plane-layered model of the crust, the Rayleigh wave group velocity minimum in the fundamental mode occurs close to a period equal to four times the travel times of P-waves from the surface to the interface. An example of such resonance, as observed in the Fourier spectrum of displacement time history from a near-field velocity gauge for the Yucca Flat explosion, Starwort (26 April 1973), is shown in Figure 12a (after Rodean, 1981, Figure 3). Multi-tapered Lg spectra of Starwort, as recorded at the four broadband stations (MNV, KNB, LAC, and ELK) of the LLNL network, were obtained by using 51.2 sec long windows and correcting for attenuation (as in the earlier work, Section 2.2). These spectra clearly indicate distinct peaks at the same resonance frequency of about 0.5 Hz (Figure 12b) at each of the four stations as well as in the network-averaged spectrum, known to suppress path effects and enhance source effects (Blandford, 1981). As pointed out earlier (Section 2.2), the theoretical dispersion curve for group velocity of the fundamental-mode Rayleigh wave for the Yucca Flat crustal model (Figure 10) also has a prominent minimum at about 0.5 Hz. These results, showing exact match between the observed resonant frequency in Rg and the spectral peak in Lg and the theoretically predicted prominent minimum in group velocity, strongly support the hypothesis of near-source scattering of Rg into S and Lg, similar to that suggested by the low-frequency nulls in Lg from explosions (Patton and Taylor, 1995; Gupta *et al.*, 1997).

In order to investigate whether such a mechanism involving resonance and the scattering of Rg into S may be operating for other Yucca Flat explosions as well, we analyzed the low-frequency Lg from 32 Yucca Flat explosions (Figure 13) that were well recorded at all four stations of the LLNL network and included two overburied shots, Borrego and Techado (Patton and Taylor, 1995, Table 2). Most of these 32 shots are of course the same as those used earlier with locations shown in Figure 3. There is considerable variation in the thickness of low velocity sediments overlying the higher velocity Paleozoic layer in the Yucca Flat region (see, *e.g.* Gaffet, 1995, Figures 2 and 3). An approximately east-west vertical cross-section across the region (Gaffet, 1995, Figure 3) shows large lateral variations in the depth of the Paleozoic layer. The shot locations in Figure 13 include eight shots approximately along a vertical section, as shown in Gaffet (1995, Figure 3), in which the depth of the Paleozoic layer first gradually increases and then decreases. As shown in Figure 14, the network-averaged spectra of these eight shots indicate prominent peaks at frequencies that initially decrease with increasing depth of the Paleozoic layer and then increase as depth of the Paleozoic layer decreases. It seems therefore that the Lg spectra of these eight explosions show prominent peaks with spectral variations consistent with resonance and the scattering of Rg into S, similar to those observed for Starwort.

Data for calculating the exact P-wave transit times between the free surface and the Paleozoic rock surface are not available for the Yucca Flat explosions. Furthermore, the large lateral variations in the sub-surface of the shot region makes the validity of a model consisting of P waves propagating through plane-parallel layers and leading to resonance somewhat questionable. However, one would expect generally larger transit times when the Paleozoic layer is deeper, so that the peak Lg or Lg(MAX) period should generally increase with depth of the Paleozoic layer. This does seem to be true, as demonstrated in Figure 15 by a plot of the observed Lg (MAX) period versus depth of the Paleozoic layer for 30 Yucca Flat explosions

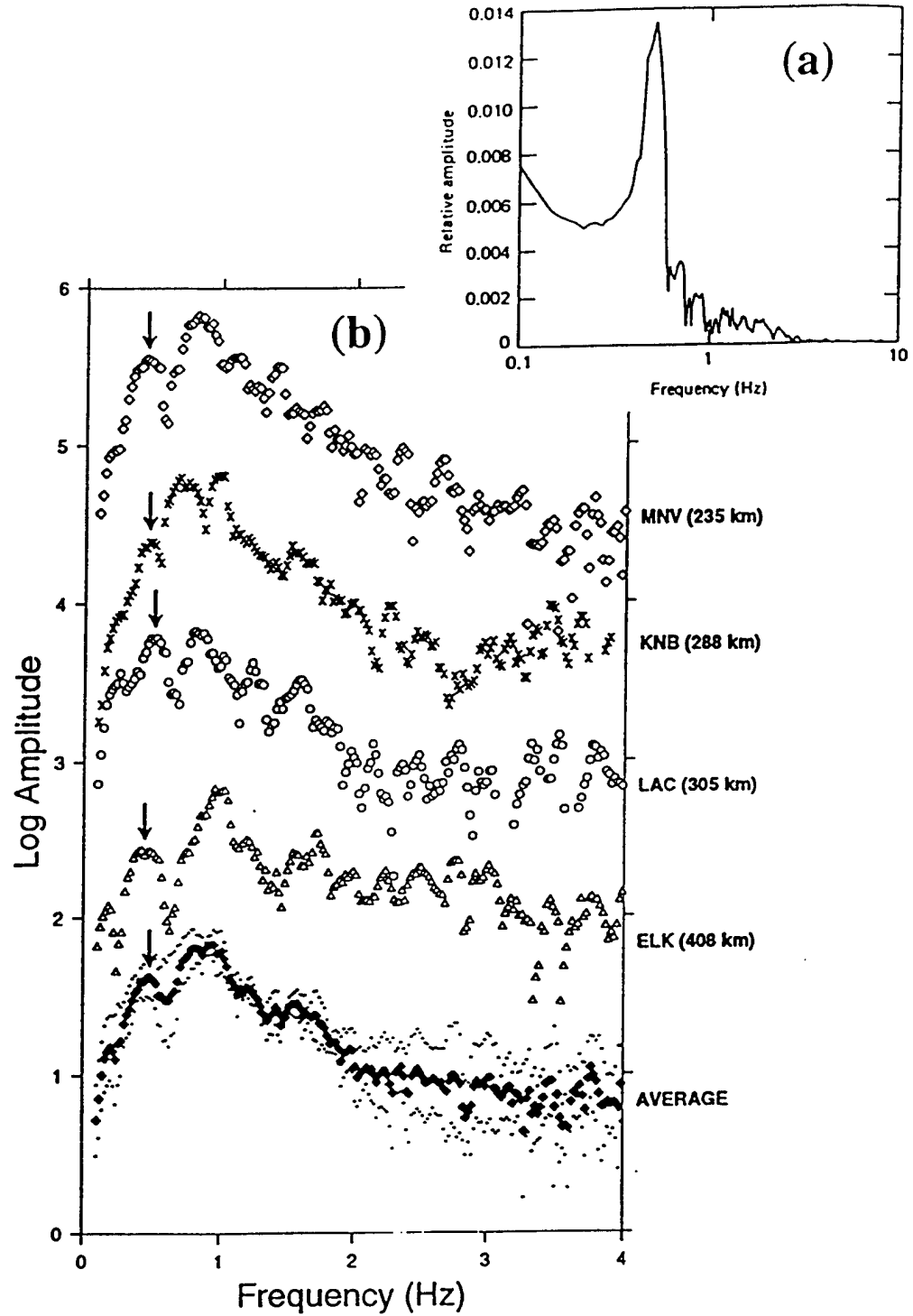


Figure 12. (a) Fourier spectrum of near-field data from Starwort indicating resonance at frequency of about 0.5 Hz. (b) Single-station and network-averaged Lg spectra, based on LLNL stations, for Starwort, each indicating a spectral peak at about 0.5 Hz.

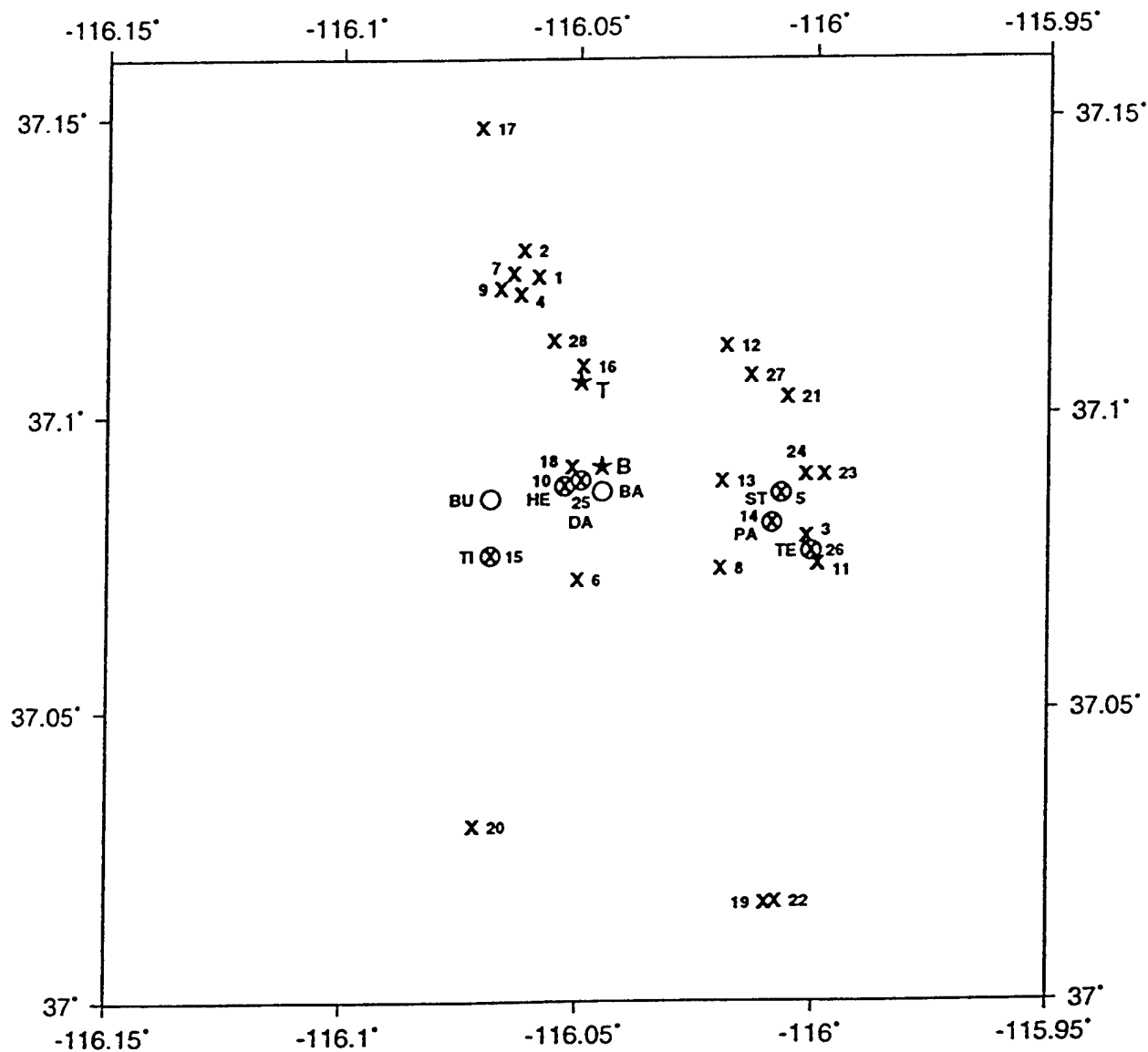


Figure 13. Location map of 32 Yucca Flat explosions used in study of spectral peaks in Lg, including eight (shot names given in Figure 14) approximately along a vertical profile (indicated by O) and two overburied shots, Borrego (B) and Techado (T).

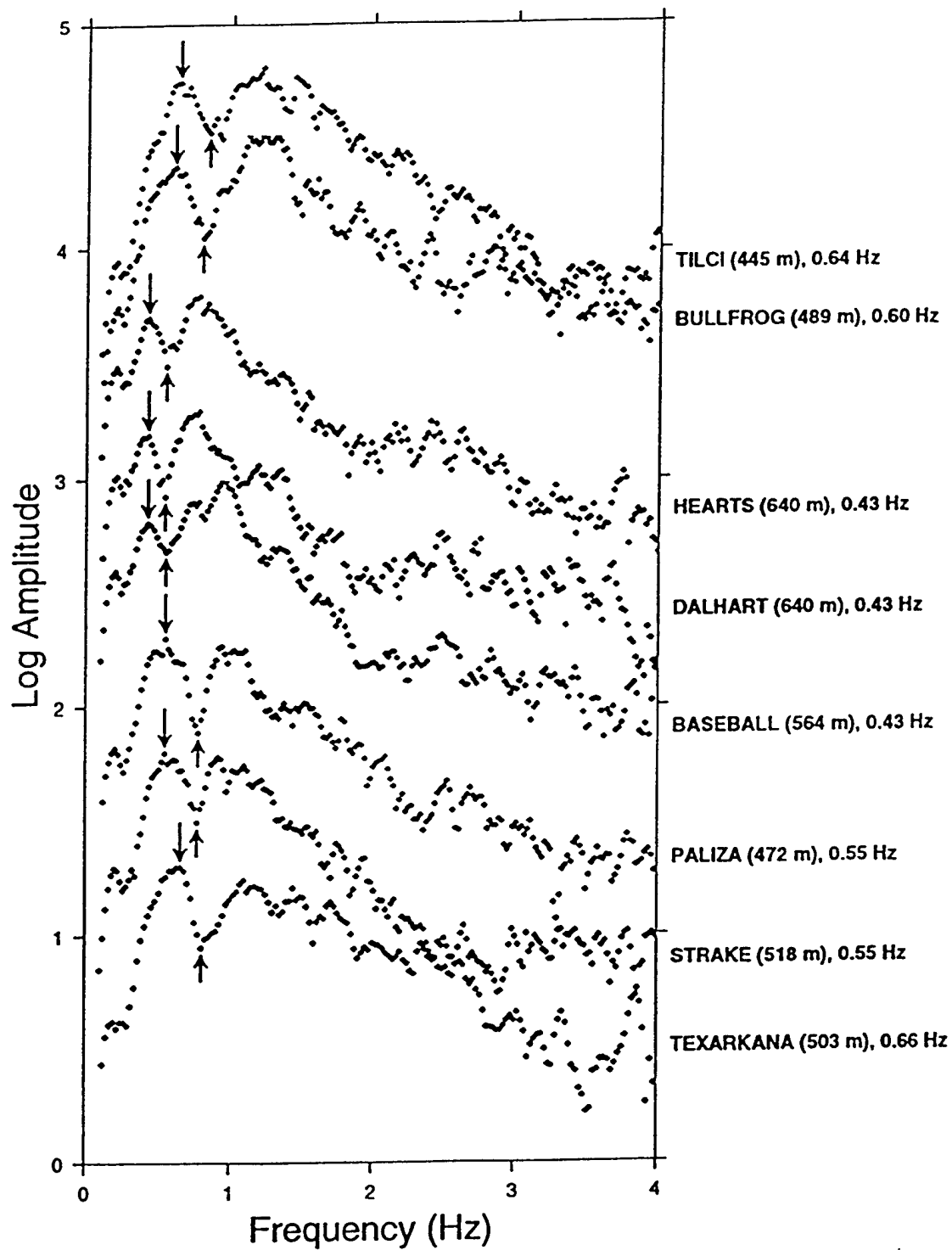


Figure 14. Network-averaged Lg spectra of eight shots, located approximately along a vertical section, showing prominent peaks (marked by arrows pointing down) at frequencies that appear to correlate with depth of the Paleozoic layer. The explosion names are given along with their shot depths and Lg(MAX) frequencies.

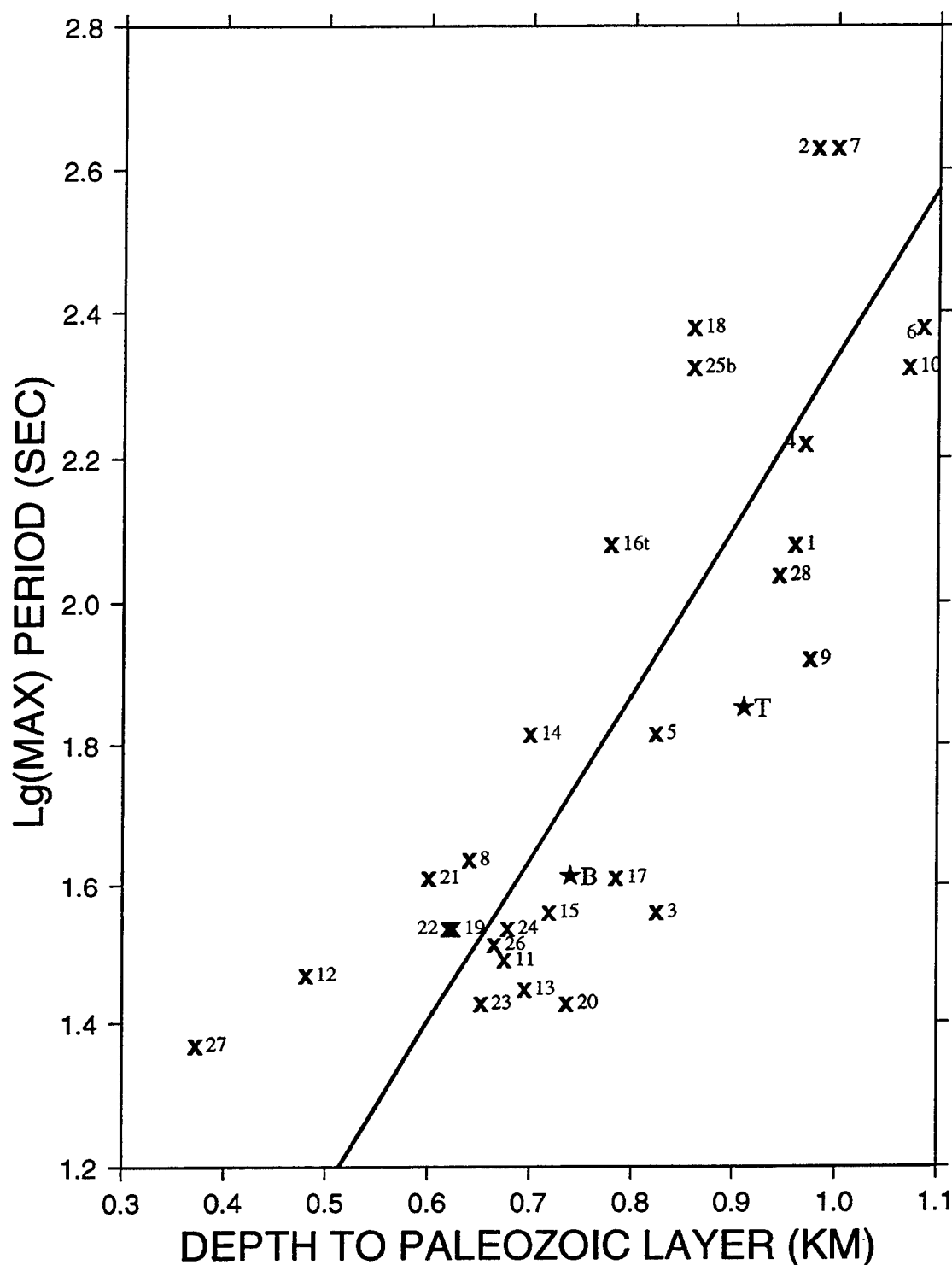


Figure 15. Plot of the observed Lg (MAX) period versus depth of the Paleozoic layer for 30 Yucca Flat explosions. Linear regression with zero intercept, based on data from 28 shots numbered as in Table 2 (Borrego (B) and Techado (T) are excluded), shows correlation coefficient of 0.82 and mean slope of 2.34. Data points for shots Dalhart and Rousanne, closest to Borrego and Techado, respectively, are denoted by 25b and 16t, respectively.

(Table 2) for which ground truth (including depth of the higher-impedance Paleozoic layer) was known. Linear regression with zero intercept, based on data from 28 shots (Borrego (B) and Techado (T) are excluded), shows a correlation coefficient of 0.82. It seems, therefore, that the low-frequency peaks in the Lg spectra of Yucca Flat explosions are due to resonance and scattering of Rg into S and Lg.

The same network-averaged spectra as used for determining the spectral peaks in Lg were also used to observe the Lg null frequencies for the same 30 explosions. Linear regressions with zero intercept, based on data from 28 shots, on plots of Lg(NULL) period versus shot depth (Figure 16) and V/f(NULL) versus shot depth (Figure 17) indicate correlation coefficients of 0.89 and 0.95, respectively. As expected, the results for the mean slope in Figure 17 are similar to those in Figure 11, again indicating that the depth of the CLVD source is about one-third of its shot depth, and a determination of the Lg null frequency of an explosion may provide an estimate of its shot depth.

It is interesting to note that the observed values of both Lg(MAX) and Lg(NULL) periods for the two overburied shots, Borrego and Techado, in Figures 15, 16, and 17 appear to be smaller than those expected from the mean trend of the remaining 28 shots. The shots closest to Borrego and Techado (Figure 13) are Dalhart (No. 25) and Rousanne (No. 16), and the path effects for these two pairs should be almost identical. A comparison of both Lg(MAX) and Lg(NULL) periods in Figures 15, 16, and 17 for the two pairs of closely located overburied and "normal" shots indicate significant differences. For example, the single-station and network-averaged low-frequency Lg spectra of Rousanne and Techado, shown in Figure 18, indicate both Lg(MAX) and Lg(NULL) frequencies of Rousanne to be somewhat smaller than those of Techado. A likely explanation is that, as compared to "normal" explosions, the overburied shots should be associated with relatively higher medium velocities because of relatively reduced degree of fracturing and other non-linear effects in their source regions. Note also that Figure 18 shows the Lg of Rousanne to be relatively rich in low (less than about 2 Hz) frequency energy as compared to the Lg of Techado, probably due to relatively stronger explosion-generated Rg from Rousanne.

3. ANALYSIS OF REGIONAL DATA FROM EXPLOSIONS IN OTHER REGIONS

3.1 Spectral Nulls in Lg from Kazakh Explosions

Regional data from the Soviet underground nuclear explosion of the Joint Verification Experiment (JVE, 14 September 1988, $m_b = 6.03$) are available at the three Natural Resources Defense Council (NRDC) stations, KSU, KKL, and BAY. These three stations lie at epicentral distances of about 160 km east, 255 km southwest, and 255 km northwest, respectively. Details of the experiment, sample records, and instrumentation have been provided by Priestley *et al.* (1990). The long- and short- period seismographs consist of 15 and 1 sec free period seismometers, respectively. Results of NBF analysis of the vertical component long-period data from KKL and BAY and short-period data (after integration using the trapezoidal rule) from KSU (the long-period data at KSU had problems; William Walter, personal

Table 2: Yucca Flats Explosions and Associated Lg Null and Peak Frequencies

No.	Date	Name	Shot Depth (m)	Depth to Paleozoic Layer (m)	Over- burden Velocity (km/sec)	Null Frequency (Hz)	Peak Frequency (Hz)
1	26 Apr 73	STARWORT	564	960	1.646	0.63	0.48
2	20 Dec 75	CHIBERTA	716	981	1.840	0.57	0.38
3	08 Dec 76	REDMUD	427	825	1.480	0.80	0.64
4	05 Apr 77	MARSILLY	690	970	1.716	0.54	0.45
5	04 Aug 77	STRAKE	518	824	1.500	0.77	0.55
6	09 Nov 77	SANDREEF	701	1085	1.853	0.54	0.42
7	23 Feb 78	REBLOCHON	658	1000	1.673	0.53	0.38
8	27 Sep 78	DRAUGHTS	442	640	1.534	0.75	0.61
9	29 Aug 79	NESSSEL	464	975	1.505	0.64	0.52
10	06 Sep 79	HEARTS	640	1071	1.763	0.55	0.43
11	24 Oct 80	DUTCHESS	427	675	1.573	0.89	0.67
12	14 Nov 80	DAUPHIN	320	480	1.420	0.82	0.68
13	16 Jul 81	PINEAU	204	695	1.125	1.00	0.69
14	01 Oct 81	PALIZA	472	700	1.497	0.78	0.55
15	11 Nov 81	TILCI	445	719	1.600	0.84	0.64
16	12 Nov 81	ROUSANNE	518	779	1.580	0.60	0.48
17	03 Dec 81	AKAVI	494	785	1.730	0.82	0.62
18	28 Jan 82	JORNADA	640	860	1.695	0.53	0.42
19	17 Apr 82	TENAJA	357	625	1.310	0.86	0.65
20	10 Dec 82	MANTECA	413	737	1.610	0.90	0.70
21	26 May 83	FAHADA	384	601	1.500	0.82	0.62
22	02 Aug 84	CORREO	335	620	1.305	0.84	0.65
23	30 Aug 84	DOLCETTO	366	652	1.410	0.88	0.70
24	27 Sep 85	PONIL	366	678	1.455	0.94	0.65
25	13 Oct 88	DALHART	640	860	1.770	0.55	0.43
26	10 Feb 89	TEXARKANA	503	665	1.720	0.81	0.66
27	15 Nov 89	MULESHOE	244	373	1.330	0.87	0.73
28	10 Mar 90	METROPOLIS	469	945	1.515	0.68	0.49

OVERBURIED SHOTS

*	29 Sep 82	BORREGO	564	740	1.860	0.80	0.62
*	22 Sep 83	TECHADO	533	910	1.610	0.71	0.54

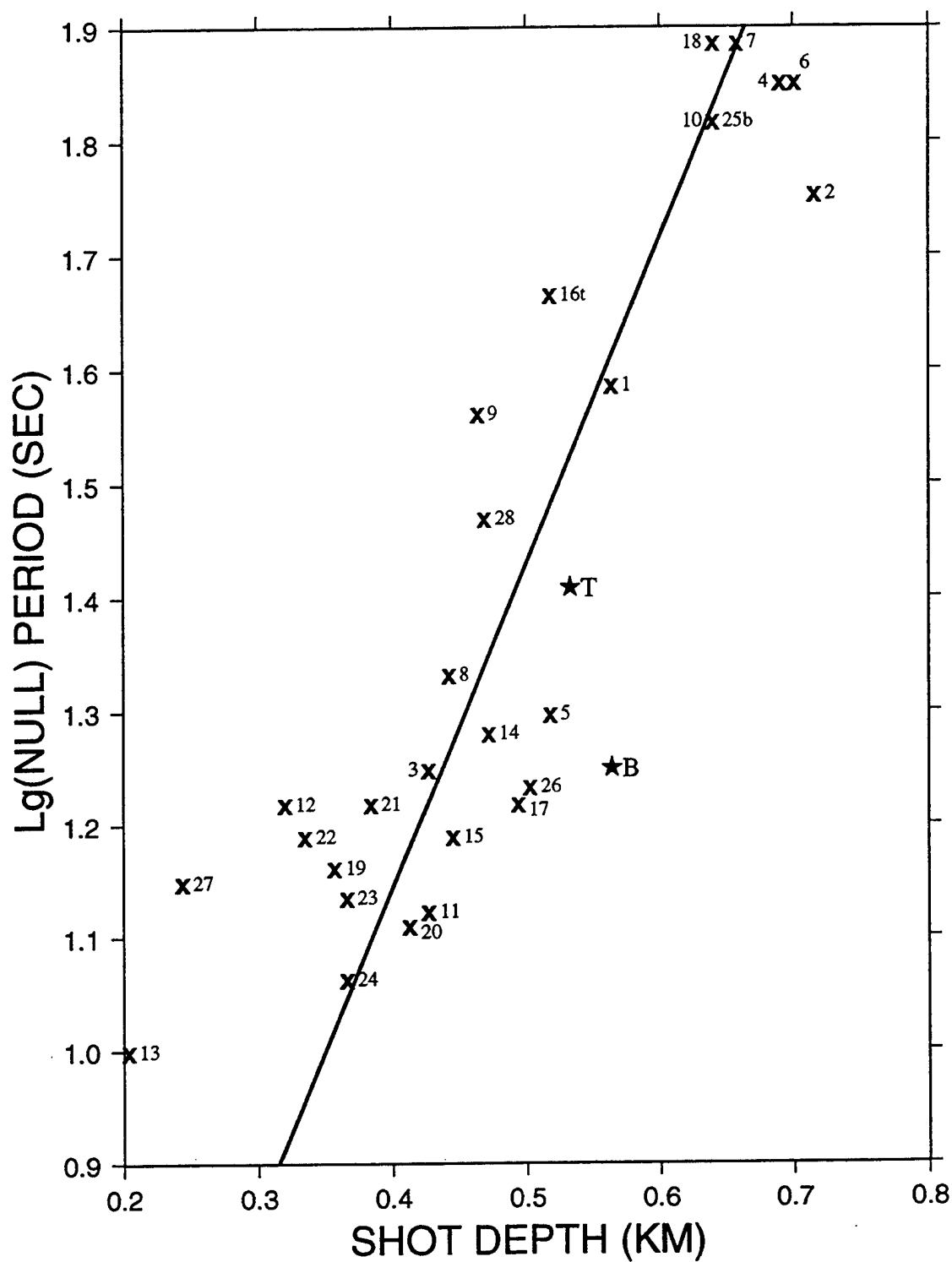


Figure 16. Similar to Figure 15 showing a plot of Lg(NULL) period versus shot depth for the same 30 explosions. Linear regression with zero intercept, based on data from 28 shots, shows a correlation coefficient of 0.89 with mean slope of 2.86.

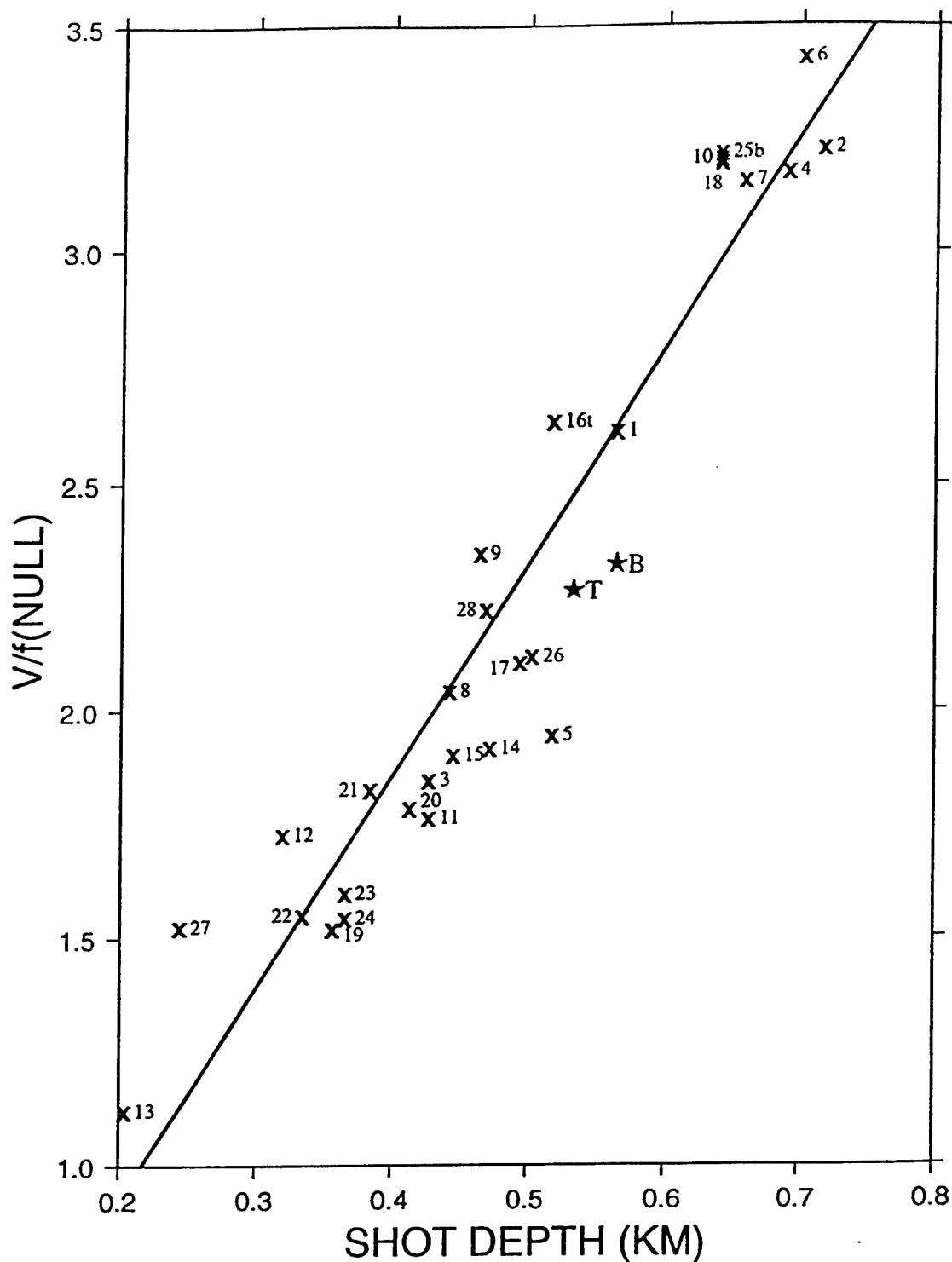


Figure 17. Similar to Figure 15 showing a plot $V/f(\text{NULL})$, where V is the overburden velocity and f is the $\text{Lg}(\text{NULL})$ frequency, versus shot depth for the same 30 explosions. Linear regression with zero intercept, based on data from 28 shots, shows a correlation coefficient of 0.95 with mean slope of 4.63.

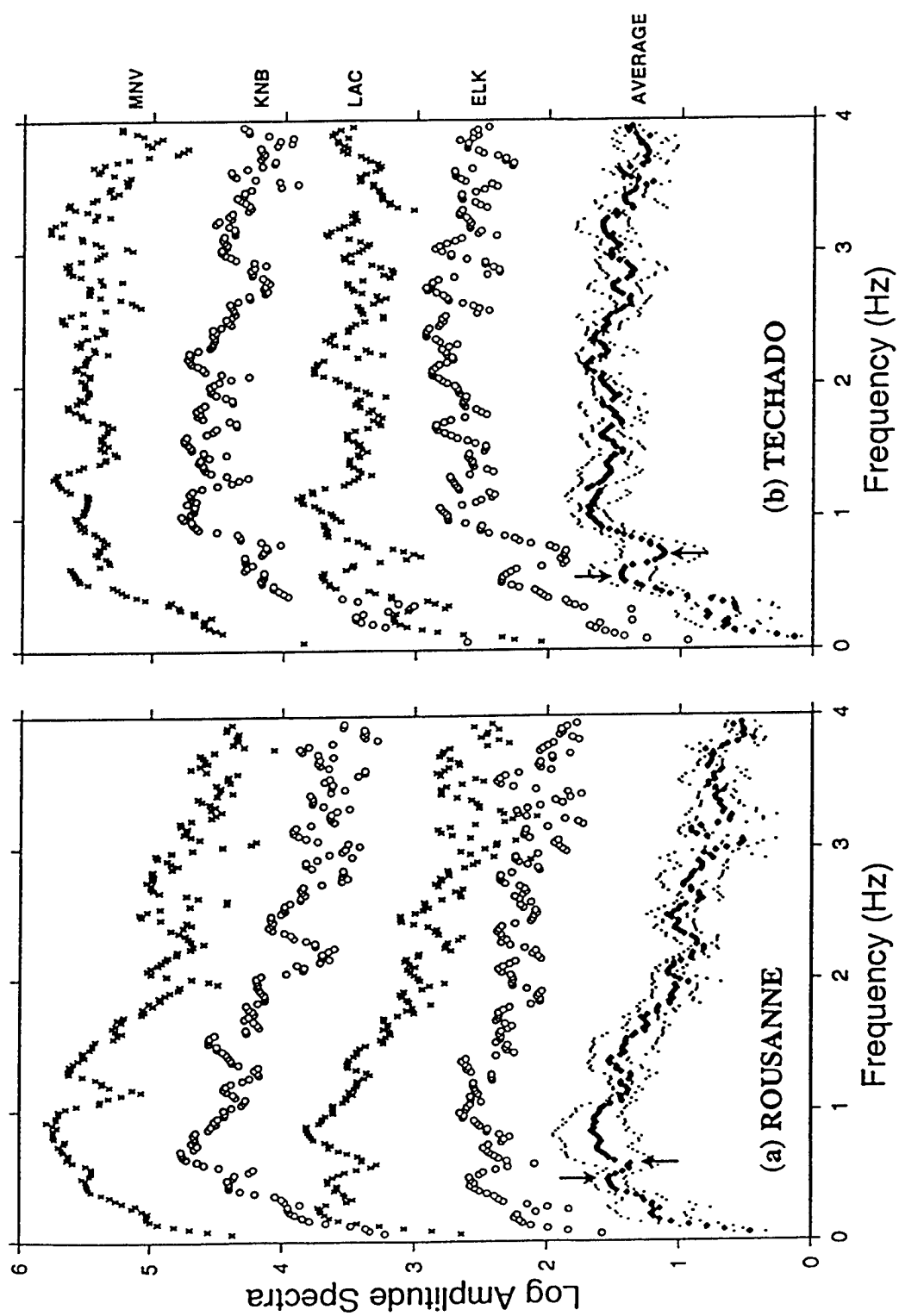


Figure 18. Single-station and network-averaged Lg spectra of closely-located shots Rousanne and Techado (overburied) indicating that both Lg(MAX) and Lg(NULL) frequencies of Rousanne are somewhat smaller than those of Techado. Lg (Rousanne) is relatively rich in low (less than about 2 Hz) frequency energy as compared to Lg (Techado).

communication) are shown in Figure 19. Severe attenuation of Rg for periods less than 1.2-1.3 sec and build-up of the shorter-period S arrivals, suggesting the scattering of shorter-period Rg into S or Lg, can be observed in the three Figures 19a, b, c. The group velocity of the scattered S wave is higher than that of Rg, indicating that scattering must take place near the source region. In each figure, a spectral null in Lg (velocity 3.0-3.5 km/sec) is observed at a period of about 0.7 sec.

Regional data from the JVE and several other East Kazakh nuclear explosions are also available at the broadband station WMQ (CDSN network) located at a distance of about 950 km from KTS. Spectral ratios of Lg from the JVE and the much smaller explosion of 12 March 1987, 87071 ($m_b = 5.31$), both recorded at WMQ (vertical component) so path effects are minimized, are shown in Figure 20a for Lg windows of 76.8, 51.2, and 25.6 sec, with seven, five, and three-point smoothing, respectively. Each of the three plots shows a spectral null at about 1.4 Hz, which corresponds to the null at period of 0.7 sec observed in the NRDC regional data. Furthermore, the plots suggest a maximum at a frequency of about 1.8 Hz, which may be due to the shallower CLVD source associated with Lg from the smaller explosion, 87071. Spectral ratios of Lg from the explosion of 3 April 1987 (87093), with $m_b = 6.12$ (somewhat larger and presumably deeper than the JVE) and the smaller explosion 87071, shown in Figure 20b, also indicate a spectral null at frequency of about 1.1 Hz, likely due to the CLVD source associated with the larger explosion 87093. Spectra of Lg (51.2 sec long windows and five-point smoothing) from seven explosions from the southwest region of KTS, recorded at WMQ and arranged in order of decreasing m_b , with Q correction from Xie *et al.* (1996), are shown in Figure 20c. The spectral nulls in Figure 20c, as indicated by arrows and selected on the basis of their prominence and consistency with those in Figures 20a and 20b, suggest a systematic increase in the Lg null frequency with decreasing m_b that should be associated with decreasing shot depth, and, therefore, with decreasing depth of the CLVD source.

As with the Yucca Flat explosions, synthetics were generated for vertically-oriented CLVD sources at several depths (Figure 21) by using the crustal structure model of Harvey (1993, Figure 15) who inverted full waveforms for structure and source parameters by using regional data recorded in Eastern Kazakhstan. In this model, the crust is 50 km thick and consists of nine layers with P-wave velocities varying over the range of about 4.60-7.15 km/sec. Note that Harvey's (1993) results are based on data collected at the NRDC station, KKL, about 250 km west-southwest of the Kazakh test site and that his observed Rg dispersion curves show significant (about 20%) lateral variation in group velocity (see his Figure 8). The synthetics in Figure 21 indicate that a spectral null at 1.4 Hz, as observed for the JVE, corresponds to a CLVD depth of about 200m. Unfortunately, the shot depths of Kazakh explosions used in this study are not known, although the JVE is believed to have a shot depth of about 600 m, or about three times the depth of the associated CLVD source.

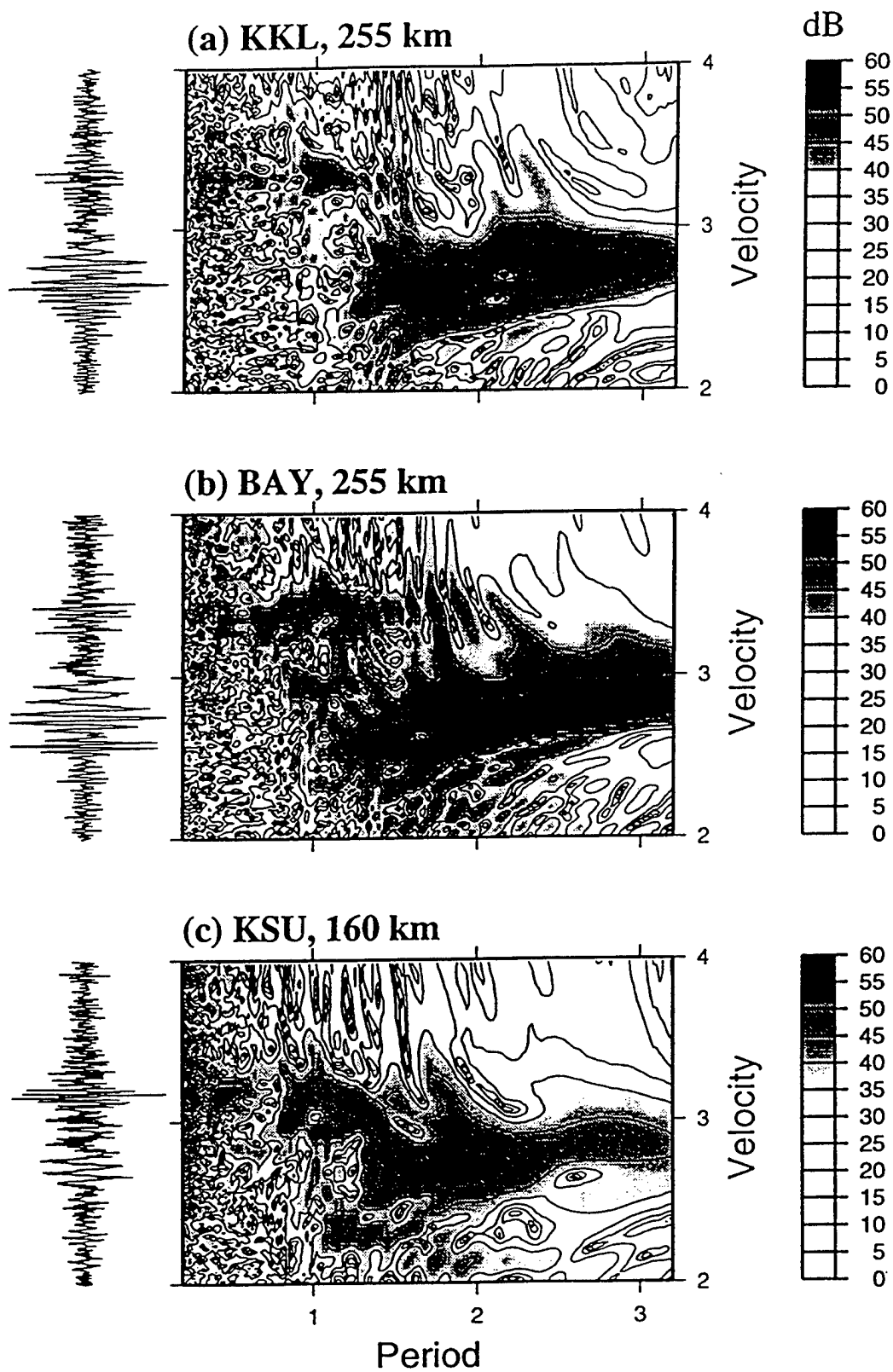


Figure 19. Narrow bandpass filtered records of the Soviet JVE shot of 14 September 1988 at the NRDC stations (a) KKL, (b) BAY, and (c) KSU, each indicating strong attenuation of Rg for periods less than about 1.2 sec and a spectral null in Lg at a period of about 0.6 to 0.7 sec.

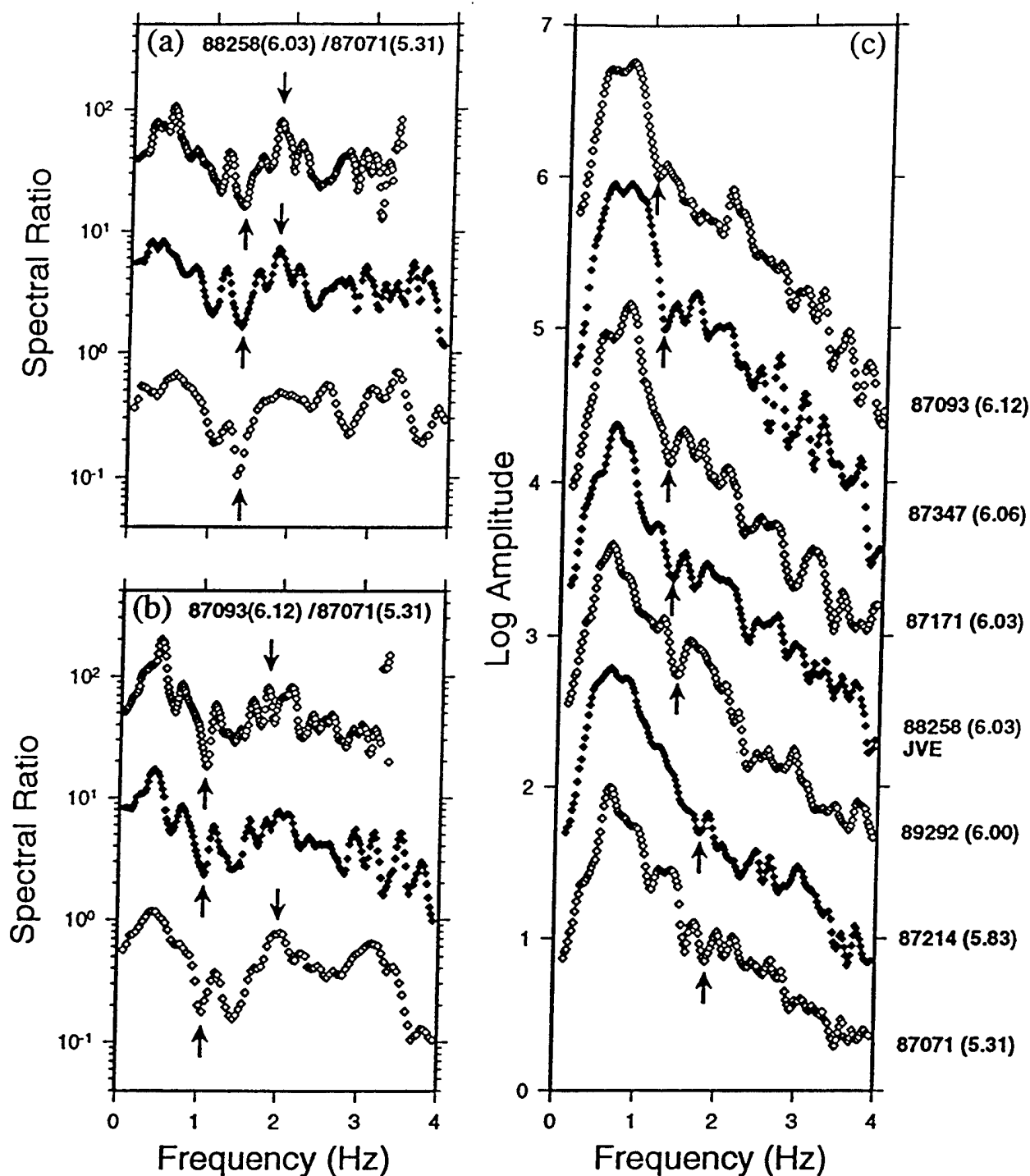


Figure 20. Lg spectral ratios for Kazakh shots recorded at WMQ (a) 88258(JVE)/87071 and (b) 87093/87071 for window lengths of 76.8 sec (top), 51.2 sec (middle), and 25.6 sec (bottom). Each of the three plots in (a) shows a spectral minimum at about 1.4 Hz and a maximum at about 1.9 Hz; plots in (b) indicate a spectral minimum at about 1.1 Hz. (c) Spectra of Lg (window length 51.2 sec) for seven Kazakh explosions suggesting a systematic increase in null frequency with decreasing m_b .

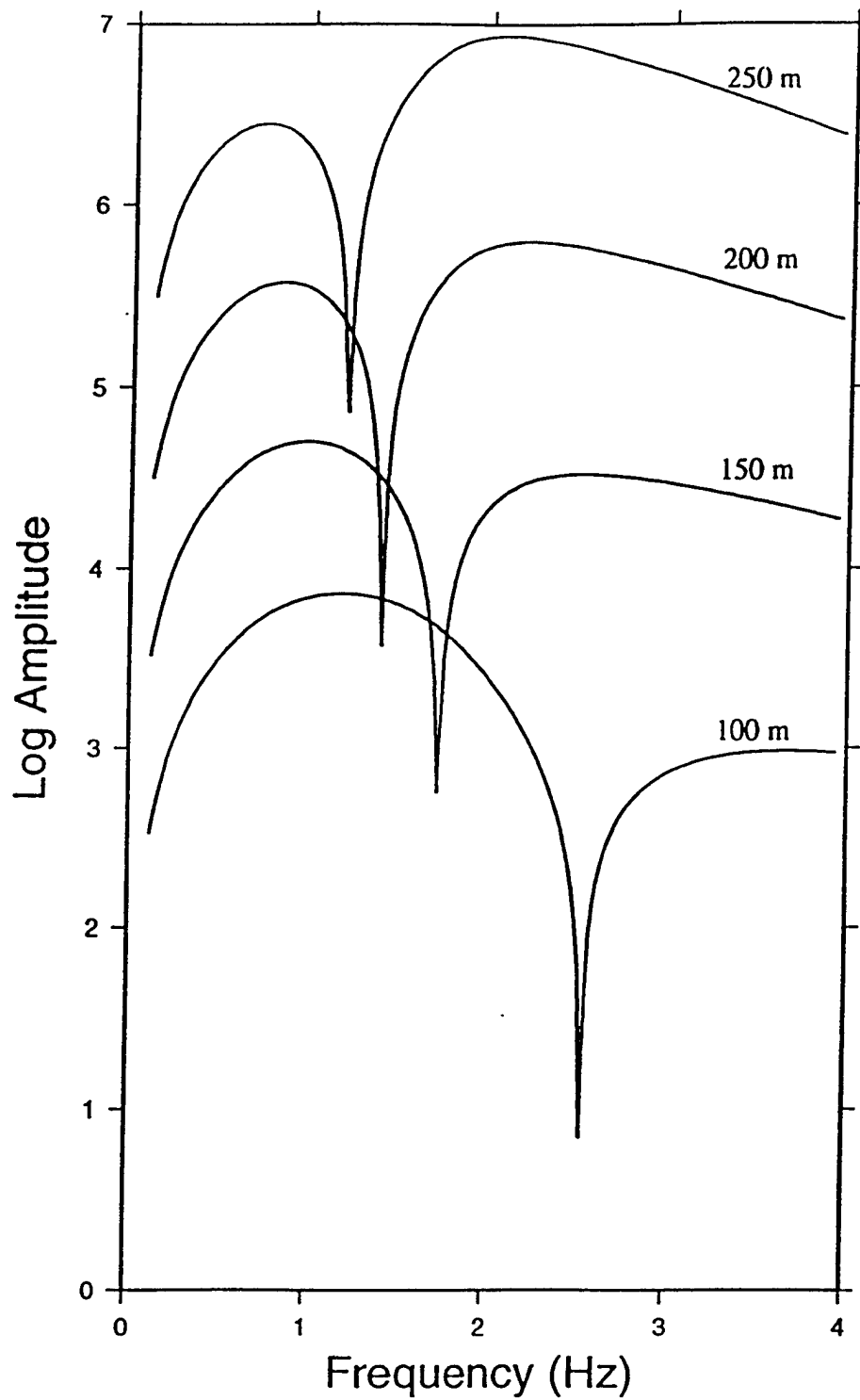


Figure 21. Spectra of Rg synthetics for CLVD source at four different depths for crustal velocity model of Eastern Kazakh derived by Harvey (1993). Note the steady increase in null frequency with a decrease in source depth, similar to the observations in Figure 20c.

3.2 Chinese Nuclear Tests at Lop Nor

There is considerable interest in nuclear explosions at the Lop Nor test site because, in contrast with the U.S., Russian, and French nuclear test sites, this test site has been active as recently as July 1996. Analysis of Lg from several Lop Nor shots recorded at stations belonging to the Kyrghizstan Network (KNET) showed distinct low-frequency nulls at most stations (Gupta, 1996). Results from 5 shots recorded at the vertical-component broadband high gain (20 samples/sec) KNET station AAK, at epicentral distances of about 1200 km, are shown in Figure 22. The following five shots were used: (1) May 21, 1992 (92142), $m_b = 6.5$, (2) 25 September 1992 (92269), $m_b = 5.0$, (3) 5 October 1993 (93278), $m_b = 5.9$, (4) 15 May 1995 (95135), $m_b = 6.1$, and (5) 17 August 1995 (95229), $m_b = 6.0$. For AAK, the instrument response is flat to ground velocity between 0.004 and 6 Hz. The individual vertical-component Lg (window length 51.2 sec) spectra, with Q correction from Xie *et al.* (1996), shown in Figure 22a, and the spectral ratios (Figure 22b) indicate the same distinct spectral nulls and a general increase in frequency with decrease in magnitude. Since smaller magnitude explosions are generally associated with shallower shot depths, these results are similar to those from the Yucca Flat explosions (Figure 7) and support the hypothesis of the scattering of Rg, originating from a CLVD source, contributing to the low-frequency Lg.

Matzko (1994) provided a detailed description of the geological structure and rock types at the test site. According to him, the largest shot of 21 May 1992 was emplaced in a shaft over 900 m deep and had a yield of about 1 megaton. Furthermore, the nuclear shots are fired in either vertically drilled shafts or horizontal tunnels, but there is hard rock coupling in both areas and the Lop Nor test site is, in several respects, more similar to the KTS than the NTS. This provides a possible explanation for the similarity of the observed Lg null frequencies at Lop Nor test site (Figure 22) and the KTS (Figure 20) for shots with similar magnitudes.

3.3 Azgir PNE at ILPA Array

Regional data from a Soviet Peaceful Nuclear Explosion (PNE) in salt on 18 December 1978 ($m_b = 5.9$) at Azgir (north of the Caspian Sea) are available at the ILPA array (Figure 23); see Grant *et al.* (1996). The vertical-component waveforms at two locations, IR1 and IR7 show considerably less energy in Lg than in Sn. A possible reason for the diminished Lg is the presence of mostly ocean-like path through the Caspian Sea. Spectra of Lg and Sn windows, each 51.2 sec long and starting at velocities of 3.5 and 4.3 km/sec, respectively, are also shown in Figure 23. Not only the Lg spectra but also the Sn spectra indicate a prominent spectral null at a frequency of about 1.1 Hz. It appears, therefore, that the source of the low frequency energy in the large Sn phase is the same as in Lg and the low-frequency energy in both phases originated from the near-source scattering of explosion-generated Rg into S.

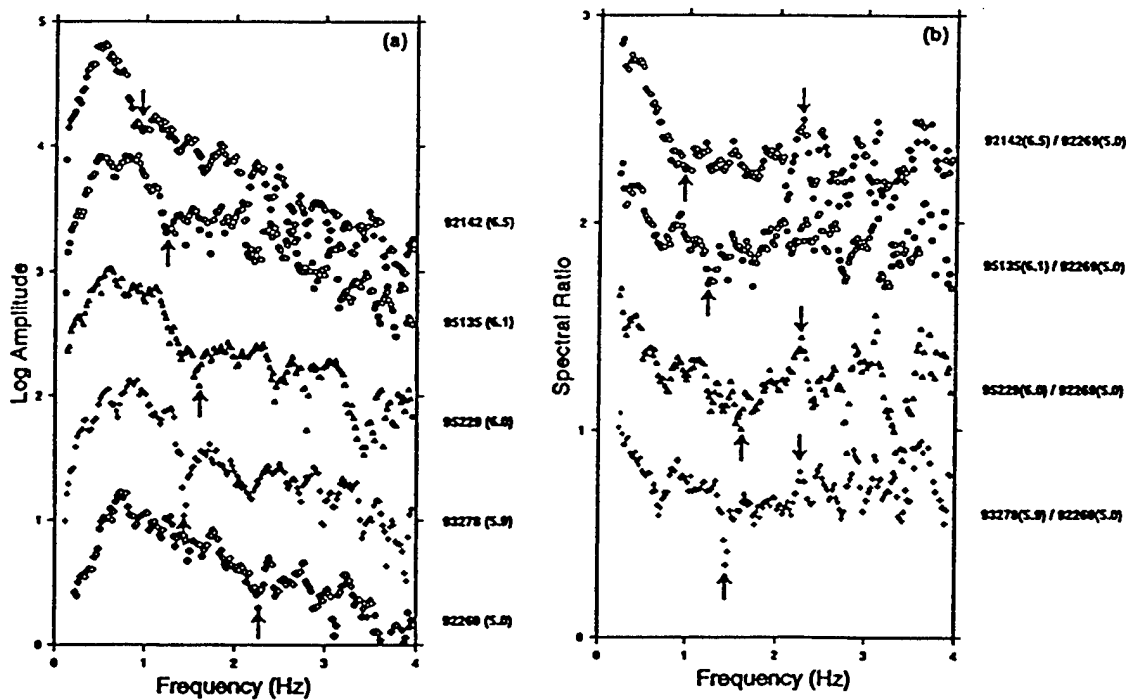
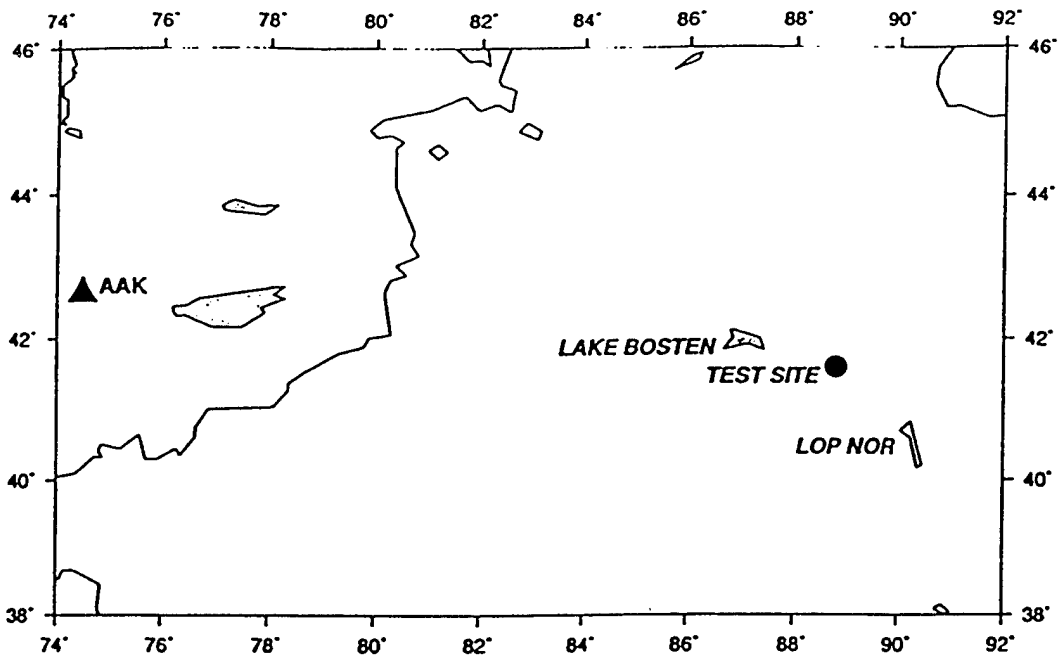


Figure 22. Results from five Lop Nor shots recorded at AAK, about 1200 km west of the test site. Both (a) spectra of Lg (window length 51.2 sec) and (b) spectral ratios indicate the same spectral nulls (indicated by arrows) and a general increase in null frequency with decrease in m_b .

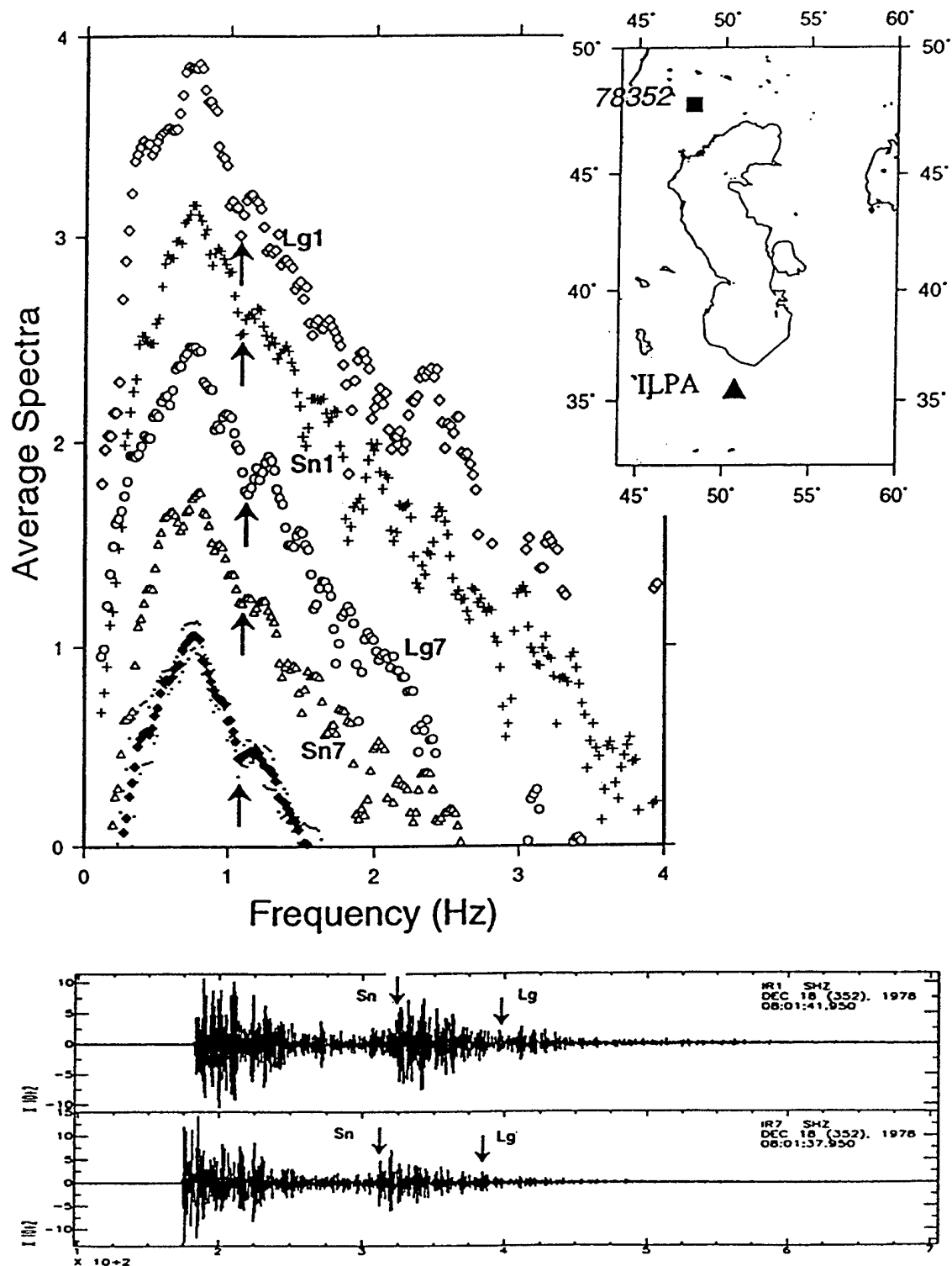


Figure 23. Waveforms and spectra of Lg and Sn from the Azgir PNE (78352) recorded at two ILPA sensors. The four spectra and their average indicate a distinct null at about 1.1 Hz, perhaps due to near-source scattering of explosion-generated Rg into S which contributes to both Sn and Lg.

4. HIGH FREQUENCY S AND Lg FROM NUCLEAR EXPLOSIONS

4.1 Importance of High-Frequency S or Lg

It is important to understand the origin of high frequency S from explosions so that the scope and limitations of the regional discriminant Lg/P, often reported to perform better at higher frequencies, are clearly known. The high frequency S or Lg from explosions may be due to the generation of new cracks generated by a tamped explosion (Blandford, 1995a, b), but the evidence presented so far has probably not been fully convincing (Murphy and Barker, 1995). We therefore test Blandford's (1995a, b) hypothesis by examining data from several sources.

4.2 Comparison of Seismic Data from Tamped and Decoupled Explosions

4.2.1 Analysis of Local Data from Azgir Tamped and Decoupled Explosions

We analyzed local data, made available by Adushkin *et al.* (1992), from a pair of explosions detonated in a salt dome. On 22 December 1971, a 64-kt tamped explosion was fired at a depth of 987 m and, on 29 March 1976, a smaller (about 8 kt) explosion was detonated in the cavity. Since we are interested in a comparison of P and S spectra, it is important that both P and S phases be available for both events. With this criterion, data from only one station, AZG08, were found to be suitable. Bandpass filtering of corrected data from this station by Blandford (1995a) showed the amplitude ratio P/S to be much larger for the decoupled shot. Our analysis of the same data, showing spectral ratios P/S for the two shots (Figure 24a) and coupled/decoupled P and S (Figure 24b) indicate significantly larger S than P for the coupled shot at higher (above 5 Hz) frequencies. These results are in agreement with Blandford's (1995a, b) hypothesis that the higher frequency S comes from cracks generated by the tamped explosion because a decoupled shot will not cause cracks (a non-linear effect).

4.2.2 Re-examination of Salmon/Sterling Data at Local Distances

Analysis of Salmon and Sterling data recorded at three common stations (10S, 20S, and PL-MS) by Blandford and Woolson (1979) and Gupta *et al.* (1986) found relatively greater decoupling of Sterling for S or Lg than for P at higher frequencies. Murphy and Barker (1995) also analyzed Salmon and Sterling data at several local distances, including 10S (16 km), 20S (32 km), and PL-MS (27 km). They found that the filtered signals at 20S and PL-MS showed larger S/P ratios for Salmon than for Sterling, in agreement with Blandford's hypothesis. However, their results for 10S, based on recording from a single sensor out of a cluster of closely spaced 12 instruments which recorded both Salmon and Sterling, did not show any obvious differences between the filtered signals for the two events (see Murphy and Barker, 1995, Figure 19).

In this study, we examined all available instruments providing data for both Salmon and Sterling at 10S; only eight (numbered 5 through 12) were found to be suitable. The raw (unfiltered) data for the two events are shown in Figures 25 through 28 for these eight vertical-component sensors. Note that although the eight sensors are close to each other, the waveforms

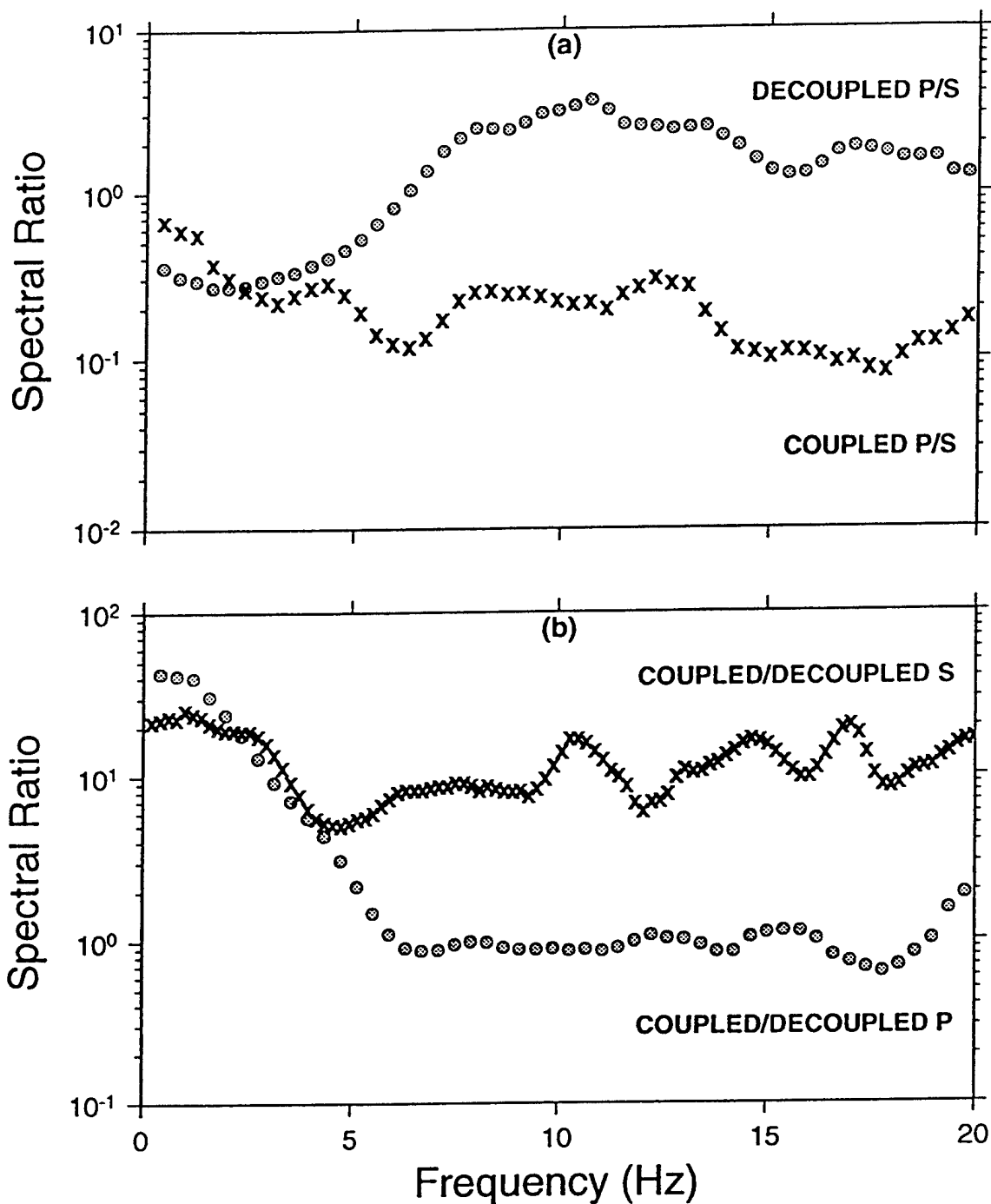


Figure 24. Spectral ratios derived from the coupled (tamped) and decoupled Azgir explosions of 22 December 1971 and 29 March 1976, respectively recorded at a common station at a distance of about 18 km. Since both figures (a) and (b) indicate significantly larger S than P for the coupled shot at higher (above 5 Hz) frequencies, these results support Blandford's hypothesis regarding the generation of high frequency S from explosions.

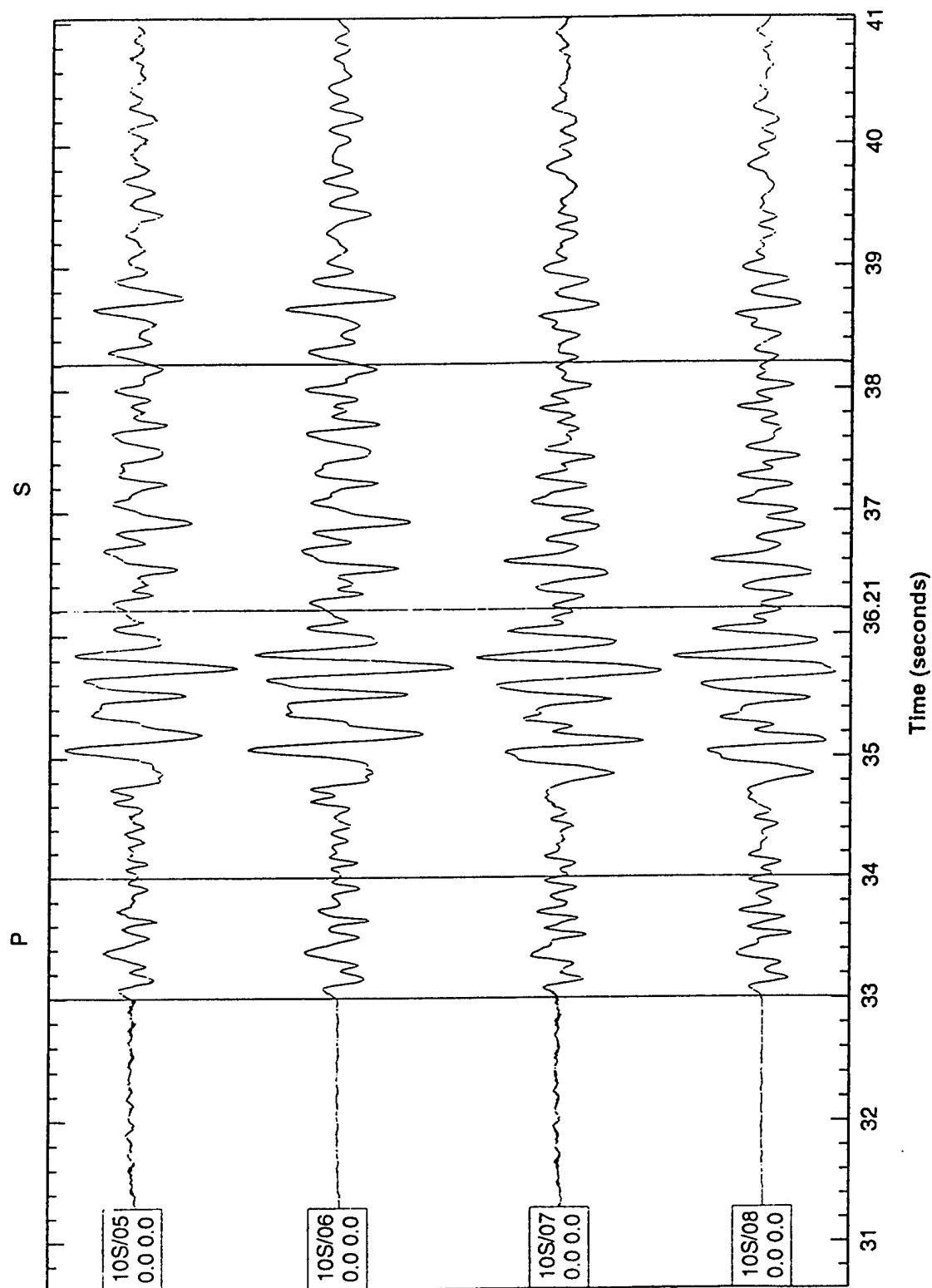


Figure 25. Raw (unfiltered) data for Salmon recorded at 10S at a distance of 16 km on sensors numbered 5 through 8.

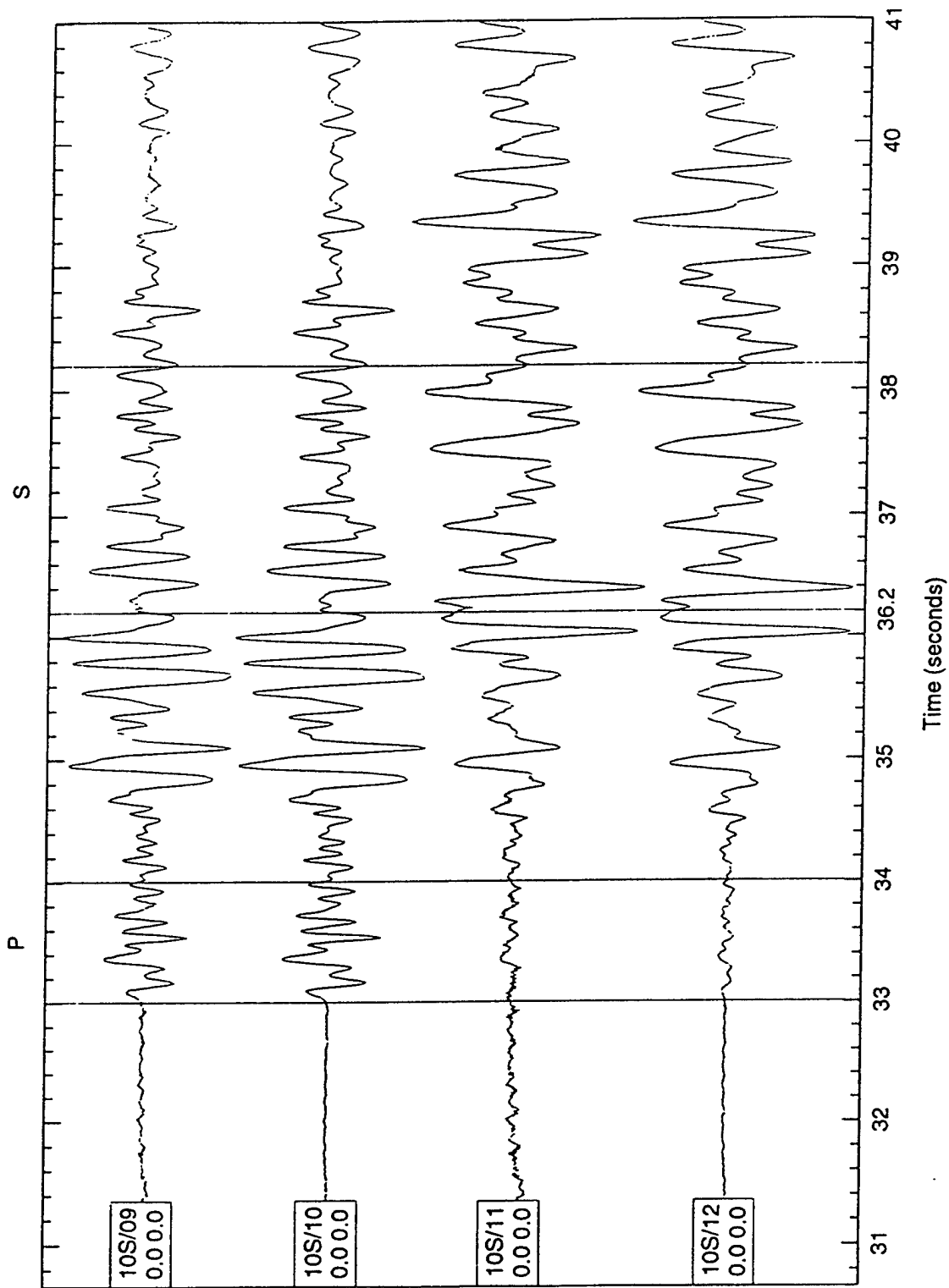


Figure 26. Raw (unfiltered) data for Salmon recorded at 10S at a distance of 16 km on sensors numbered 9 through 12.

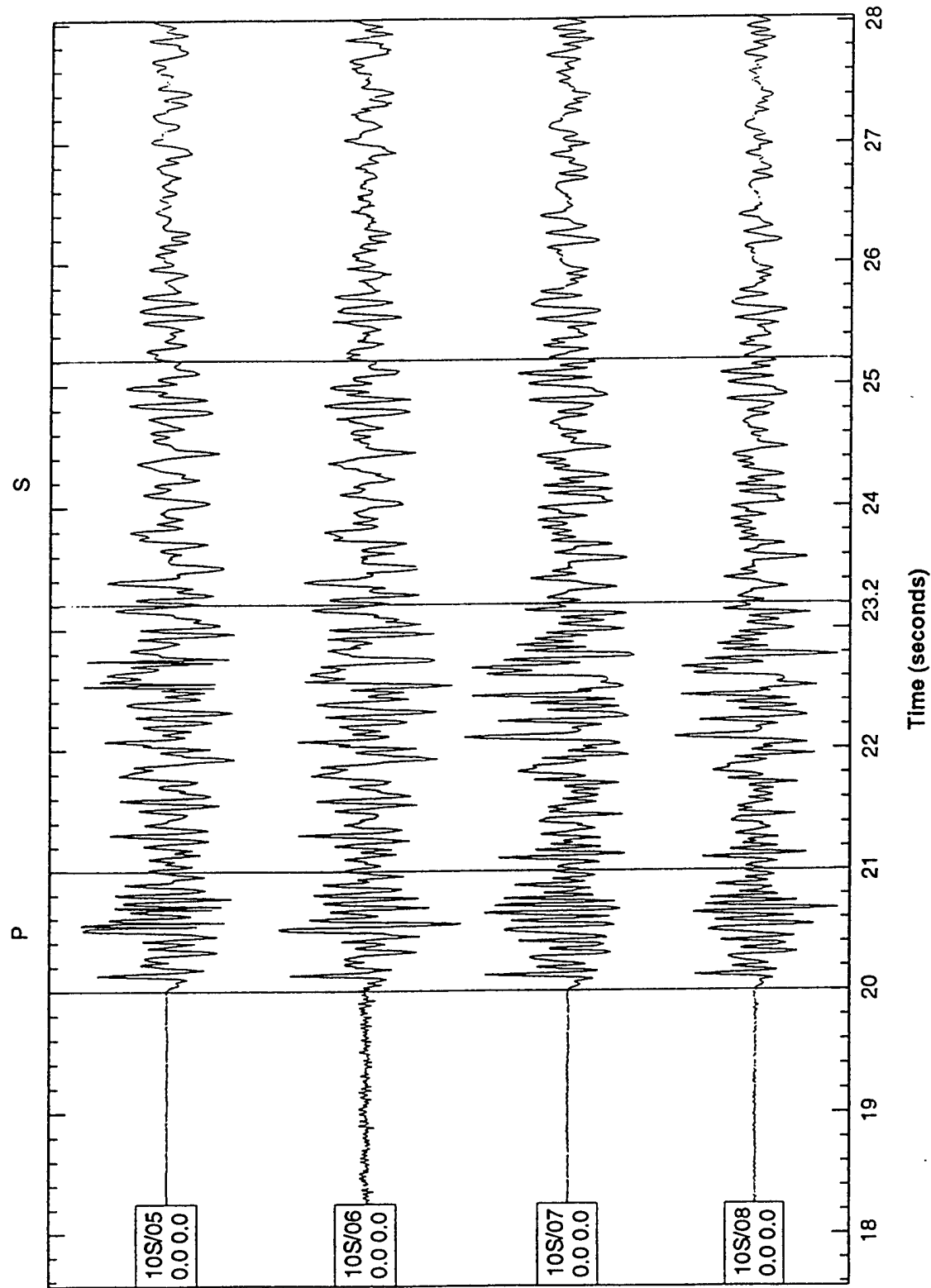


Figure 27. Raw (unfiltered) data for Sterling recorded at 10S at a distance of 16 km on sensors numbered 5 through 8.

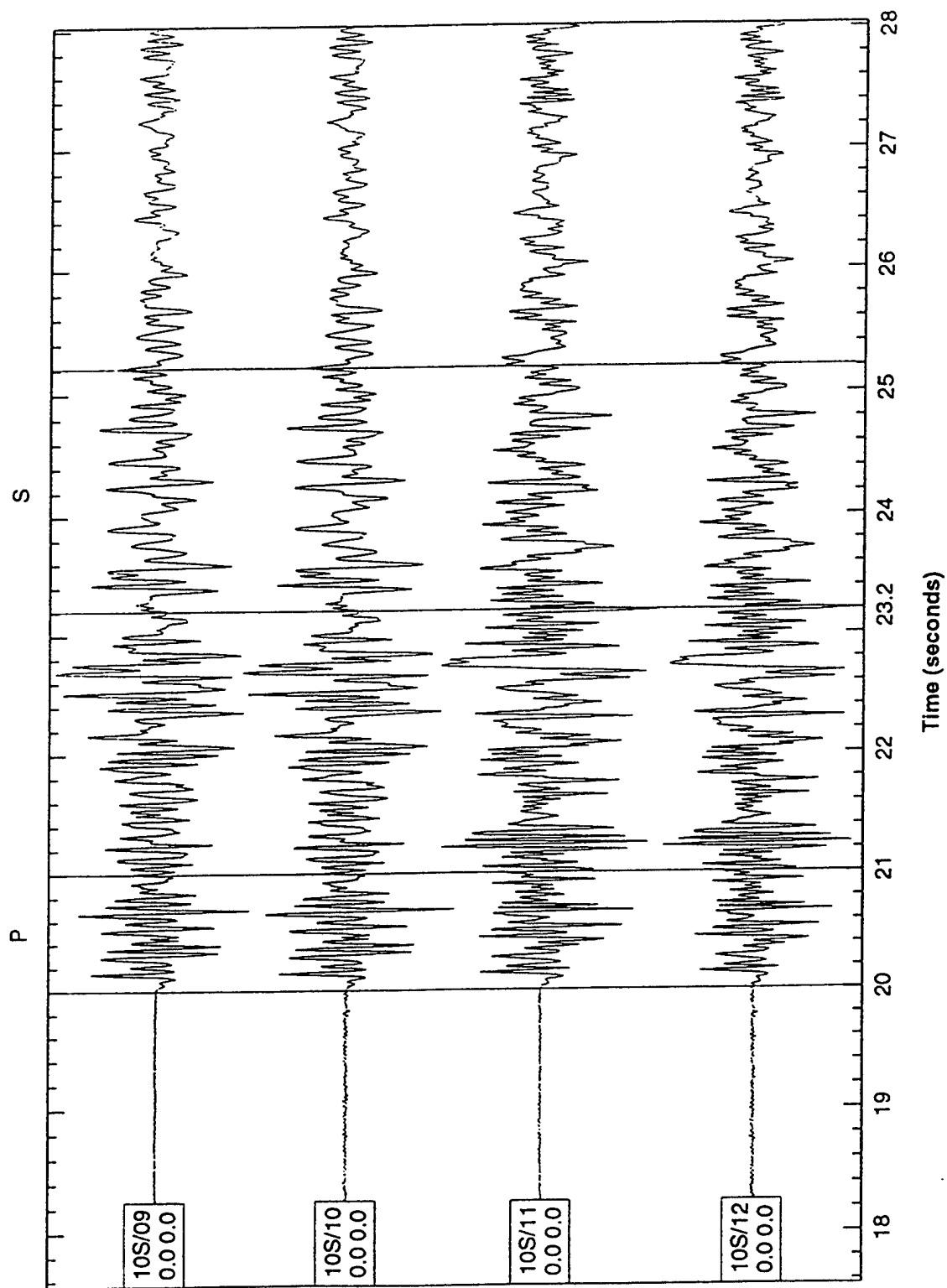


Figure 28. Raw (unfiltered) data for Sterling recorded at 10S at a distance of 16 km on sensors numbered 9 through 12.

for each event show significant differences from one sensor to another. A possible reason is site effects. In Figures 26 and 28, the data from Sensor 9 are the same as those used by Murphy and Barker (1995, Figure 19). The beginning of the P and S windows are the same used by Murphy and Barker (1995) and vertical lines have been drawn to indicate window lengths of 1 and 2 sec for P and S, respectively. Bandpassed outputs for frequency ranges of 12-16, and 16-20 Hz for the two events (Salmon in red and Sterling in black) are shown in Figures 29 through 32, in which the peak amplitudes in the P windows for the two events have been adjusted to be the same. This means that amplitudes in only the S windows need to be examined for comparing the high frequency amplitudes for the two events. Results from Sensor 9 indicate no significant differences in the S windows for the two sources, as noted by Murphy and Barker (1995). However, most other sensors (especially Sensors 6, 7, 8 in Figure 29, Sensors 11 and 12 in Figure 30, and Sensor 12 in Figure 32) show the S wave peak amplitudes to be significantly larger for Salmon than for Sterling. Note that results from none of the 8 sensors show the S wave amplitudes for Salmon to be smaller than for Sterling. It seems therefore that most data from 10S show results consistent with Blandford's hypothesis. It will be interesting to find out in the future why different sensors show considerably different results; possible reasons are site effects and radiation patterns, which are generally believed to be more variable at higher frequencies.

4.3 High Frequency Lg from Nuclear Explosions Recorded at Regional Distances

4.3.1 Analysis of Regional Data from NTS Explosions

We examined the origin of high frequency S from explosions by analyzing the regional phases Pn, Pg, and Lg from several closely-located and other Yucca Flat (NTS) explosions recorded at common stations so that path effects are minimized. Figure 33 shows locations of over 100 explosions, including 13 which provided high frequency data with fairly good signal/noise ratio at the four stations of the LLNL network. Estimated damage zones for these 13 and earlier shots with epicenters within 500 m of them are indicated by circles around their epicenters. The radius of damage zone is assumed to be three times the explosion cavity radius; a conservative estimate on the basis of Johnson's (1997) study of the damage zone associated with the chemical explosion (an overburied shot) of the Non-Proliferation Experiment. Cavity radii for various shots are calculated by using the empirical relationships developed for NTS shots by Closmann (1969). As shown in Figure 33, at least two large earlier shots were so close to Dalhart that their damage zones probably produced a highly fractured region around its shot point which could have prevented or at least inhibited the growth of new cracks, presumed to be responsible for the higher frequency S. A comparison of the spectral ratios Pg (12.8 sec)/Lg (25.6 sec) and Pn (3.2 sec)/Lg (25.6 sec) from Dalhart, with those from the earliest shot Hearts, is shown in Figure 34. Nearly all stations and their average show significant differences at higher (above 8-10 Hz) frequencies. Similar comparison between Hearts and Baseball, with their damage zones well separated from each other, showed no such differences. A possible explanation for the relative deficiency of higher frequency Lg from Dalhart is lack of new explosion-generated cracks because its shot-point lies within the previously damaged zone.

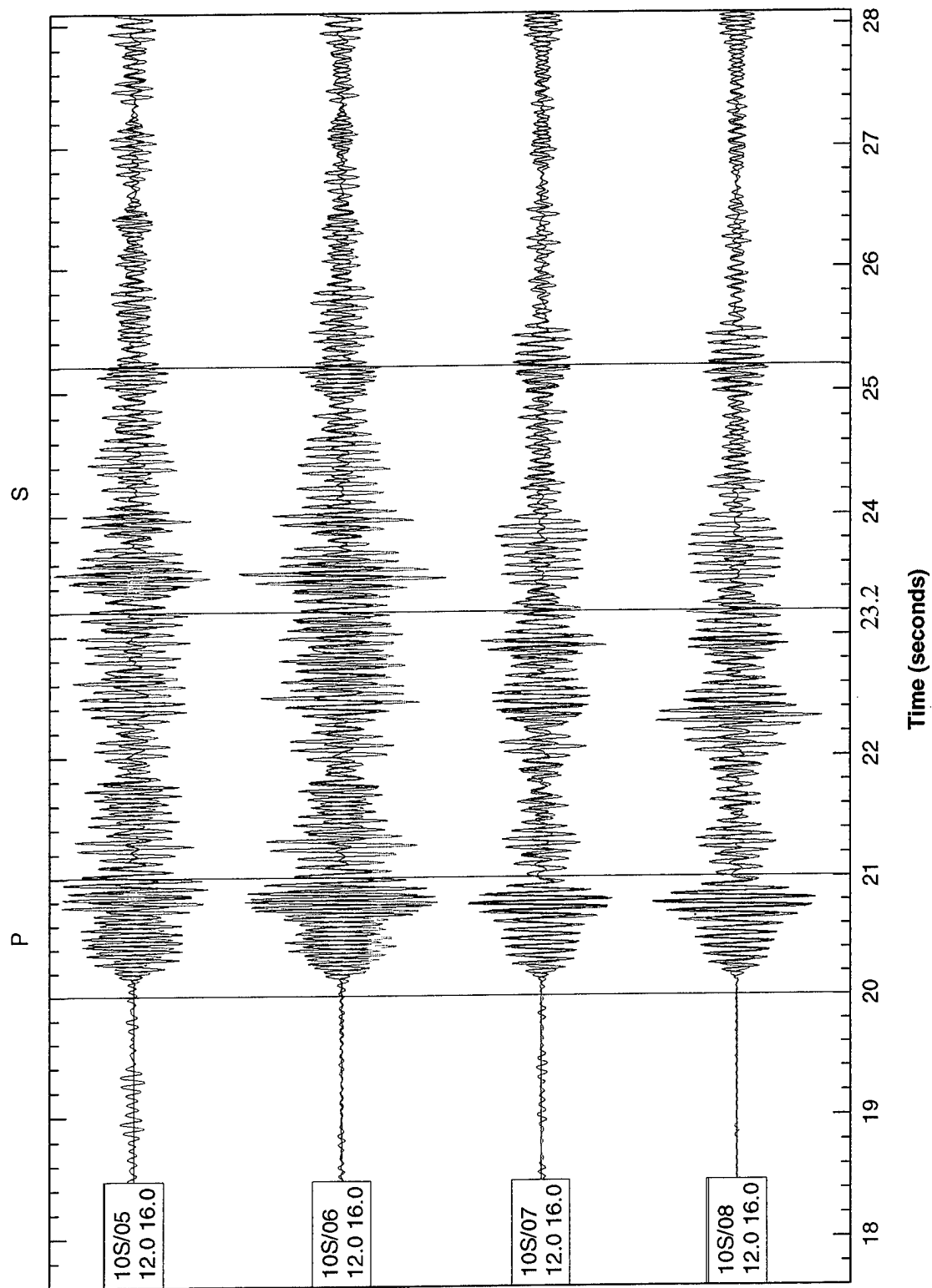


Figure 29. Bandpassed outputs for 12-16 Hz for Salmon (red color) and Sterling recorded at 10S on sensors numbered 5 through 8.

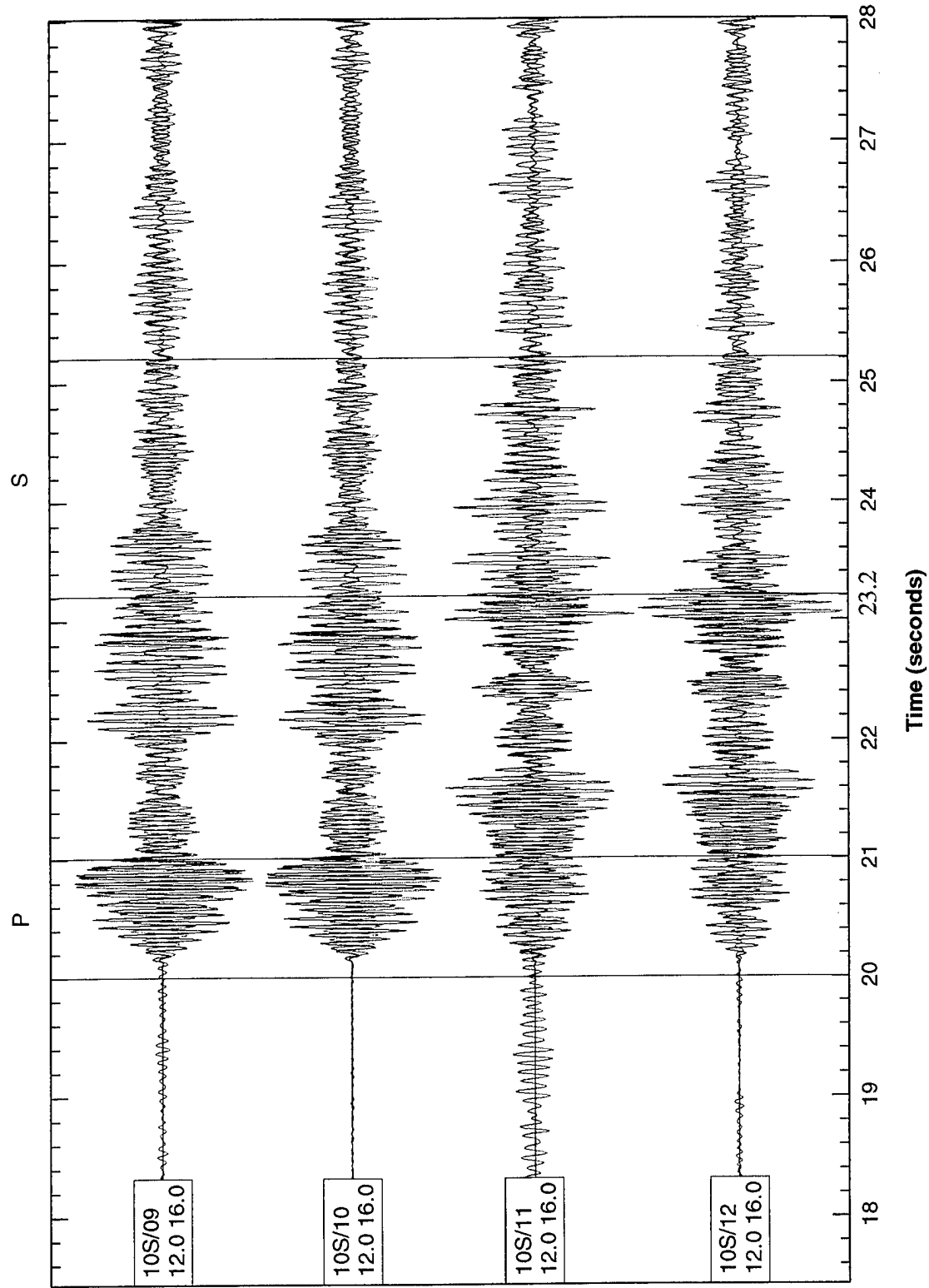


Figure 30. Bandpassed outputs for 12-16 Hz for Salmon (red color) and Sterling recorded at 10S on sensors numbered 9 through 12.

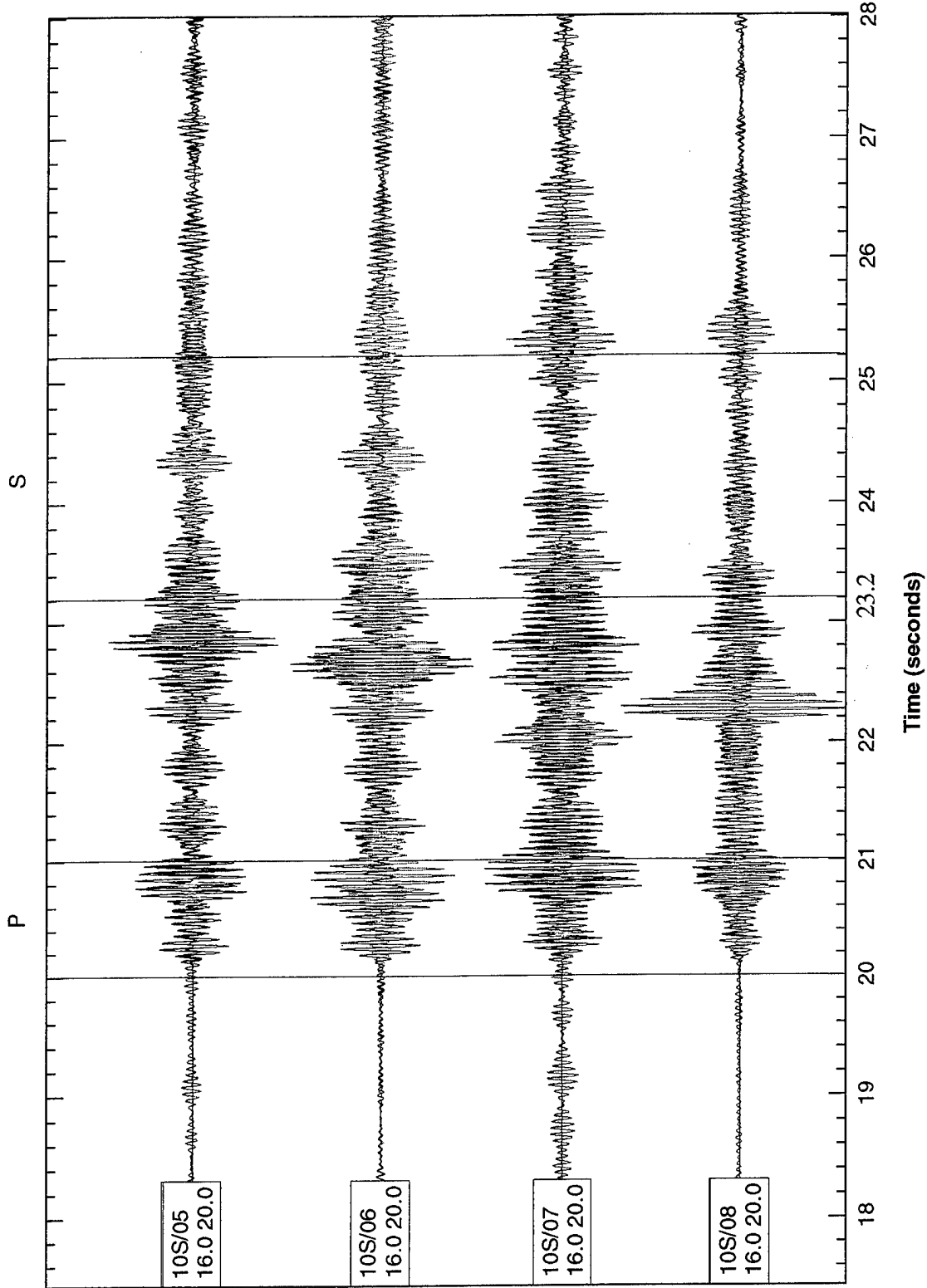


Figure 31. Bandpassed outputs for 16-20 Hz for Salmon (red color) and Sterling recorded at 10S on sensors numbered 5 through 8.

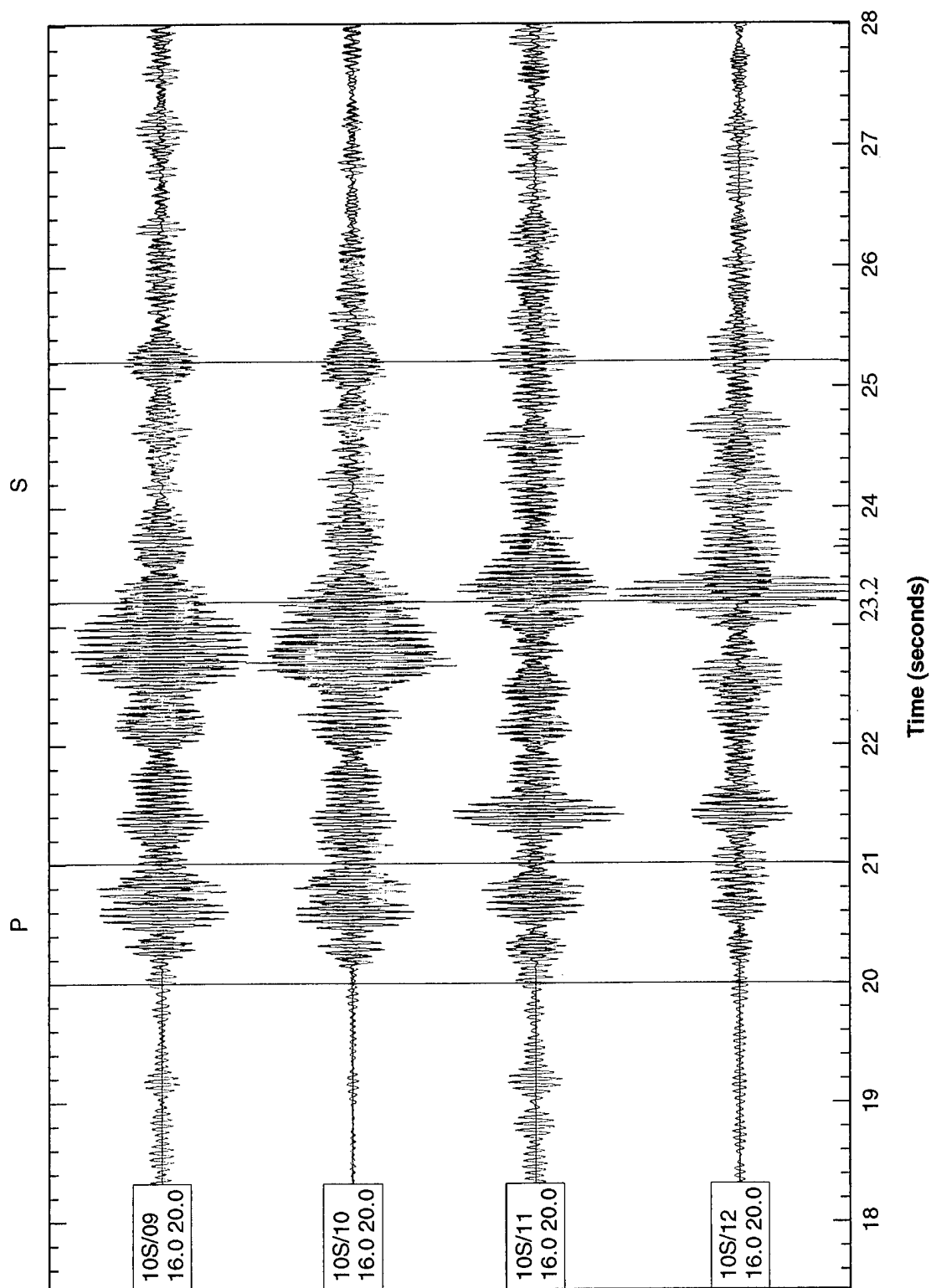


Figure 32. Bandpassed outputs for 16-20 Hz for Salmon (red color) and Sterling recorded at 10S on sensors numbered 9 through 12.

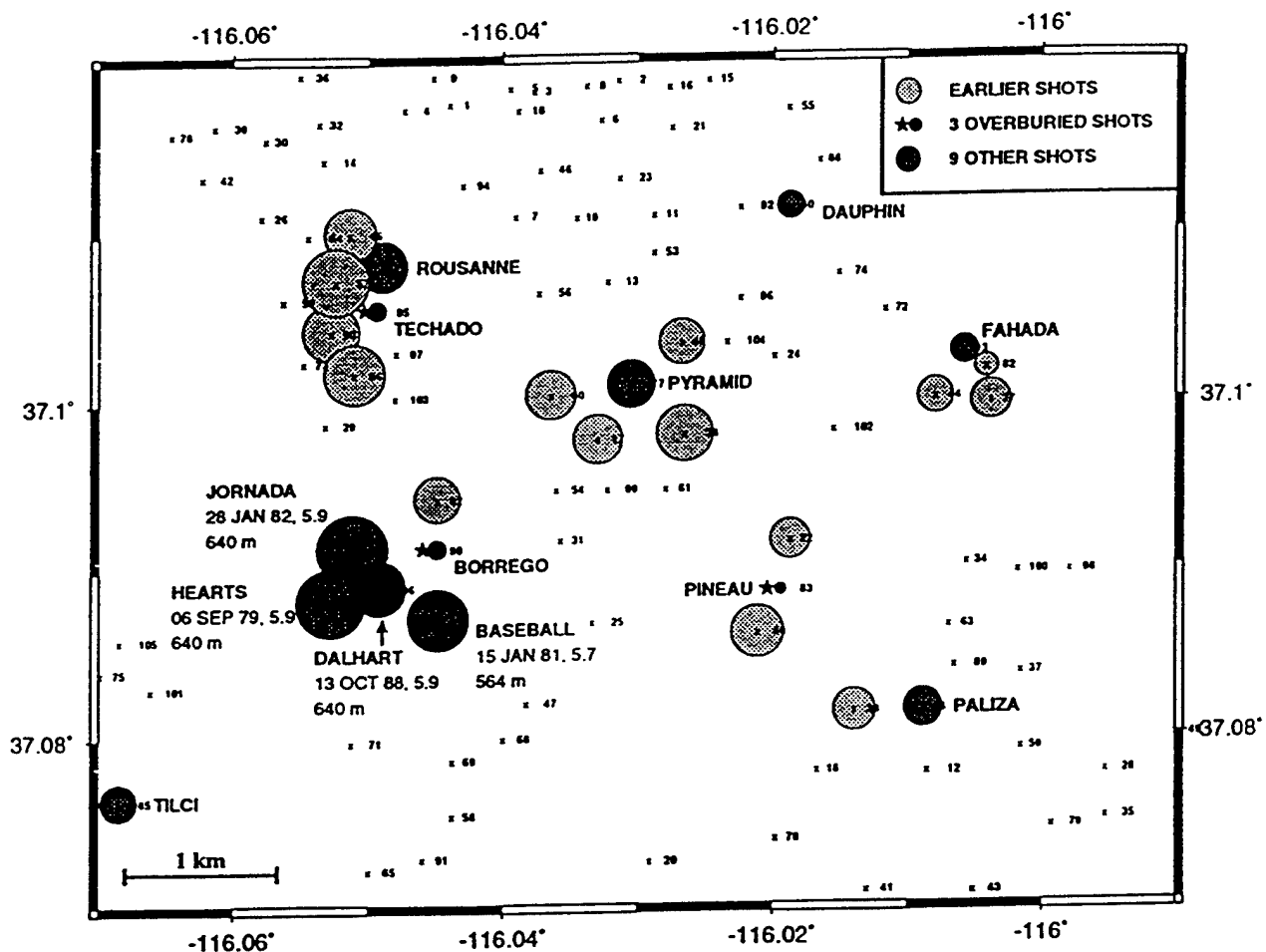


Figure 33. Location map of over 100 explosions in the northern Yucca Flat region showing the estimated damage zones for the Yucca Flat explosion, Dalhart and many other shots. Dalhart is nearly surrounded by at least two (probably three) large earlier shots with their damage zones intersecting its shot point.

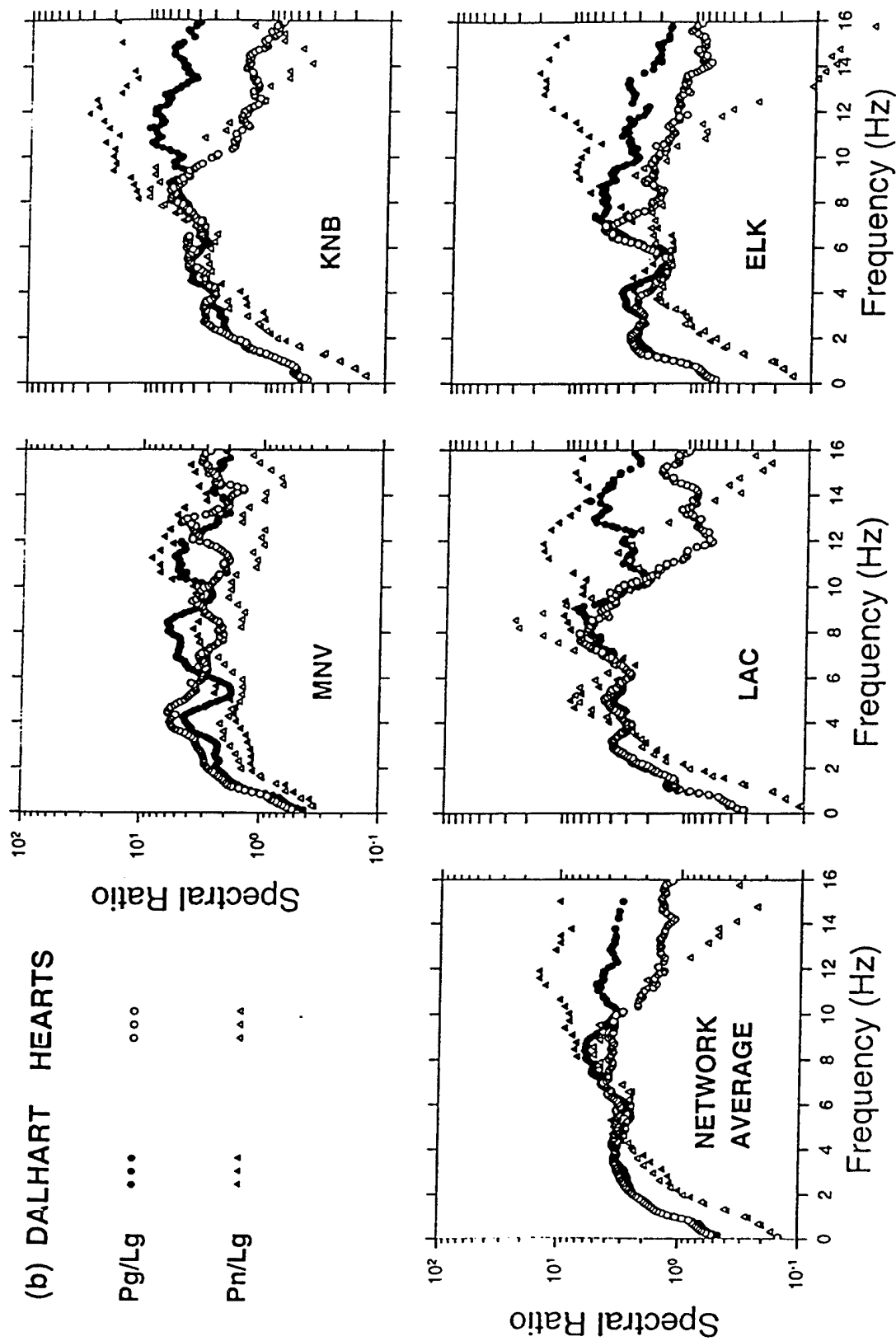


Figure 34. Network-averaged and single-station spectral ratios of Pg/Lg and Pn/Lg indicating large differences at higher (above 8-10 Hz) frequencies between Dalhart and Hearts. The relative deficiency of higher frequency Lg from Dalhart is probably due to lack of new explosion-generated cracks because of the damage zones from earlier shots extending up to its shot point.

Evidence supporting a cracking mechanism also comes from a comparison of deeper and shallower shots for their frequency dependence of Pg/Lg . We analyzed the LLNL network data from nine explosions, obtained by excluding the three overburied shots and Dalhart from the 13 explosions specified by name in Figure 33. Linear regression of average Pg/Lg versus shot depth for several frequency passbands, each about 2 Hz in width, were carried out; an example is shown in Figure 35a. The average values for depths of 640 and 300m, obtained from the linear regressions, were used to obtain a plot of log average Pg/Lg versus center frequency. As suggested by the results in Figure 35b, differences in Pg/Lg due to variation in shot depth are larger for both high (greater than 6 Hz) and low (less than 4 Hz) frequencies. The increasing difference at higher frequency may be due to the generation of high frequency S by explosion-generated cracks that are inhibited by overburden pressure and contribute more to the higher frequencies, as suggested by Blandford (1995a,b). The increase in Pg/Lg for lower (less than 4 Hz) frequencies is probably due to Rg being larger for shallower depths, playing a more dominant role at lower frequencies, and the scattering of Rg into S and Lg.

4.3.2 Results from Analysis of High Frequency Data from Station NLS

We also analyzed the high frequency (50 samples/sec) data from Dalhart, Hearts, and several other Yucca Flat explosions recorded at the station NLS belonging to the SNL network. The results are shown in Figures 36 and 37. The results in Figure 36 are obtained by averaging the spectral ratios over successive frequency bands about 4 Hz wide. The Pn, Pg and Lg windows are 5.12, 10.24 and 20.48 sec, respectively, whereas Lg1 denotes the first 10.24 sec of the Lg window and Lg2 the next 10.24 sec. The results are similar to those in Figure 34; the relative deficiency of higher frequency Lg from Dalhart is again probably due to lack of new explosion-generated cracks because of its shot point lying within the damage zones of earlier shots including Hearts. It is interesting to note that a comparison of spectral ratios $Pg/Lg1$ and $Pg/Lg2$ shows somewhat larger higher-frequency separation between Dalhart and Hearts for the later Lg window. A possible reason for this is that most of the higher frequency S generated by the creation of new cracks is somewhat delayed.

The NLS data are also used to obtain a comparison of deeper and shallower shots for their frequency dependence of Pg/Lg by using data from ten Yucca Flat explosions. The results, shown in Figure 37, are similar to those in Figure 35, and once again support Blandford's (1995a,b) hypothesis regarding the influence of overburden pressure on the generation of new cracks which contribute to the higher frequency S.

4.3.3 Analysis of Regional Data from Kazakh Explosions

High-frequency data from 14 KTS shots recorded by the short-period (sampling rate 40 samples/sec), vertical-component instrument at WMQ were analyzed to obtain a comparison of deeper and shallower shots for their frequency dependence of Pn/Lg . Most of these explosions were the same as used in Gupta *et al.* (1992, Table 1a). Since the shot depths for KTS shots are not known, the comparison actually involved average values for large and small magnitude shots, assuming that the larger magnitude shots are deeper than the smaller magnitude shots.

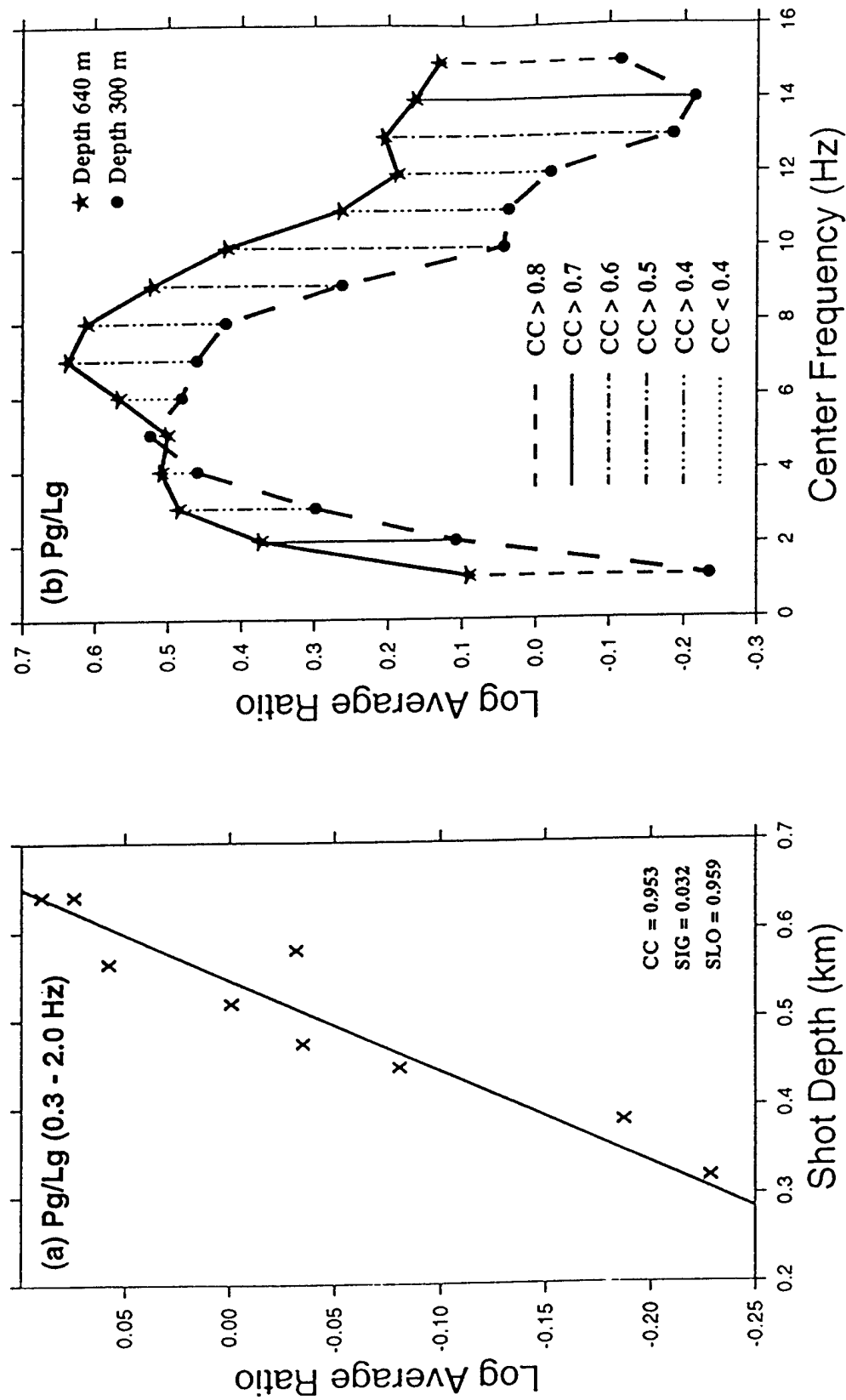


Figure 35. Network-averaged spectral differences in Pg/Lg for shallow (depth 300 m) and deep (depth 640 m) Yucca Flat explosions obtained by linear regression of average ratio versus shot depth for nine shots for several passbands; an example is shown in (a). Differences in Pg/Lg appear to be larger for both high (greater than 6 Hz) and low (less than 4 Hz) frequencies. The increasing difference at higher frequency may be due to the generation of high frequency S by explosion-generated cracks that are inhibited by overburden pressure, whereas that at lower frequency is probably due to scattering of explosion-generated Rg into S.

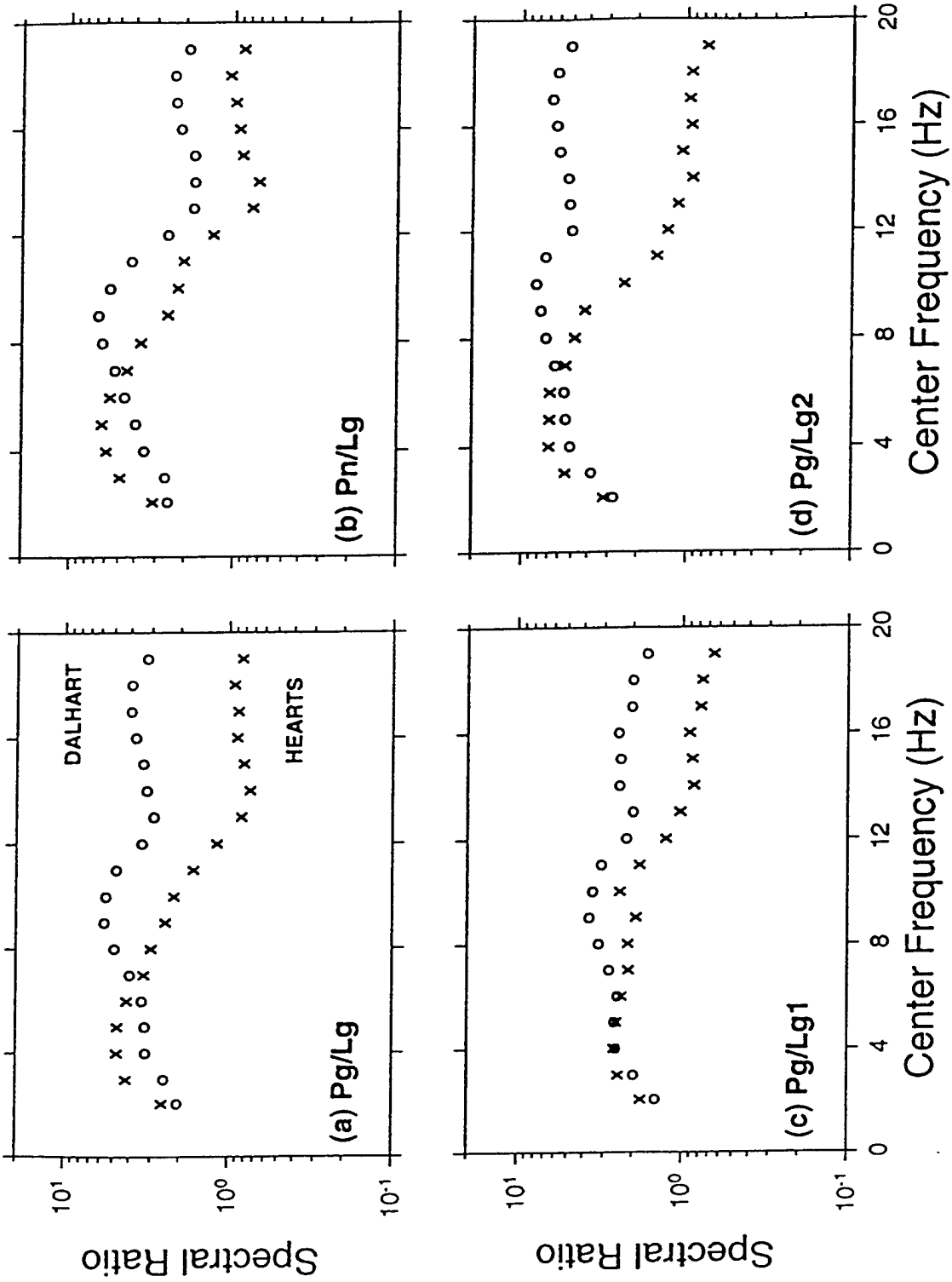


Figure 36. Similar to Figure 34 for station NLS showing spectral ratios of (a) Pg/Lg, (b) Pn/Lg, (c) Pg/Lg1, and (d) Pg/Lg2, all indicating significant differences at higher (above about 8 Hz) frequencies between Dalhart and Hearts.

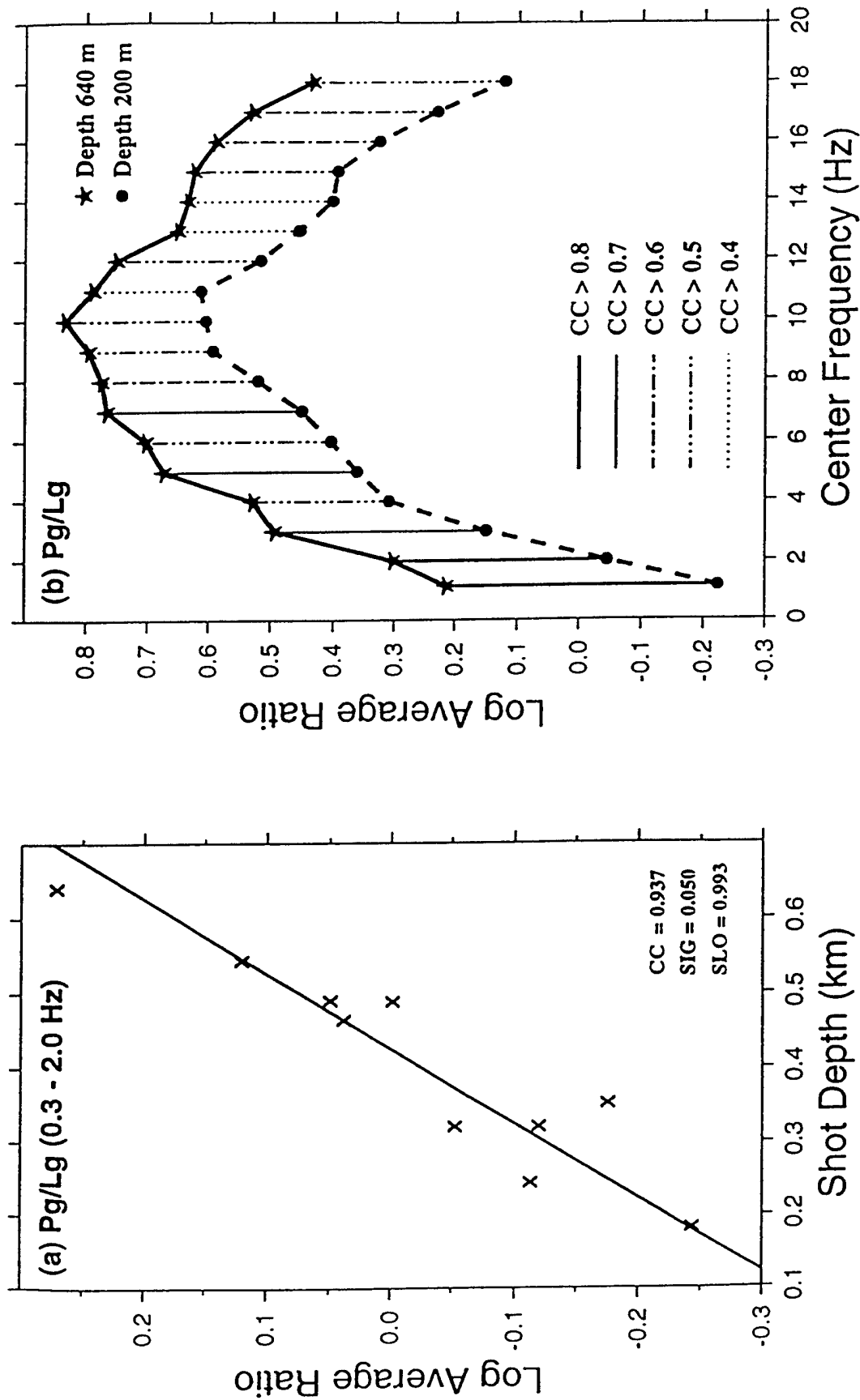


Figure 37. Similar to Figure 35 but derived from 10 Yucca Flat explosions recorded at NLS. The increasing difference at higher frequency between shallow and deep shots may again be due to the generation of high frequency S by explosion-generated cracks that are inhibited by overburden pressure, in agreement with Blandford's hypothesis.

Following a procedure similar to that used for the Yucca Flat explosions (Section 4.3.1), results shown in Figure 38 were obtained. The differences in Pn/Lg due to variation in magnitude and therefore in shot depth are larger for higher (greater than 5 Hz) frequencies. These results are therefore similar to those from Yucca Flat explosions (Figures 35 and 37) and support Blandford's (1995a,b) hypothesis.

5. APPLICATION TO REGIONAL DISCRIMINATION

5.1 Scattering of Rg into S and Regional Discrimination

Most regional discrimination methods are based on the differences in the frequency content of the seismic waves radiated from the source region of explosions and earthquakes. Several recent studies (Gupta *et al.*, 1992; Patton and Taylor, 1995; Gupta and Wagner, 1997; Gupta *et al.*, 1997) have provided new insight into the generation of Lg from explosions by suggesting that the low-frequency part of the Lg spectra is mainly due to the near-source scattering of explosion-generated Rg into S. The scattering mechanism (Rg-S-Lg) not only explains the spectral characteristics (such as peaks and nulls) of the low-frequency Lg from explosions (Gupta and Wagner, 1997) but also provides a good explanation of why the discriminant P/Lg may work at higher (above about 3 Hz) frequencies but fail at low frequencies. Since most regional discriminants make use of Lg, an improved understanding of this prominent regional phase should be useful not only for improving the performance of several existing regional discriminants but also for exploring the possibility and effectiveness of new discriminants.

Most geological sites where explosions and earthquakes may occur will have crustal heterogeneities, including lateral variations, which will generally diminish with depth. Since the explosions generally occur at depths that are shallower than those for earthquakes, they will generate much larger Rg, a considerable portion of which will be scattered into both S and P (more into S than P). The scattering process will contribute low frequency energy to both S and P from explosions because Rg has dominant energy only for low frequencies (less than about 2-3 Hz). Moreover, since explosions directly generate P waves, the influence of Rg scattering will generally be more distinct and observable on the spectra of S or Lg rather than on the various P phases (such as Pn or Pg).

5.2 Evaluation of Discriminants Using Galilee Ground-Truth Dataset

In order to test the discrimination potential of these concepts, we analyzed data from known mine blasts and earthquakes in the Galilee region recorded by the Israel Seismic Network (Gitterman *et al.*, 1996; Grant *et al.*, 1997). The analysis was restricted to events well recorded at common stations so that the influence of recording site effects is minimal. A set of 20 events (10 mine blasts and 10 earthquakes, numbered 1-10 and 11-20, respectively; Figure 39), recorded at the station MML, were found to be suitable for this purpose. The instrument used at MML is the short-period Teledyne-Geotech S-13 and the available signals, shown in Figures 40 and 41, had been bandpass filtered (0.2 to 12.5 Hz). The source-receiver distances varied from about 20 to 50 km, so that the first arrival was always Pg.

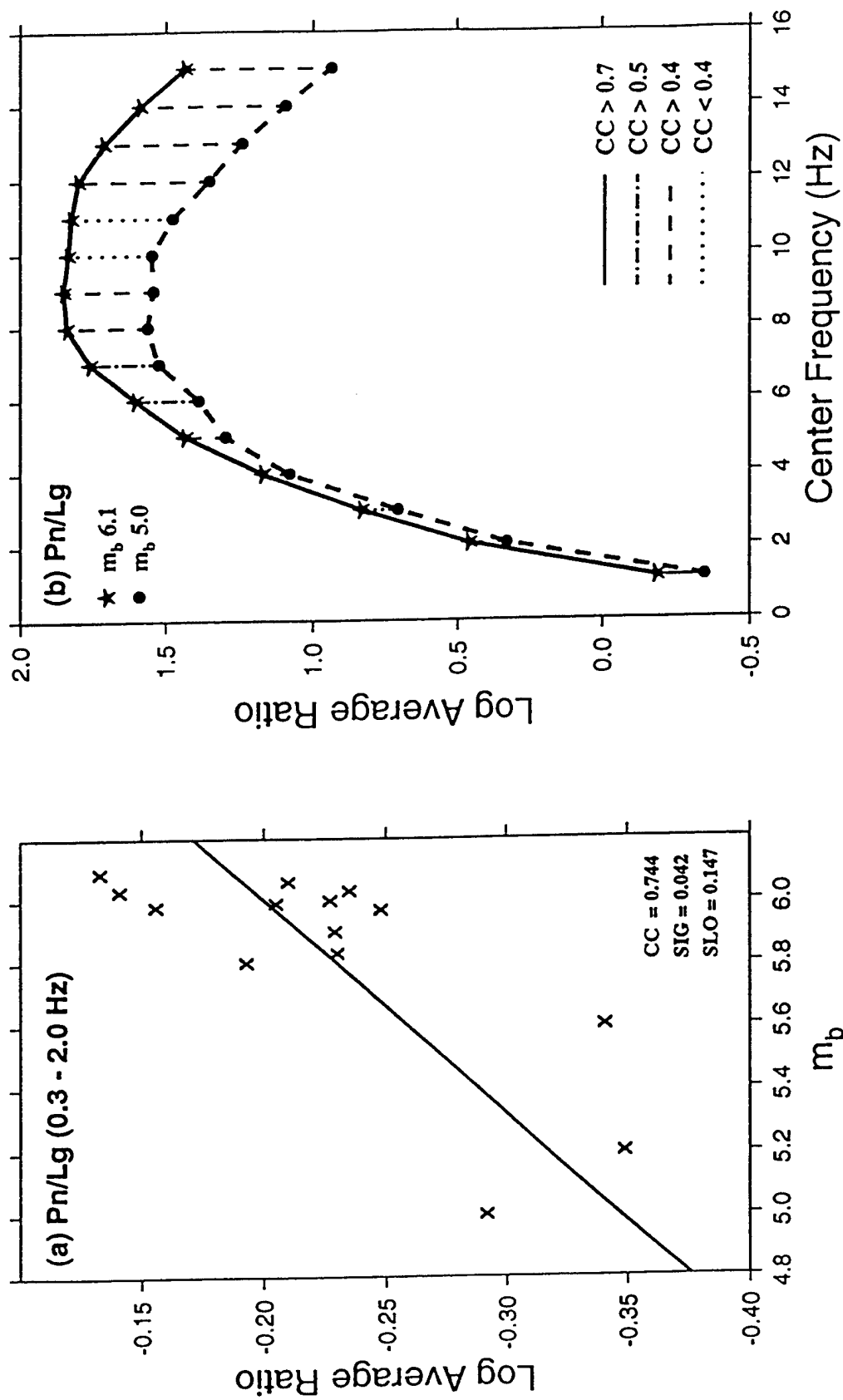


Figure 38. Spectral differences in Pn/Lg for small (m_b 5.0) and large (m_b 6.1) Kazakh explosions obtained by linear regression of average ratio versus m_b for various frequency bands, based on data from 14 shots recorded at WMQ. An example of regression is shown in (a). Differences in Pn/Lg appear to be larger for higher (larger than 5 Hz) frequencies. These results are similar to those for Yucca Flats (NTS) because m_b and shot depths are strongly correlated.

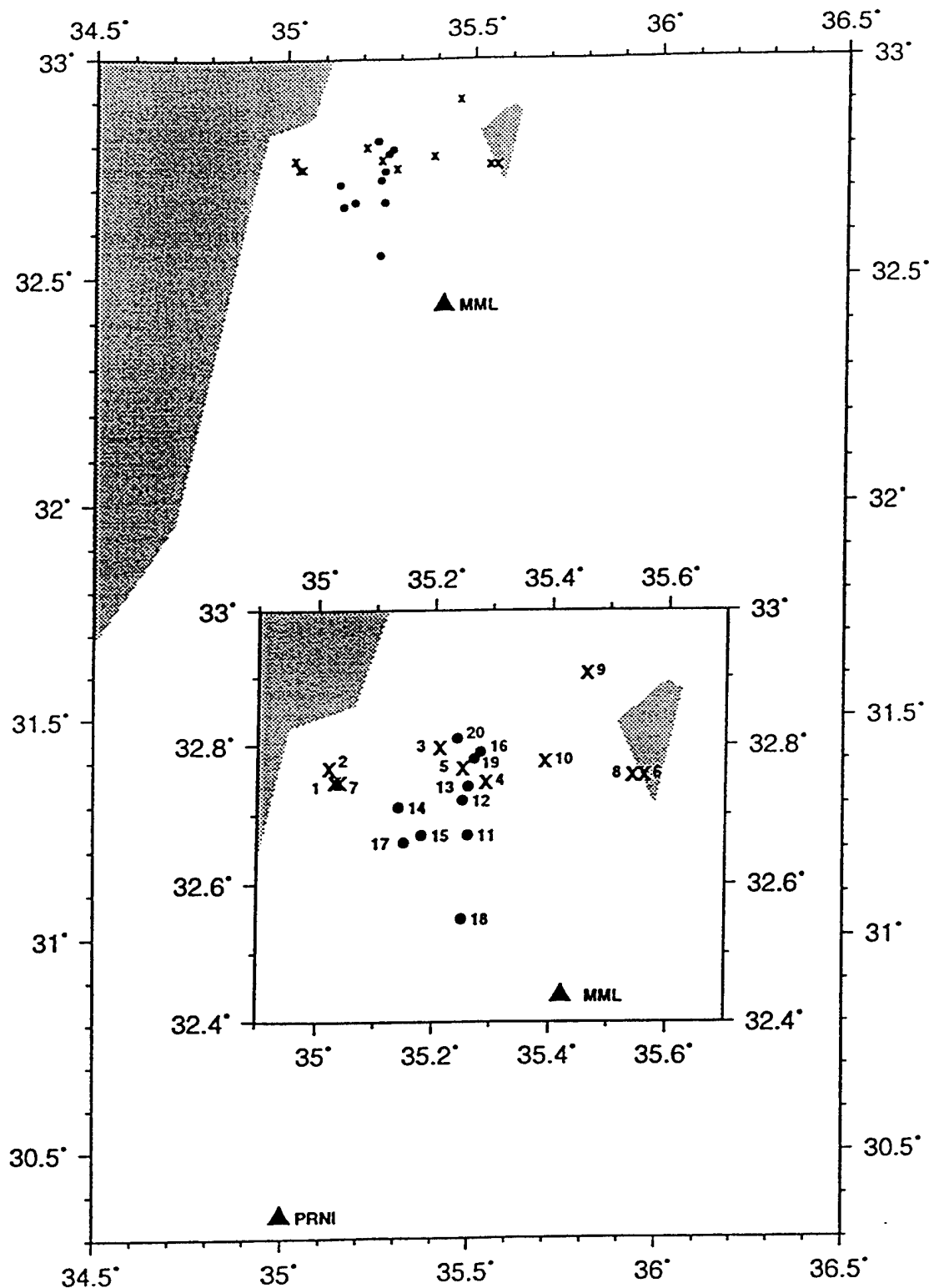


Figure 39. Location map of 20 events, including 10 quarry blasts (numbered 1 through 10) and 10 earthquakes (numbered 11 through 20) recorded at station MML. The recording station PRNI is also shown.

10 QUARRY BLASTS MML SHZ

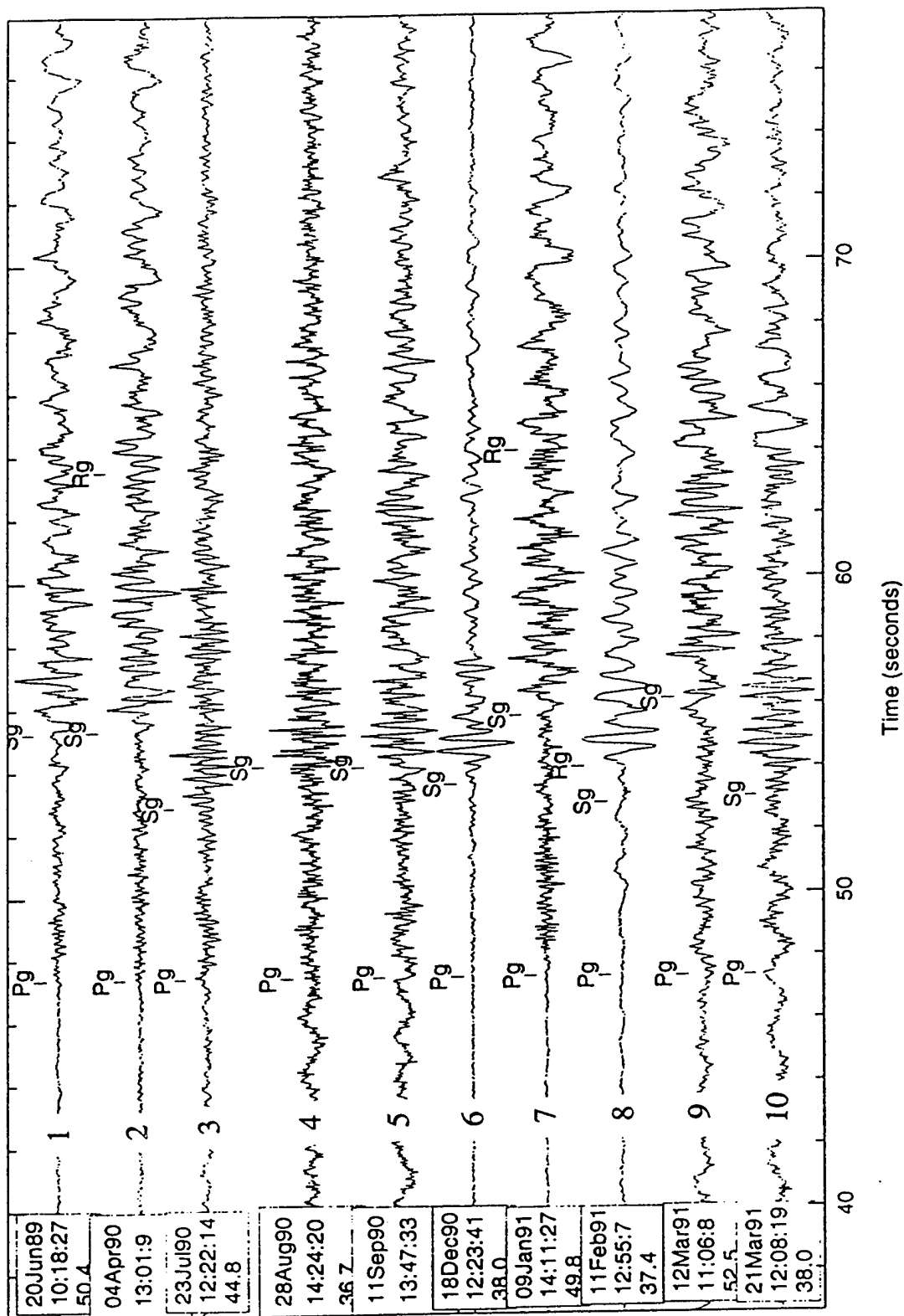


Figure 40. Station MML records of 10 quarry blasts (numbered 1 through 10).

10 EARTHQUAKES MML SHZ

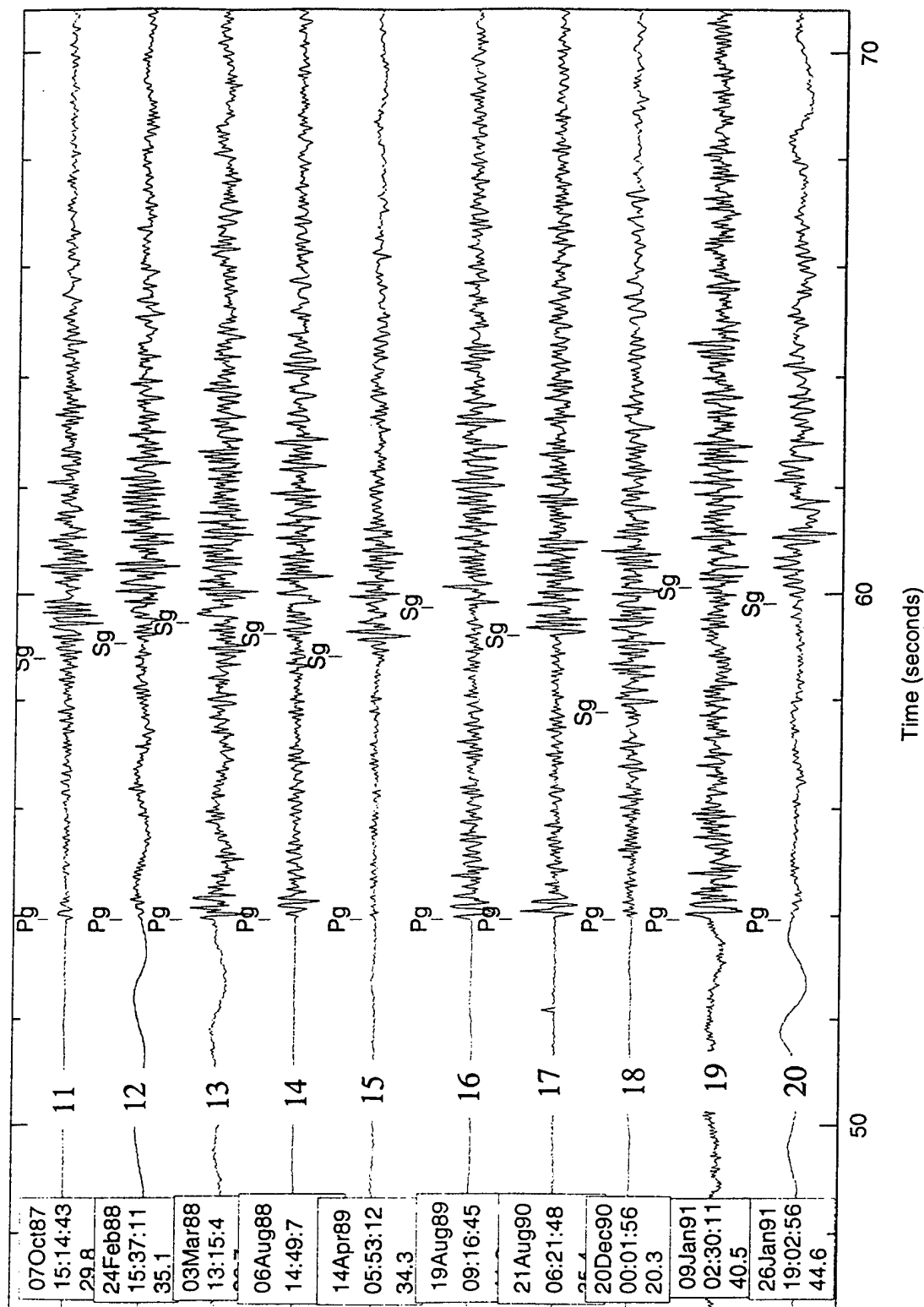


Figure 41. Station MML records of 10 earthquakes (numbered 11 through 20).

Multi-tapered spectra were obtained for the initial Pg (5.12 sec) and Sg (10.24 sec) and a correction for noise was applied by using a sample of noise before the onset of Pg. The amplitude ratios Pg/Sg were obtained by using only those data points for which the signal/noise power ratio was at least 1.5. Results (in log units) for each of the 20 events for the frequency band of 1-3 Hz (center frequency 2 Hz) are shown in Figure 42a in which the mean values for the ten quarry blasts and ten earthquakes are also indicated along with one standard deviation error bars. There is considerable overlap between the Pg/Sg values for the two types of sources. Combined results for the mean values for nine frequency bands, each 2 Hz in width, and with center frequencies at 2, 3, 4, 5, 6, 7, 8, 9, and 10 Hz are shown in Figure 42b which indicates rapid increase in the Pg/Sg ratio with frequency for the quarry blasts. This suggests that for the quarry blasts, the Pg amplitude is increasing with frequency and/or the Sg amplitude is decreasing with frequency. Earlier work based on spectral observations of Lg from nuclear explosions (Gupta *et al.*, 1992) would suggest that the rapid decrease in Sg amplitude with frequency is mainly responsible for the increase in Pg/Sg with frequency. The increase in Pg/Sg with frequency for earthquakes in Figure 42b is not as rapid so that there appears to be significant separation between the mean values for quarry blast and earthquake populations at both low and high frequency ends.

Considering the nature of Rg-to-S and Rg-to-P scattering as discussed earlier and the results in Figure 42, several other phase and spectral ratios for various frequency bands were computed for both the explosion and earthquake populations; the results are shown in Figures 43 through 46. The results in Figure 43 are similar to those in Figure 42 except that the two frequency ranges have been somewhat enlarged for greater stability. Note that there is larger separation between the mean values of Pg/Sg for the explosion and earthquake populations for the frequency band of 1-4 Hz (-0.21 log units) than for the higher frequency band of 8-12 Hz (0.13 log units). Figure 44 is based on a comparison of Pg/Sg within low (1-4 Hz) and two high frequency bands (8-12 Hz and 6-10 Hz) and shows somewhat better separations between the mean values (-0.34 log units and -0.28 log units) than those in Figure 43. Nevertheless, both Figures 43 and 44 show considerable overlap between data points belonging to the two different sources.

A comparison of amplitudes within a single phase (Pg or Sg) between the low and high frequency bands was also made by first removing the instrument response. Results based on a comparison of 1-4 Hz and 8-12 Hz amplitudes, shown in Figure 45, indicate surprisingly large separation between the two populations (0.67 and 0.98 log units for Pg and Sg, respectively). Moreover, the data points for the two sources are completely separated from each other, except for Event No. 7 for Pg (Figure 45a). A likely explanation is that both Pg and Sg from explosions at these rather small epicentral distances are rich in low frequencies because of large contributions from the scattering of Rg into both P and S. Results in Figure 46, based on the mean slope over the frequency range of 1-9 Hz for the Pg and Lg spectra (corrected for instrument response), also show the two populations as well separated, especially for Sg, similar to the results in Figure 45.

Investigations of S or Lg coda have been found to be useful for source discrimination and related studies because of their greater stability as compared to the direct S (e.g. Su *et al.*, 1991;

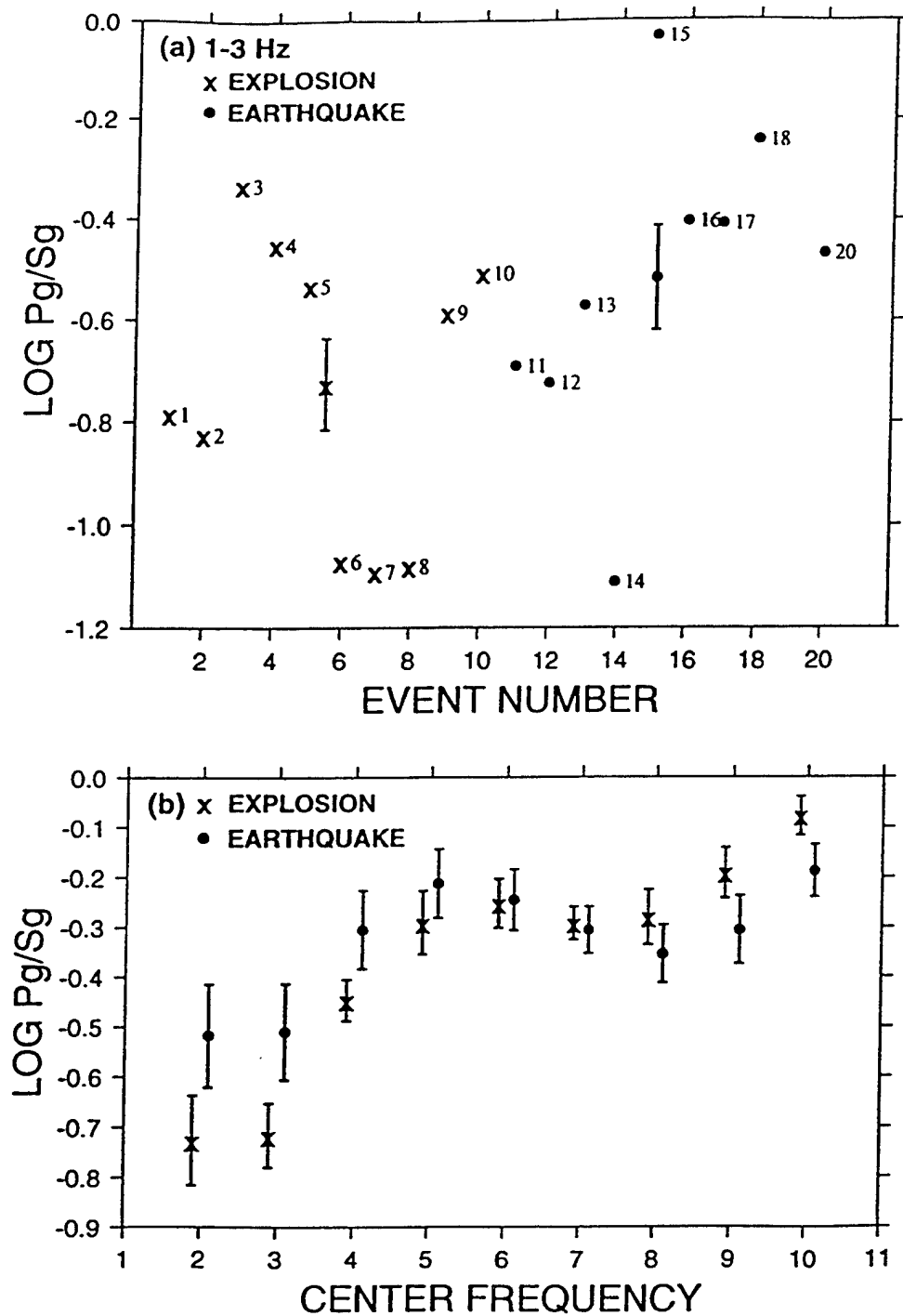


Figure 42. (a) Log Pg (5.12 sec)/Sg (10.24 sec), averaged over 1-3 Hz, for 10 quarry blasts and 10 earthquakes. Mean values for the two different types of sources are indicated along with one standard deviation error bars. (b) Mean values of Pg/Sg for quarry blasts and earthquakes for nine frequency bands with center frequencies ranging from 2 to 10 Hz. Note that the mean Pg/Sg for explosions is smaller than that for earthquakes at the lowest (2-5 Hz) frequencies, but the opposite is true at the highest (8-10 Hz) frequencies.

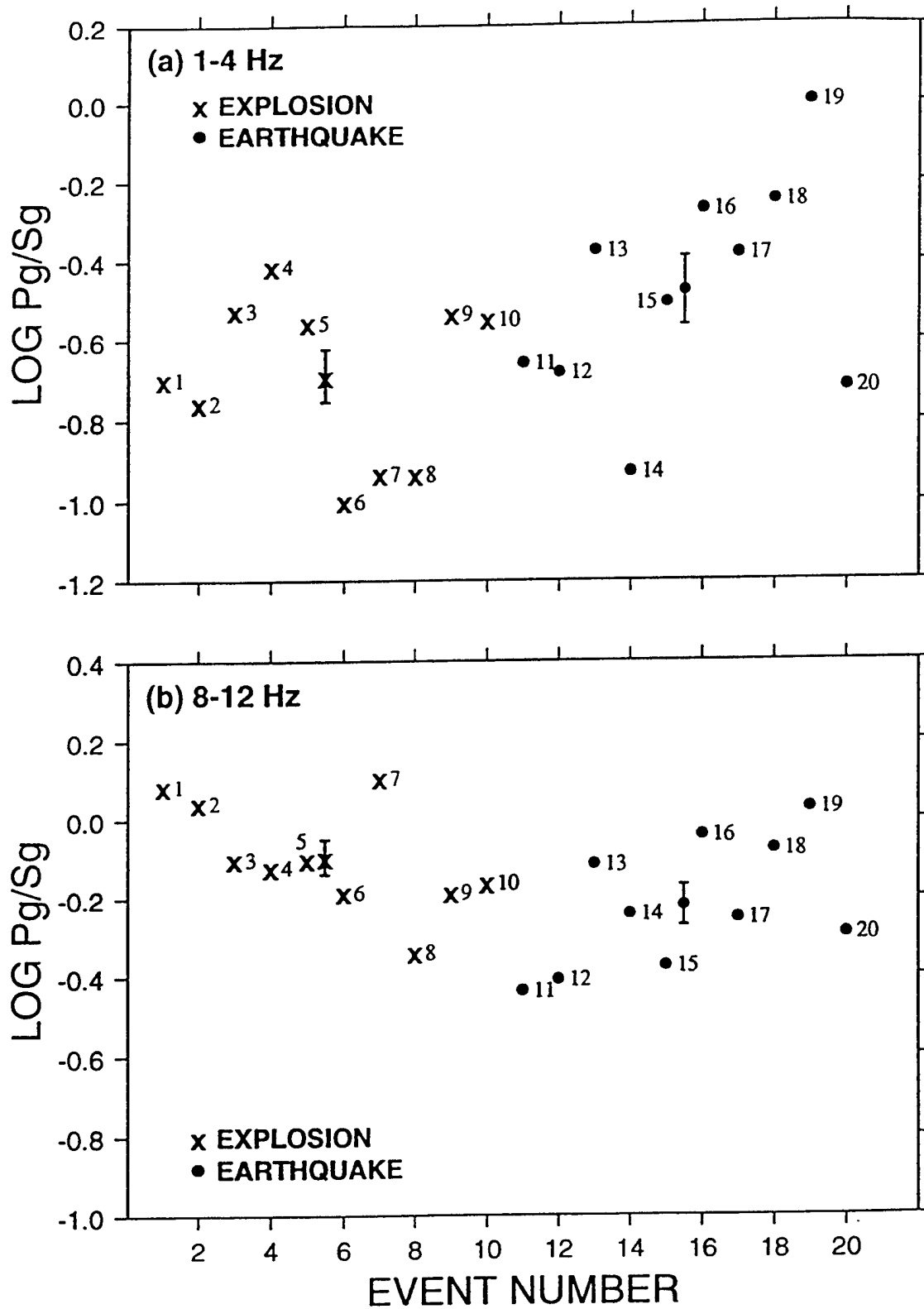


Figure 43. Similar to Figure 42a for frequency ranges of (a) 1-4 Hz and (b) 8-12 Hz showing mean values of Pg/Sg for the explosion and earthquake populations separated by -0.21 and 0.13 log units, respectively.

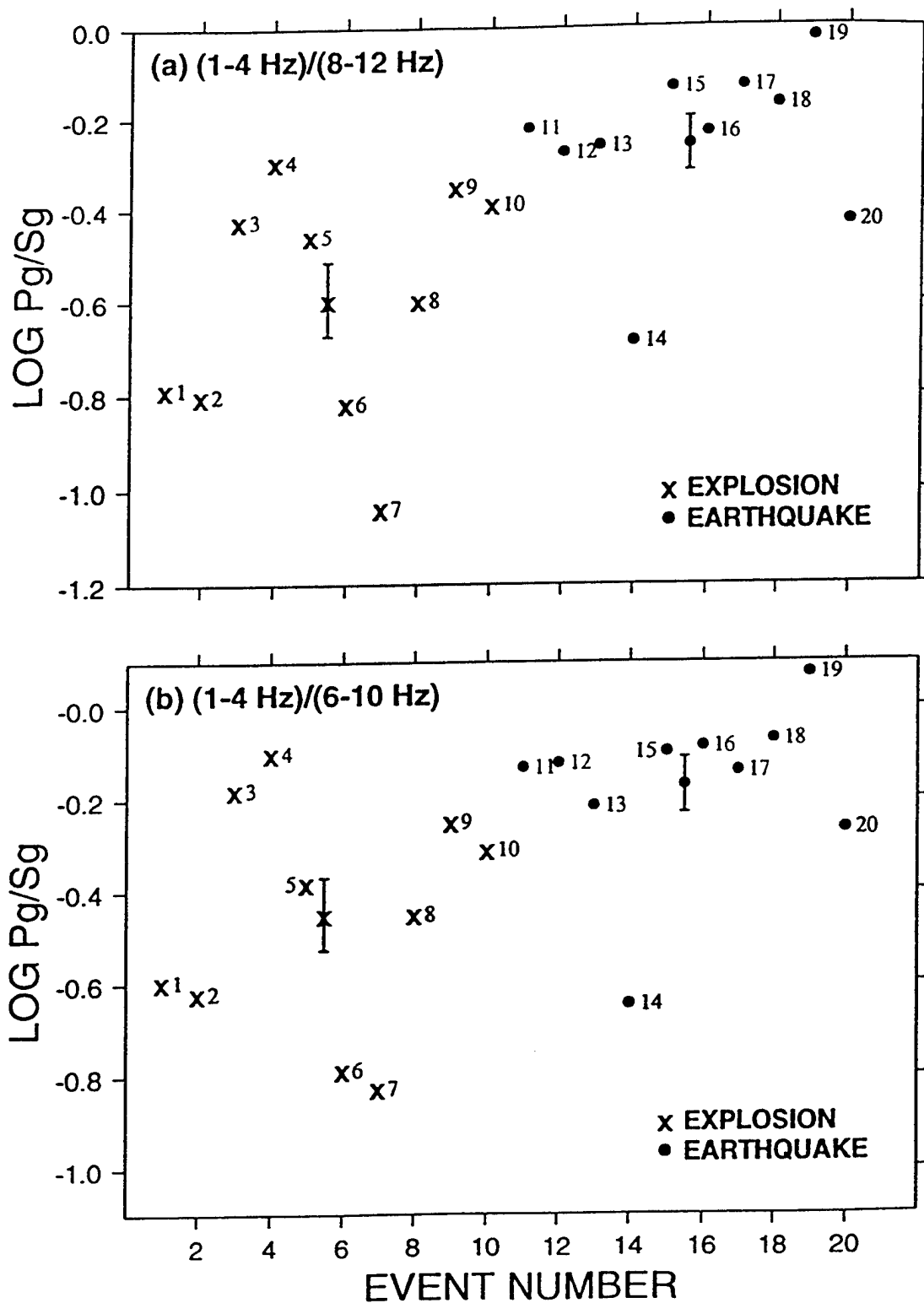


Figure 44. Similar to Figure 42a for Log Pg/Sg for (a) (1-4 Hz)/(8-12 Hz) and (b) (1-4 Hz)/(6-10 Hz) with mean values of the two populations separated by -0.34 and -0.28 log units, respectively.

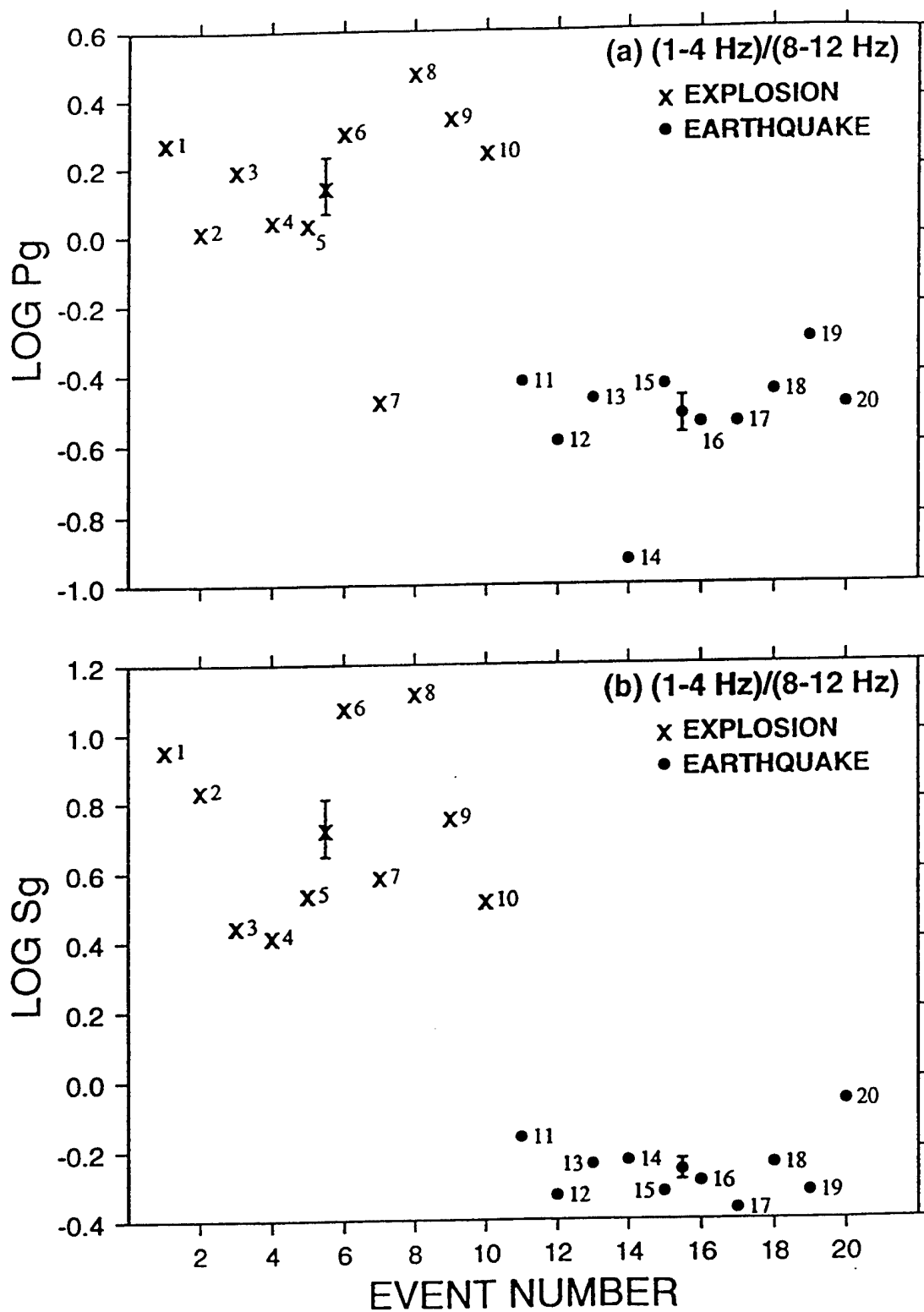


Figure 45. Similar to Figure 42a for (1-4 Hz)/(8-12 Hz) derived from instrument-response corrected (a) Pg and (b) Sg, indicating the mean values of the explosion and earthquake populations separated by 0.67 and 0.98 log units, respectively and no overlap (except for explosion no. 7 for Pg) between data points from the two types of sources.

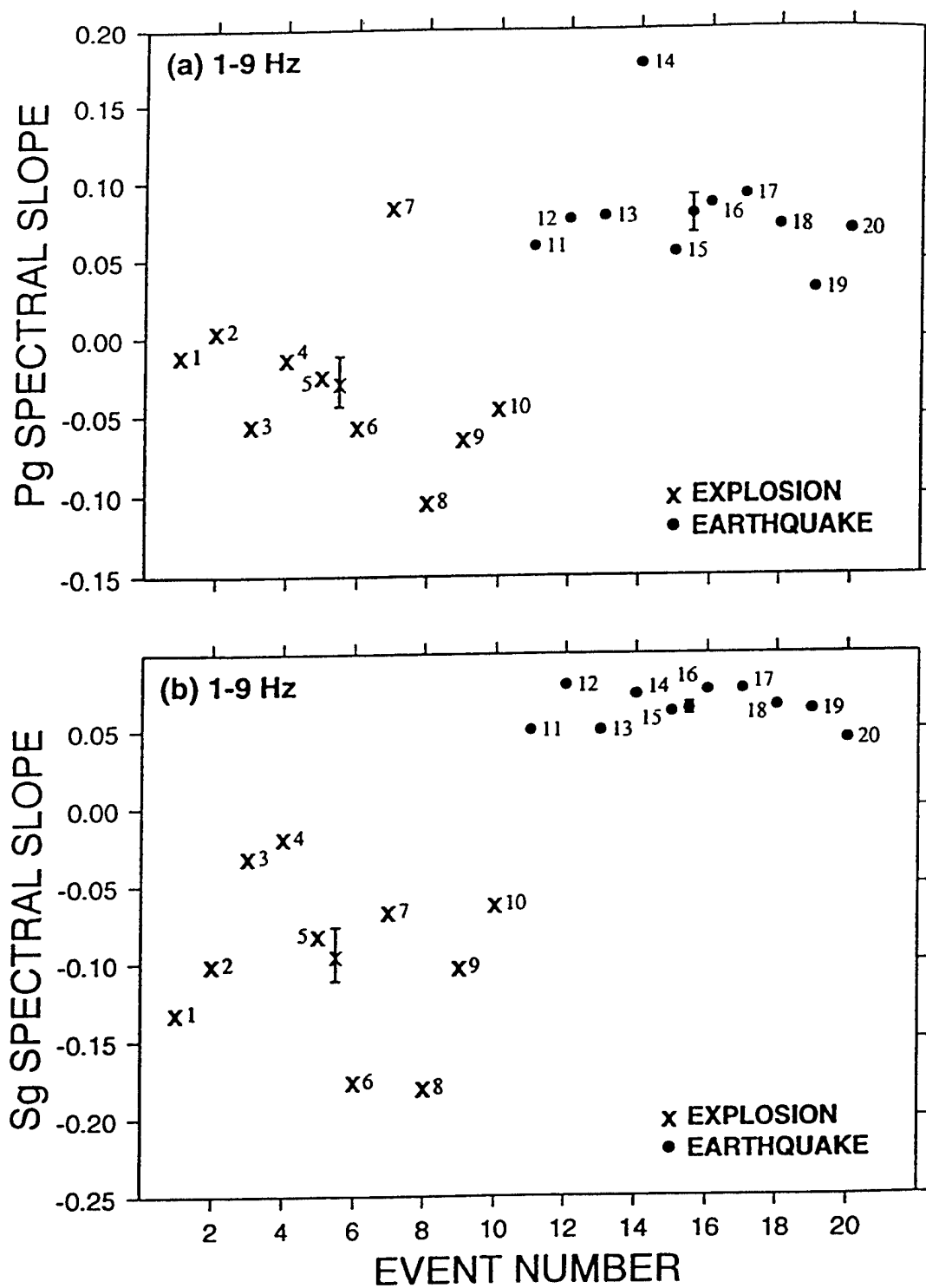


Figure 46. Similar to Figure 42a for mean slope over the frequency range of 1-9 Hz for the (a) Pg and (b) Sg spectra (corrected for instrument response), showing the mean values for the explosion and earthquake populations separated by -0.11 and -0.16 log units/Hz, respectively. The two sources are well separated, especially for Sg with no overlap between the two sets of data points.

Phillips and Aki, 1986; Steensma and Biswas, 1988). We applied the single-station spectral discrimination method based on the use of coda waves, successfully used by Hartse *et al.* (1995). Because of short recording times, coda immediately following the Sg arrival was used by applying a source-receiver distance correction as outlined in Roecker *et al.* (1982). The method we used also corrected for noise by using a sample of noise before the onset of Pg. Figure 47 shows the results for source factor (SF) difference between (a) 2-4 Hz band and 6-8 Hz band, and (b) 2-4 Hz band and 4-6 Hz band. The mean values for explosion and earthquake populations are well separated (by 0.51 and 0.34 log units, respectively) and there is no overlap among data points belonging to the two sources, except for one explosion. Considering Figures 42 through 47, the most effective source discriminants appear to be those based on the spectral content of Sg and the coda waves.

We next analyzed all available, well-recorded events at station PRNI; only 14 events (5 quarry blasts and 9 earthquakes) were found to have fairly good signal/noise ratio at higher frequencies. Waveforms of these 14 events are shown in Figures 48 and 49. The source-receiver distances varied from about 260 to 300 km. The Pn spectra of most events had poor S/N for frequencies less than about 2 Hz, although the Lg spectra were good for frequencies above 1 Hz. Some of the results are shown in Figures 50 and 51. Unlike the poor source discrimination shown by the high-frequency Pg/Sg in Figure 43b, Pn/Lg, averaged over 5-8 Hz, showed good separation (no overlap) between data points from the two sources (Figure 50a). Even better source discrimination is indicated by the instrument-response corrected Lg (1-3 Hz)/(5-8 Hz), as shown in Figure 50b; this result is similar to that for Sg in Figure 45b.

Results for the mean slope over the frequency range of 1-5 Hz for the instrument-response corrected Pn and Lg spectra are shown in Figure 51a, and 51b, respectively. There is hardly any separation for Pn, unlike the results for Pg in Figure 46a which showed fairly good separation. The spectra of Lg (Figure 51b) indicate excellent source discrimination, similar to the result for Sg in Figure 46b.

5.3 Discussion of Results

An examination of the above results from the Galilee dataset suggests several interesting possibilities for improved source discrimination. It seems that, for purposes of source discrimination, Sg and Lg are considerably more useful and stable phases to work with than are Pn or Pg. Although ripple firing is known to influence drastically the observed spectra of quarry blasts used in this study (Gitterman and Eck, 1993), the discrimination capability of Sg or Lg did not seem to be affected. There have been a few earlier studies of spectral slope as a discriminant but with ambiguous results. Analyzing high frequency data, Chael (1988) found the spectral slope of Pg to be a good discriminant for NTS explosions and southwestern U.S. earthquakes, whereas Carr's (1992) study of events recorded at the NORESS array indicated that the spectral slope of Pn did not distinguish between mine blasts and earthquakes. Wuster's (1993) study of chemical explosions and earthquakes in central Europe recorded at the ARCESS array showed examples of spectra in which the S-wave groups from earthquakes were relatively richer in high frequency energy than those from the mine blasts. Our study of spectral slope of S and Lg is perhaps the first detailed and successful investigation of this type,

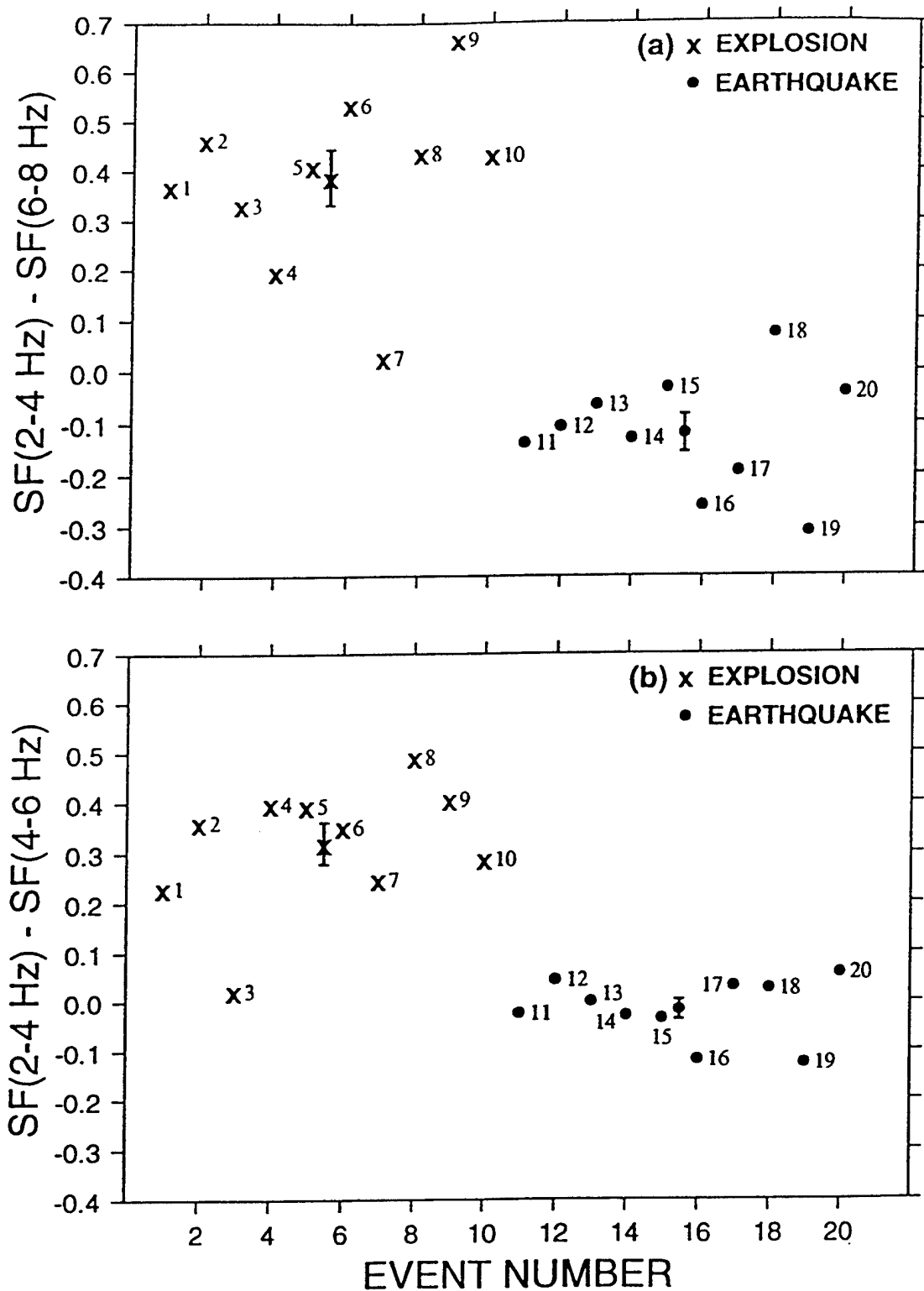


Figure 47. Similar to Figure 42a for source factor (SF) difference between (a) 2-4 Hz band and 6-8 Hz band, and (b) 2-4 Hz band and 4-6 Hz band, showing the mean values for explosion and earthquake populations differing by 0.51 and 0.34 log units and no overlap except for one event.

5 QUARRY BLASTS PRNI SHZ

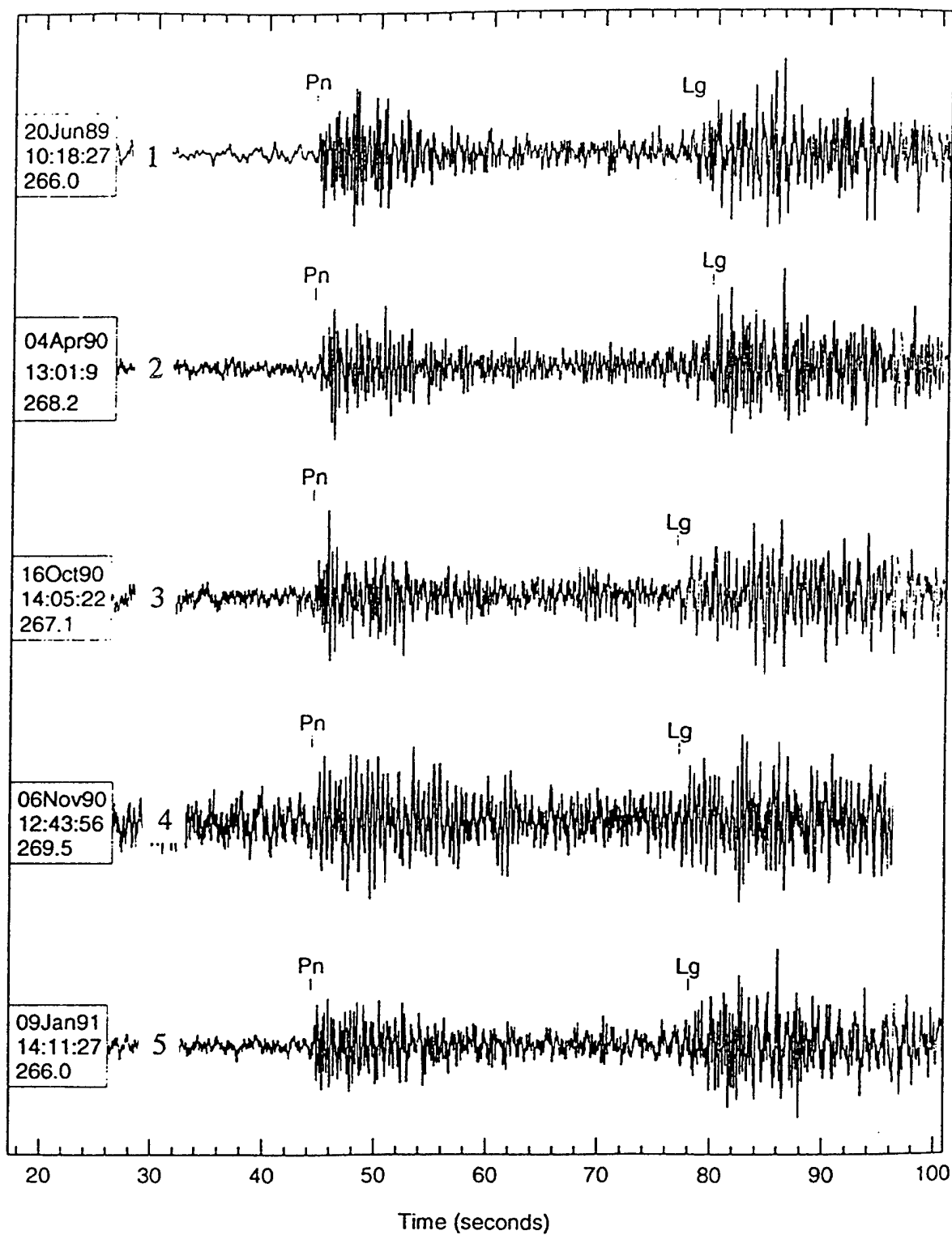


Figure 48. Station PRNI records of 5 quarry blasts (numbered 1 through 5).

9 EARTHQUAKES PRNI SHZ

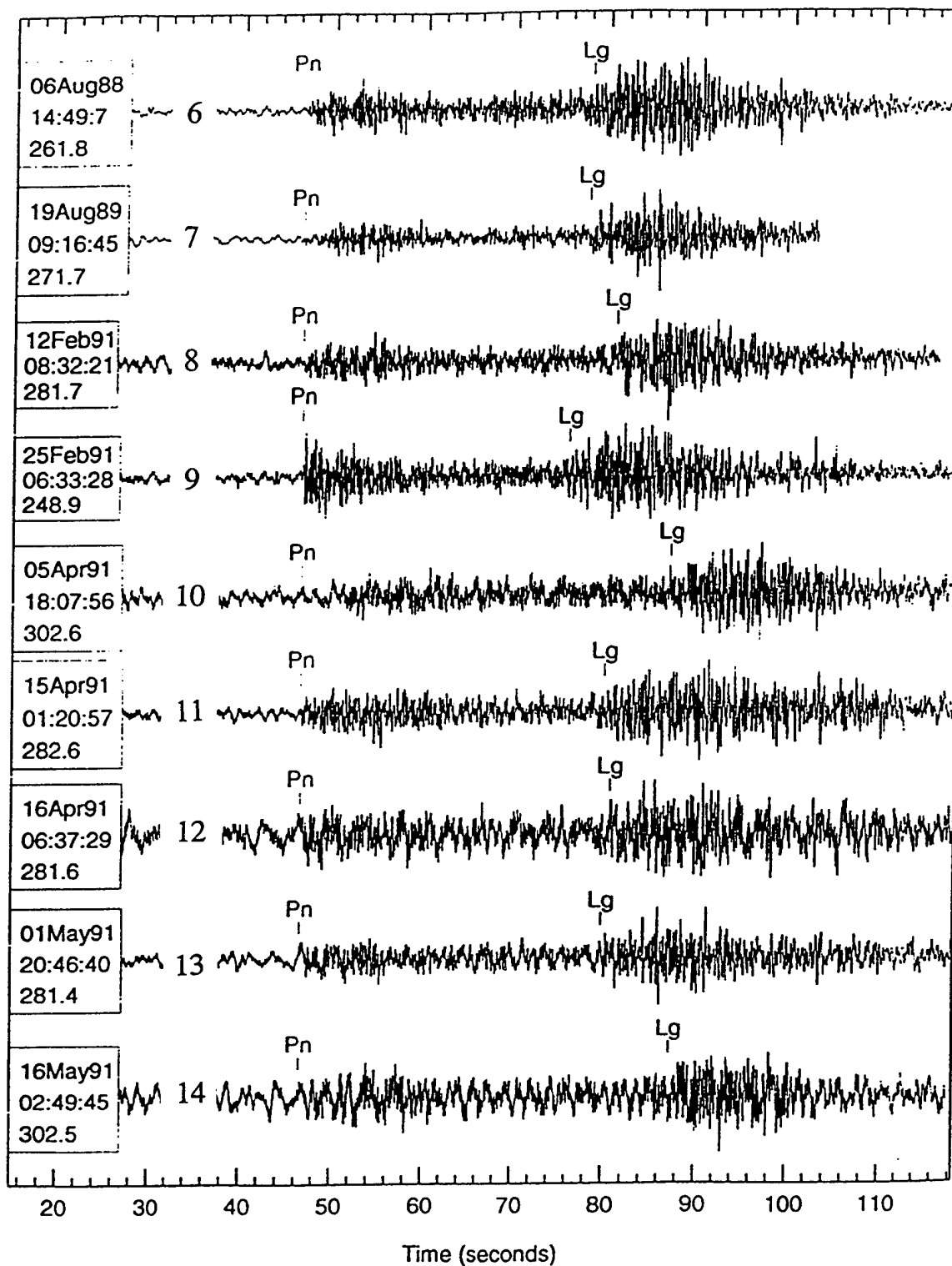


Figure 49. Station PRNI records of 9 earthquakes (numbered 6 through 14).

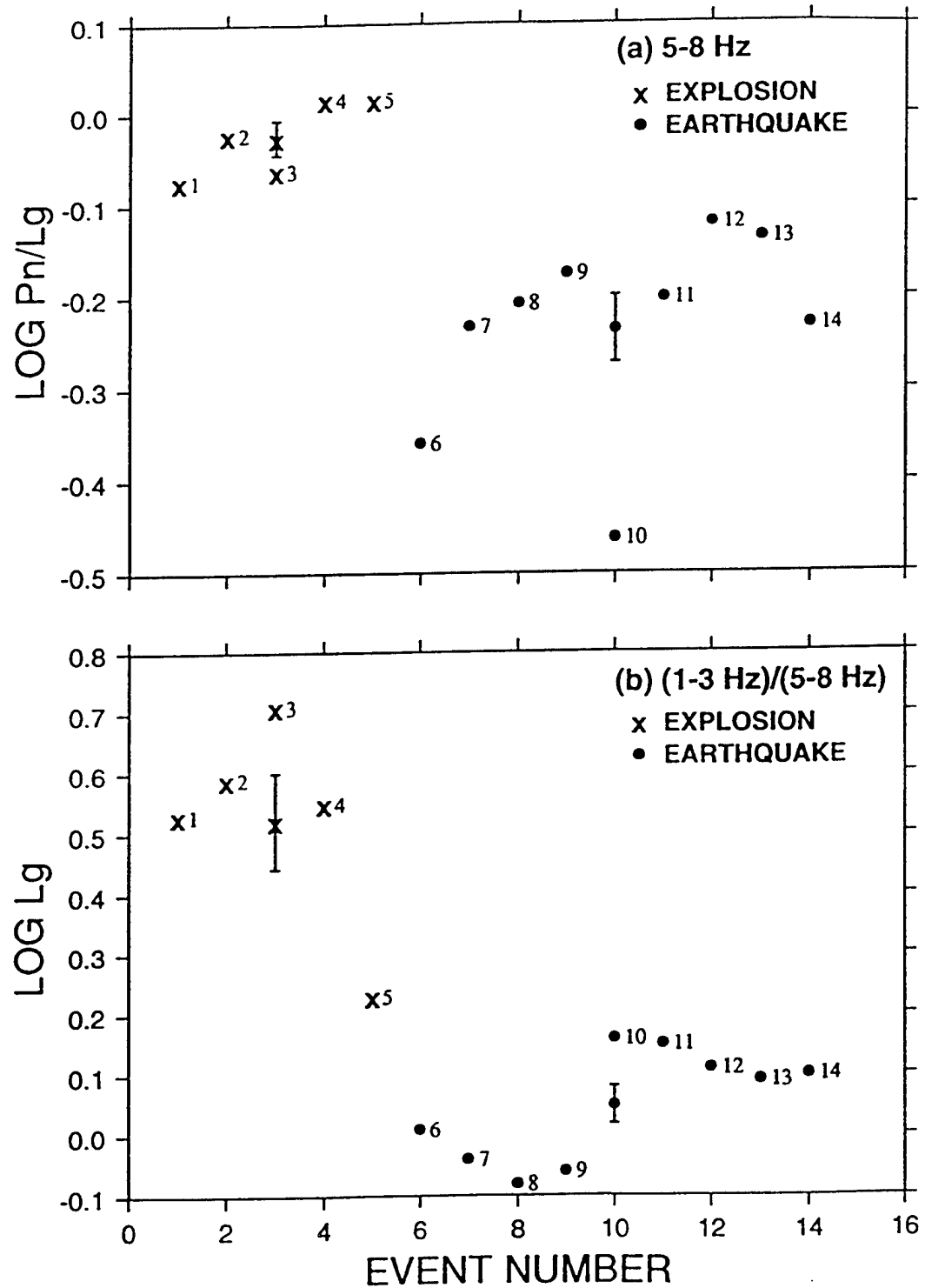


Figure 50. (a) $\text{Log Pn (10.24 sec)/Lg (20.48 sec)}$, averaged over 5-8 Hz, for 5 quarry blasts and 9 earthquakes, indicating the mean values for the two different types of sources separated by 0.21 log units. (b) Instrument-response corrected $\text{Lg (1-3 Hz)/(5-8 Hz)}$, indicating the mean values of the explosion and earthquake populations separated by 0.45 log units. Both (a) and (b) show no overlap between the two sets of data points.

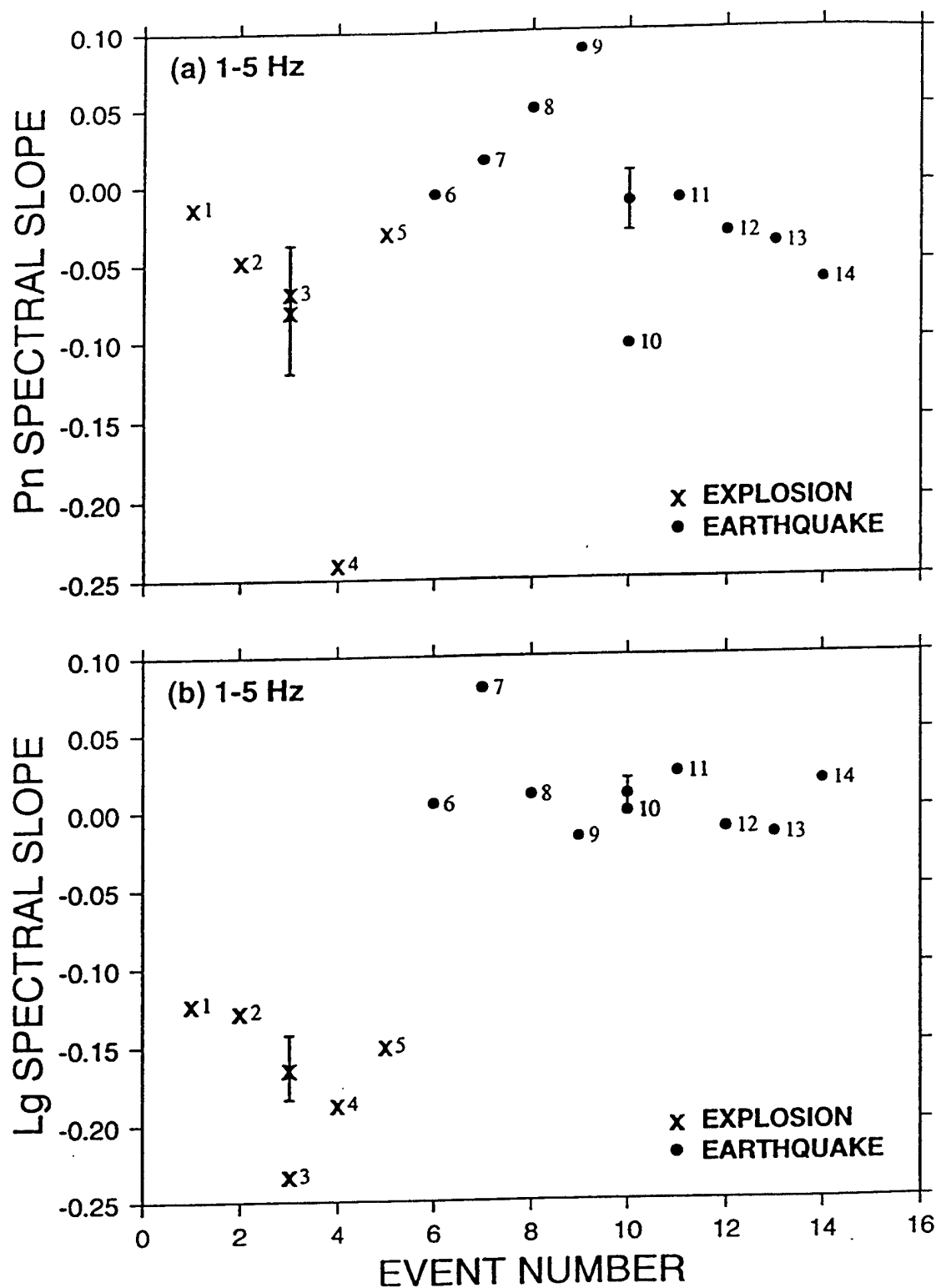


Figure 51. Similar to Figure 50 for mean slope over the frequency range of 1-5 Hz for (a) Pn and (b) Lg spectra (corrected for instrument response), showing the mean values of explosion and earthquake populations separated by -0.07 and -0.17 log units/Hz, respectively. Data points for the two sources are well separated only for Lg, with no overlap.

because (1) it is based on the mechanism of generation of the low-frequency S or Lg from explosions, (2) analyzes data from two stations well separated from each other, and (3) shows excellent separation between the explosion and earthquake populations. Lastly, our preliminary results demonstrate the need for using a combination of several source discriminants for improved reliability and effectiveness. For example, analysis of the station MML data, as shown in Figures 45a, 46a, and 47a indicate Event 7 (an explosion) to be an outlier, or the most like an earthquake. But the same event appearing in Figures 43a, 43b, 44a, and 44b behaves like an event most likely to be an explosion. Several other figures (such as Figures 45b, 46b, and 47b) easily identify Event 7 as an explosion.

6. CONCLUSIONS AND RECOMMENDATIONS

Our analysis of both low- and high-frequency data from a large number of underground nuclear explosions, most of them with known ground truth and recorded at both local and regional distances, leads to the following principal conclusions:

- (1) Excellent agreement between observation and theory, mostly for Yucca Flat (NTS) explosions, confirms the dominant contribution of Rg-to-S scattering to the low-frequency Lg from explosions, as suggested earlier by Gupta *et al.* (1992) and Patton and Taylor (1995).
- (2) An effective CLVD source appears to be present not only for Lg from Yucca Flat (NTS) explosions, as suggested by Patton and Taylor (1995), but also for explosions from other test sites in significantly different geological environments.
- (3) Shot depth and subsurface structure are important in defining the spectral characteristics of the low-frequency (less than about 3 Hz) Lg, including the most important spectral null and peak.
- (4) Spectral null frequency in the low-frequency Lg depends strongly on shot depth and local velocity structure so that a comparison with theory can provide useful source information, including shot depth with an accuracy not possible by other methods.
- (5) Spectral peak in the low-frequency Lg from Yucca Flat explosions is associated with resonance caused by sharp impedance contrast in the source region.
- (6) Analyses of regional phases from explosions at both Nevada and Kazakh test sites support Blandford's (1995a,b) suggestion that the high frequency S or Lg from explosions is due to the generation of new cracks created by a tamped explosion and that these cracks should decrease as overburden increases.
- (7) A comparison of both low (less than about 3 Hz) and high frequency Lg may be useful for identifying clandestine cavity decoupled explosions.

(8) As demonstrated by our analysis of the Israeli Seismic Network data, new insight into the generation of broadband Lg from explosions suggests potentially useful discriminants for seismic monitoring of the CTBT.

On the basis of results obtained in this study, the following recommendations are made for future work:

- (1) The broadband characteristics of Lg should be further investigated for regions other than the NTS so that the role of near-source scattering of explosion-generated Rg is clearly understood and exploited for deriving source and near-source information.
- (2) Improve the results obtained in this study by using more sophisticated theoretical and analytical methods and extend such work to other test regions.
- (3) Analyze local data from Salmon and Sterling, such as that discussed in Section 4.2.3, to understand why results from closely-located sensors are significantly different from one sensor to another.
- (4) In order to fully understand the generation of high-frequency S from explosions, analyze additional near-field, local, and regional high-frequency data from tamped, decoupled, and overburied explosions.

7. ACKNOWLEDGMENTS

Discussions with Bob Blandford and Howard Patton are greatly appreciated. Software development by Tien Zhang and David Salzberg and seismic analysis by Claudia Carabajal contributed to this study. We are especially grateful to Bill Walter, Eric Chael, Lori Grant, Flori Ryall, Terri Hauk, Albert Smith, and the IRIS staff for providing the waveform data. Thanks are also due to Winston Chan and Wilmer Rivers for guidance and a critical review of the manuscript. This study was supported by the Department of Energy, Contract No. F19628-95-C-0176.

8. REFERENCES

- Adushkin, V. V., I. O. Kitov, and D. D. Sultanov (1992). Experimental results of USSR nuclear explosion decoupling measurements, *C92-04*, Center for Seismic Studies, Arlington, Virginia.
- Aki, K. and P. G. Richards (1980). *Quantitative Seismology*, Chapter 7, W. H. Freeman and Company.
- Blandford, R. R. (1981). Seismic discrimination problems at regional distances, *in* Identification of Seismic Sources - Earthquake or Underground Explosion, E. S. Husebye and S. Mykkeltveit, Editors, D. Reidel Publishing Co., Dordrecht, The Netherlands, 695-740.
- Blandford, R. R. (1995a). Discrimination of mining, cratering, tamped, and decoupled explosions using high frequency S-to-P ratios, *AFTAC-TR-95-002*, Patrick AFB, Florida.
- Blandford, R. R. (1995b). Regional seismic event discrimination, *in* Monitoring a Comprehensive Test Ban Treaty, NATO ASI Series, Husebye, E. S. and Dainty, A. M. (eds), vol. 303, 689-719.
- Blandford, R., A. Dainty, R. Lacoss, R. Maxion, A. Ryall, B. Stump, C. Thurber, and T. Wallace (1992). Report on the DARPA Seismic Identification Workshop, DARPA.
- Blandford, R. R., R. Hartenberger, and R. Naylor (1981). Regional amplitude-distance relations, discrimination and detection, *VSC-TR-81-15*, Teledyne Geotech, Alexandria, Virginia. ADA105722.
- Blandford, R. R. and J. R. Woolson (1979). Experimental spectral analysis of Salmon/Sterling decoupling, *SDAC-TR-79-3*, Teledyne Geotech, Alexandria, Virginia.
- Carr, D. B. (1992). Discrimination using spectral slopes at frequencies up to 50 Hz, *Bull. Seism. Soc. Am.* 82, 337-351.
- Carter, T. B. (1992). Nuclear Explosion Quick Reference V1.0, July 1945 – September 1992, *Technical Report C92-03*, Center for Seismic Studies, Arlington, Virginia.
- Chael, E. P. (1988). Spectral discrimination of NTS explosions and earthquakes in the southwestern United States using high-frequency regional data, *Geophys. Res. Lett.* 15, 625-628.
- Closmann, P. J. (1969). On the prediction of cavity radius produced by an underground nuclear explosion, *Jour. Geophys. Res.* 74, 3935-3939.
- Day, S. M. and K. L. McLaughlin (1991). Seismic source representations for spall, *Bull. Seism. Soc. Am.* 81, 191-201.

Denny, M. D. and D. M. Goodman (1990). A case study of the seismic source function: Salmon and Sterling reevaluated, *Jour. Geophys. Res.* 95, 19,705-19,723.

Edwards, C. L. and D. F. Baker (1993). Integrated verification experiment data collected as part of the Los Alamos National Laboratory's source region program, Appendix E: Local and near-regional data for IVEs, *LAUR-93-854*, Los Alamos National Laboratory, Los Alamos, New Mexico.

Frankel, A. (1989). Effects of source depth and crustal structure on the spectra of regional phases determined from synthetic seismograms, DARPA/AFTAC Annual Seismic Research Review, 97-118, Patrick Air Force Base, Florida.

Gaffet, S. (1995). Teleseismic waveform modeling including geometrical effects of superficial geological structures near to seismic sources, *Bull. Seism. Soc. Am.* 85, 1068-1079.

Gitterman, Y. and van Eck, T. (1993). Spectra of quarry blasts and microearthquakes recorded at local distances in Israel, *Bull. Seism. Soc. Am.* 83, 1799-1812.

Gitterman, Y., V. Pinsky, and A. Shapira (1996). Discrimination of seismic sources using Israel Seismic Network, PL-TR-96-2207, Phillips Laboratory, Hanscom Air Force Base, Massachusetts. ADA317385

Grant, L., R. Wagner, F. Ryall, W. Rivers, and I. Henson (1997). Ground truth database for regional seismic discrimination research in the Middle East and North America, Proc. 19th Annual Seismic Research Symposium on Monitoring a Comprehensive Test Ban Treaty (Editors: M. J. Shore, R. S. Jih, A. Dainty, and J. Erwin), Defense Special Weapons Agency, Alexandria, pp. 867-876.

Gupta, I. N. (1996). Improved understanding of broadband Lg/P ratio and its application to discriminating earthquakes from explosions, including decoupled shots, *PL-TR-96-2251*, Phillips Laboratory, Hanscom Air Force Base, Massachusetts.

Gupta, I. N., W. W. Chan, and R. A. Wagner (1992). A comparison of regional phases from underground nuclear explosions at East Kazakh and Nevada test sites, *Bull. Seism. Soc. Am.* 82, 352-382.

Gupta, I. N., C. S. Lynnes, and R. A. Wagner (1990). Broadband f-k analysis of array data to identify sources of local scattering, *Geophys. Res. Lett.* 17, 183-186.

Gupta, I. N., C. S. Lynnes, and R. A. Wagner (1991a). Studies of near-source and near-receiver scattering and low-frequency Lg from East Kazakh and NTS explosions, *PL-TR-91-2287*, Phillips Laboratory, Hanscom Air Force Base, Massachusetts. ADA248046

Gupta, I. N., C. S. Lynnes, and R. A. Wagner (1993). An array study of the effects of a known local scatterer on regional phases, *Bull. Seism. Soc. Am.* 83, 53-63.

Gupta, I. N., T. W. McElfresh, and R. A. Wagner (1991b). Near-source scattering of Rayleigh to P in teleseismic arrivals from Pahute Mesa (NTS) shots, in *Explosion Source Phenomenology*, Am. Geophys. Union Monograph 65, 151-159.

Gupta, I. N., K. L. McLaughlin, and others (1986). Studies in decoupling, *TGAL-86-08*, Teledyne Geotech, Alexandria, Virginia.

Gupta, I. N. and R. A. Wagner (1997). Low and high frequency Lg from explosions - new insights, Proc. 19th Annual Seismic Research Symposium on Monitoring a Comprehensive Test Ban Treaty (Editors: M. J. Shore, R. S. Jih, A. Dainty, and J. Erwin), Defense Special Weapons Agency, Alexandria, pp. 594-603.

Gupta, I. N. and T. R. Zhang (1996). Study of low-frequency Lg from explosions at Nevada, Kazakh, Lop Nor, and Azgir test sites, *PL-TR-96-2153*, Phillips Laboratory, Hanscom Air Force Base, Massachusetts, 328-337. ADA313692

Gupta, I. N., T. R. Zhang, and R. A. Wagner (1997). Low-frequency Lg from NTS and Kazakh nuclear explosions - observations and interpretation, *Bull. Seism. Soc. Am.* 87, 1115-1125..

Hartse, H. E., W. S. Phillips, M. C. Fehler, and L. S. House (1995). Single-station spectral discrimination using coda waves, *Bull. Seism. Soc. Am.* 85, 1464-1474.

Harvey, D. J. (1993). Full waveform inversion for structure and source parameters using regional data recorded in Eastern Kazakhstan, *PL-TR-93-2078*, Phillips Laboratory, Hanscom Air Force Base, Massachusetts. ADA266405

Herrmann, R. B. and C. Y. Wang (1985). A comparison of synthetic seismograms, *Bull. Seism. Soc. Am.* 75, 41-56.

Hudson, J. A. and A. Douglas (1975). Rayleigh wave spectra and group velocity minima, and the resonance of P waves in layered structures, *Geophys. J. R. astr. Soc.* 42, 175-188.

Israelsson, H. (1992). A spectral decomposition of Lg waves from explosions and scaling of RMS magnitudes, in RMS Lg as a yield estimator in Eurasia, *PL-TR-92-2117(I)*, 143-166, Phillips Laboratory, Hanscom Air Force Base, Massachusetts. ADA256692

Jih, R. S. (1995). Numerical investigation of relative contributions of Rg scattering and attenuation to Lg excitation, in Proc. 17th PL/AFOSR Seismic Research Symposium, *PL-TR-95-2108*, Phillips Laboratory, Hanscom AFB, MA, pp. 401-410. ADA310037

Johnson, L. R. (1997). Generation of S waves by explosions, Proc. 19th Annual Seismic Research Symposium on Monitoring a Comprehensive Test Ban Treaty (Editors: M. J. Shore, R. S. Jih, A. Dainty, and J. Erwin), Defense Special Weapons Agency, Alexandria, pp. 625-631.

Kafka, A. L. (1990). Rg as a depth discriminant for earthquakes and explosions: a case study in New England, *Bull. Seism. Soc. Am.* 80, 373-394.

Kennett, B. L. N. (1989). On the nature of regional seismic phases - I. Phase representations for Pn, Pg, Sn, Lg, *Geophys. J.* 98, 447-456.

Kim, W. Y., D. W. Simpson, and P. G. Richards (1993). Discrimination of earthquakes and explosions in the eastern United States using regional high-frequency data, *Geophys. Res. Lett.* 20, 1507-1510.

Matzko, J. R. (1994). Geology of the Chinese nuclear test site near Lop Nor, Xinjiang Uygur Autonomous Region, China, *Engineering Geology* 36, 173-181.

Mayeda, K. M. and W. R. Walter (1994). Lg coda moment rate spectra and discrimination using Lg coda envelopes, Proliferation Experiment at the Livermore NTS network, Proc. Symposium on the Non-Proliferation Experiment, *CONF-9404100*, Department of Energy, Rockville, Maryland, 6-202 to 6-212.

Murphy, J. R. and B. W. Barker (1995). A comparative analysis of the seismic characteristics of cavity decoupled nuclear and chemical explosions, *PL-TR-95-2177*, Phillips Laboratory, Hanscom Air Force Base, Massachusetts. ADA304812

Patton, H. J. (1988). Application of Nuttli's method to estimate yield of Nevada Test Site explosions recorded on Lawrence Livermore National Laboratory's digital seismic system, *Bull. Seism. Soc. Am.* 78, 1759-1772.

Patton, H. J. and S. R. Taylor (1995). Analysis of Lg spectral ratios from NTS explosions: implications for the source mechanisms of spall and the generation of Lg waves, *Bull. Seism. Soc. Am.* 85, 220-236.

Phillips, W. S. and K. Aki (1986). Site amplification of coda waves from local earthquakes in central California, *Bull. Seism. Soc. Am.* 76, 627-648.

Priestley, K. F., W. R. Walter, V. Martynov, and M. V. Rozhkov (1990). Regional seismic recordings of the Soviet nuclear explosion of the Joint Verification Experiment, *Geophys. Res. Lett.* 17, 179-182.

Roecker, S. W., B. Tucker, J. King, and D. Hatzfeld (1982). Estimates of Q in central Asia as a function of frequency and depth using the coda of locally recorded earthquakes, *Bull. Seism. Soc. Am.* 72, 129-149.

Rodean, H. C. (1981). Inelastic processes in seismic wave generation by underground explosions, in *Identification of Seismic Sources - Earthquake or Underground Explosion*, E. S. Husebye and S. Mykkeltveit (eds), D. Reidel, Dordrecht, Holland, 97-189.

Seneff, S. (1978). A fast new method for frequency-filter analysis of surface waves: application in the west Pacific, *Bull. Seism. Soc. Am.* 68, 1031-1048.

Steensma, G. J. and N. N. Biswas (1988). Frequency dependent characteristics of coda wave quality factor in central and southcentral Alaska, *PAGEOPH* 128, 295-307.

Stead, R. J. and D. V. Helmberger (1988). Numerical-analytical interfacing in two dimensions with application to modeling NTS seismograms, *PAGEOPH* 128, nos. 1/2, 157-193.

Su, F., K. Aki, and N. N. Biswas (1991). Discriminating quarry blasts from earthquakes using coda waves, *Bull. Seism. Soc. Am.* 81, 162-178.

Taylor, S. R. (1993). Integrated verification experiment data collected as part of the Los Alamos National Laboratory's source region program, Appendix F: Regional data from Lawrence Livermore National Laboratory and Sandia National Laboratory seismic networks, *LAUR-93-2150*, Los Alamos National Laboratory, Los Alamos, New Mexico.

Walter, W. R., K. Mayeda, and H. J. Patton (1994). Regional seismic observations of the Non-Proliferation Experiment at the Livermore NTS network, Proc. Symposium on the Non-Proliferation Experiment, *CONF-9404100*, Department of Energy, Rockville, Maryland, 6-193 to 6-201.

Walter, W. R., K. M. Mayeda, and H. J. Patton (1995). Phase and spectral ratio discrimination between NTS earthquakes and explosions. Part1: empirical observations, *Bull. Seism. Soc. Am.* 85, 1050-1067.

Wuster, J. (1993). Discrimination of chemical explosions and earthquakes in central Europe – a case study, *Bull. Seism. Soc. Am.* 83, 1184-1212.

Xie, J., L. Cong, and B. J. Mitchell (1996). Spectral characteristics of the excitation and propagation of Lg from underground nuclear explosions in central Asia, *J. Geophys. Res.* 101, 5813-5822.

Xie, X. B. and T. Lay (1994). The excitation of Lg waves by explosions: a finite-difference investigation, *Bull. Seism. Soc. Am.* 84, 324-342.

THOMAS AHRENS
SEISMOLOGICAL LABORATORY 252-21
CALIFORNIA INST. OF TECHNOLOGY
PASADENA, CA 91125

AIR FORCE RESEARCH LABORATORY
ATTN: VSOP
29 RANDOLPH ROAD
HANSKOM AFB, MA 01731-3010 (2 COPIES)

AIR FORCE RESEARCH LABORATORY
ATTN: RESEARCH LIBRARY/TL
5 WRIGHT STREET
HANSKOM AFB, MA 01731-3004

AIR FORCE RESEARCH LABORATORY
ATTN: AFRL/SUL
3550 ABERDEEN AVE SE
KIRTLAND AFB, NM 87117-5776 (2 COPIES)

RALPH ALEWINE
NTPO
1901 N. MOORE STREET, SUITE 609
ARLINGTON, VA 22209

G. ELI BAKER
MAXWELL TECHNOLOGIES
8888 BALBOA AVE.
SAN DIEGO, CA 92123-1506

MUAWIA BARAZANGI
INSTOC
3126 SNEE HALL
CORNELL UNIVERSITY
ITHACA, NY 14853

DOUGLAS BAUMGARDT
ENSCO INC.
5400 PORT ROYAL ROAD
SPRINGFIELD, VA 22151

THERON J. BENNETT
MAXWELL TECHNOLOGIES
11800 SUNRISE VALLEY
SUITE 1212
RESTON, VA 22091

WILLIAM BENSON
NAS/COS
ROOM HA372
2001 WISCONSIN AVE. NW
WASHINGTON DC 20007

JONATHAN BERGER
UNIV. OF CALIFORNIA, SAN DIEGO
SCRIPPS INST. OF OCEANOGRAPHY IGPP, 0225
9500 GILMAN DRIVE
LA JOLLA, CA 92093-0225

ROBERT BLANDFORD
AFTAC
1300 N. 17TH STREET
SUITE 1450
ARLINGTON, VA 22209-2308

LESLIE A. CASEY
DEPT. OF ENERGY/NN-20
1000 INDEPENDENCE AVE. SW
WASHINGTON DC 20585-0420

CENTER FOR MONITORING RESEARCH
ATTN: LIBRARIAN
1300 N. 17th STREET, SUITE 1450
ARLINGTON, VA 22209

FRANCESCA CHAVEZ
LOS ALAMOS NATIONAL LAB
P.O. BOX 1663, MS-D460
LOS ALAMOS, NM 87545 (5 COPIES)

ANTON DAINTY
DTRA/PMA
45045 AVIATION DRIVE
DULLESVA 20166-7517

CATHERINE DE GROOT-HEDLIN
UNIV. OF CALIFORNIA, SAN DIEGO
IGPP
8604 LA JOLLA SHORES DRIVE
SAN DIEGO, CA 92093

DIANE DOSER
DEPT. OF GEOLOGICAL SCIENCES
THE UNIVERSITY OF TEXAS AT EL PASO
EL PASO, TX 79968

DTIC
8725 JOHN J. KINGMAN ROAD
FT BELVOIR, VA 22060-6218 (2 COPIES)

MARK D. FISK
MISSION RESEARCH CORPORATION
735 STATE STREET
P.O. DRAWER 719
SANTA BARBARA, CA 93102-0719

LORI GRANT
MULTIMAX, INC.
311C FOREST AVE. SUITE 3
PACIFIC GROVE, CA 93950

HENRY GRAY
SMU STATISTICS DEPARTMENT
P.O. BOX 750302
DALLAS, TX 75275-0302

I. N. GUPTA
MULTIMAX, INC.
1441 MCCORMICK DRIVE
LARGO, MD 20774

DAVID HARKRIDER
BOSTON COLLEGE
24 MARTHA'S PT. RD.
CONCORD, MA 01742

THOMAS HEARN
NEW MEXICO STATE UNIVERSITY
DEPARTMENT OF PHYSICS
LAS CRUCES, NM 88003

MICHAEL HEDLIN
UNIVERSITY OF CALIFORNIA, SAN DIEGO
SCRIPPS INST. OF OCEANOGRAPHY
9500 GILMAN DRIVE
LA JOLLA, CA 92093-0225

DONALD HELMBERGER
CALIFORNIA INST. OF TECHNOLOGY
DIV. OF GEOL. & PLANETARY SCIENCES
SEISMOLOGICAL LABORATORY
PASADENA, CA 91125

EUGENE HERRIN
SOUTHERN METHODIST UNIVERSITY
DEPT. OF GEOLOGICAL SCIENCES
DALLAS, TX 75275-0395

ROBERT HERRMANN
ST. LOUIS UNIVERSITY
DEPT. OF EARTH & ATMOS. SCIENCES
3507 LACLEDE AVENUE
ST. LOUIS, MO 63103

VINDELL HSU
HQ/AFTAC/TTR
1030 S. HIGHWAY A1A
PATRICK AFB, FL 32925-3002

RONG-SONG JIH
DTRA/PMA
45045 AVIATION DRIVE
DULLES, VA 20166-7517

THOMAS JORDAN
MASS. INST. OF TECHNOLOGY
BLDG 54-918
CAMBRIDGE, MA 02139

LAWRENCE LIVERMORE NAT'L LAB
ATTN: TECHNICAL STAFF (PLS ROUTE)
PO BOX 808, MS L-208
LIVERMORE, CA 94551

LAWRENCE LIVERMORE NAT'L LAB
ATTN: TECHNICAL STAFF (PLS ROUTE)
PO BOX 808, MS L-205
LIVERMORE, CA 94551

LAWRENCE LIVERMORE NAT'L LAB
ATTN: TECHNICAL STAFF (PLS ROUTE)
PO BOX 808, MS L-200
LIVERMORE, CA 94551

THORNE LAY
UNIV. OF CALIFORNIA, SANTA CRUZ
EARTH SCIENCES DEPARTMENT
EARTH & MARINE SCIENCE BUILDING
SANTA CRUZ, CA 95064

ANATOLI L. LEVSHIN
DEPARTMENT OF PHYSICS
UNIVERSITY OF COLORADO
CAMPUS BOX 390
BOULDER, CO 80309-0309

JAMES LEWKOWICZ
WESTON GEOPHYSICAL CORP.
325 WEST MAIN STREET
NORTHBORO, MA 01532

LOS ALAMOS NATIONAL LABORATORY
ATTN: TECHNICAL STAFF (PLS ROUTE)
PO BOX 1663, MS D460
LOS ALAMOS, NM 87545

LOS ALAMOS NATIONAL LABORATORY
ATTN: TECHNICAL STAFF (PLS ROUTE)
PO BOX 1663, MS F665
LOS ALAMOS, NM 87545

LOS ALAMOS NATIONAL LABORATORY
ATTN: TECHNICAL STAFF (PLS ROUTE)
PO BOX 1663, MS C335
LOS ALAMOS, NM 87545

GARY MCCARTOR
SOUTHERN METHODIST UNIVERSITY
DEPARTMENT OF PHYSICS
DALLAS, TX 75275-0395

KEITH MCLAUGHLIN
CENTER FOR MONITORING RESEARCH
SAIC
1300 N. 17TH STREET, SUITE 1450
ARLINGTON, VA 22209

BRIAN MITCHELL
DEPT OF EARTH & ATMOSPHERIC SCIENCES
ST. LOUIS UNIVERSITY
3507 LACLEDE AVENUE
ST. LOUIS, MO 63103

RICHARD MORROW
USACDA/VI
320 21ST STREET, N.W.
WASHINGTON DC 20451

JOHN MURPHY
MAXWELL TECHNOLOGIES
11800 SUNRISE VALLEY DRIVE
SUITE 1212
RESTON, VA 22091

JAMES NI
NEW MEXICO STATE UNIVERSITY
DEPARTMENT OF PHYSICS
LAS CRUCES, NM 88003

ROBERT NORTH
CENTER FOR MONITORING RESEARCH
1300 N. 17th STREET, SUITE 1450
ARLINGTON, VA 22209

OFFICE OF THE SECRETARY OF DEFENSE
DDR&E
WASHINGTON DC 20330

JOHN ORCUTT
INST. OF GEOPH. & PLANETARY PHYSICS
UNIV. OF CALIFORNIA, SAN DIEGO
LA JOLLA, CA 92093

PACIFIC NORTHWEST NAT'L LAB
ATTN: TECHNICAL STAFF (PLS ROUTE)
PO BOX 999, MS K5-12
RICHLAND, WA 99352

FRANK PILOTTE
HQ AFTAC/TT
1030 S. HIGHWAY A1A
PATRICK AFB, FL 32925-3002

KEITH PRIESTLEY
DEPARTMENT OF EARTH SCIENCES
UNIVERSITY OF CAMBRIDGE
MADINGLEY RISE, MADINGLEY ROAD
CAMBRIDGE, CB3 0EZ UK

JAY PULLI
BBN SYSTEMS AND TECHNOLOGIES, INC.
1300 NORTH 17TH STREET
ROSSLYN, VA 22209

DELAINE REITER
WESTON GEOPHYSICAL CORP.
73 STANDISH ROAD
WATERTOWN, MA 0472

PAUL RICHARDS
COLUMBIA UNIVERSITY
LAMONT-DOHERTY EARTH OBSERV.
PALISADES, NY 10964

MICHAEL RITZWOLLER
DEPARTMENT OF PHYSICS
UNIVERSITY OF COLORADO
CAMPUS BOX 390
BOULDER, CO 80309-0309

DAVID RUSSELL
HQ AFTAC/TTR
1030 SOUTH HIGHWAY A1A
PATRICK AFB, FL 32925-3002

CHANDAN SAIKIA
WOODWARD-CLYDE FED. SERVICES
566 EL DORADO ST., SUITE 100
PASADENA, CA 91101-2560

SANDIA NATIONAL LABORATORY
ATTN: TECHNICAL STAFF (PLS ROUTE)
DEPT. 5704
MS 0979, PO BOX 5800
ALBUQUERQUE, NM 87185-0979

SANDIA NATIONAL LABORATORY
ATTN: TECHNICAL STAFF (PLS ROUTE)
DEPT. 9311
MS 1159, PO BOX 5800
ALBUQUERQUE, NM 87185-1159

SANDIA NATIONAL LABORATORY
ATTN: TECHNICAL STAFF (PLS ROUTE)
DEPT. 5736
MS 0655, PO BOX 5800
ALBUQUERQUE, NM 87185-0655

AVI SHAPIRA
SEISMOLOGY DIVISION
IPRG
P.O.B. 2286 NOLON 58122 ISRAEL

MATTHEW SIBOL
ENSCO, INC.
445 PINEDA CT.
MELBOURNE, FL 32940

JEFFRY STEVENS
MAXWELL TECHNOLOGIES
8888 BALBOA AVE.
SAN DIEGO, CA 92123-1506

TACTEC
BATTELLE MEMORIAL INSTITUTE
505 KING AVENUE
COLUMBUS, OH 43201 (FINAL REPORT)

LAWRENCE TURNBULL
ACIS
DCI/ACIS
WASHINGTON DC 20505

FRANK VERNON
UNIV. OF CALIFORNIA, SAN DIEGO
SCRIPPS INST. OF OCEANOGRAPHY
9500 GILMAN DRIVE
LA JOLLA, CA 92093-0225

RU SHAN WU
UNIV. OF CALIFORNIA, SANTA CRUZ
EARTH SCIENCES DEPT.
1156 HIGH STREET
SANTA CRUZ, CA 95064

JAMES E. ZOLLWEG
BOISE STATE UNIVERSITY
GEOSCIENCES DEPT.
1910 UNIVERSITY DRIVE
BOISE, ID 83725

SANDIA NATIONAL LABORATORY
ATTN: TECHNICAL STAFF (PLS ROUTE)
DEPT. 5704
MS 0655, PO BOX 5800
ALBUQUERQUE, NM 87185-0655

THOMAS SERENO JR.
SAIC
10260 CAMPUS POINT DRIVE
SAN DIEGO, CA 92121

ROBERT SHUMWAY
410 MRAK HALL
DIVISION OF STATISTICS
UNIVERSITY OF CALIFORNIA
DAVIS, CA 95616-8671

DAVID SIMPSON
IRIS
1200 NEW YORK AVE., NW
SUITE 800
WASHINGTON DC 20005

BRIAN SULLIVAN
BOSTON COLLEGE
INSITUTE FOR SPACE RESEARCH
140 COMMONWEALTH AVENUE
CHESTNUT HILL, MA 02167

NAFI TOKSOZ
EARTH RESOURCES LABORATORY
M.I.T.
42 CARLTON STREET, E34-440
CAMBRIDGE, MA 02142

GREG VAN DER VINK
IRIS
1200 NEW YORK AVE., NW
SUITE 800
WASHINGTON DC 20005

TERRY WALLACE
UNIVERSITY OF ARIZONA
DEPARTMENT OF GEOSCIENCES
BUILDING #77
TUCSON, AZ 85721

JIAKANG XIE
COLUMBIA UNIVERSITY
LAMONT DOHERTY EARTH OBSERV.
ROUTE 9W
PALISADES, NY 10964